BIANCA APOLÔNIO FONTES

PHYSIOLOGICAL, BIOCHEMICAL, AND MOLECULAR ASPECTS OF INDUCED RESISTANCE IN SOYBEAN AGAINST RUST USING A NITROGEN-AND CALCIUM-POLYPHENOLS COMPOUND AND A PHOSPHITE OF NICKEL AND POTASSIUM

Thesis submitted to the Graduate Program in Plant Pathology of the Universidade Federal de Viçosa in partial fulfillment of the requirements for the degree of *Doctor Scientiae*.

Advisor: Fabrício de Ávila Rodrigues

VIÇOSA - MINAS GERAIS

2023

Ficha catalográfica elaborada pela Biblioteca Central da Universidade Federal de Viçosa - Campus Viçosa

T
F683p
2023

Fontes, Bianca Apolônio, 1995-
Physiological, biochemical, and molecular aspects of induced resistance in soybean against rust using a nitrogen-and calcium-polyphenols compound and a phosphite of nickel and potassium / Bianca Apolônio Fontes. – Viçosa, MG, 2023.
1 tese eletrônica (101 f.): il. (algumas color.).

Texto em inglês.
Orientador: Fabrício Ávila Rodrigues.
Tese (doutorado) - Universidade Federal de Viçosa, Departamento de Fitopatologia, 2023.
Inclui bibliografia.
DOI: https://doi.org/10.47328/ufvbbt.2023.762
Modo de acesso: World Wide Web.

1. Ferrugem da soja (Doença). 2. Soja - Doenças e pragas. I. Rodrigues, Fabrício Ávila, 1974-. II. Universidade Federal de Viçosa. Departamento de Fitopatologia. Programa de Pós-Graduação em Fitopatologia. III. Título.

CDD 22. ed. 633.3494

Bibliotecário(a) responsável: Alice Regina Pinto Pires CRB-6/2523

BIANCA APOLÔNIO FONTES

PHYSIOLOGICAL, BIOCHEMICAL, AND MOLECULAR ASPECTS OF INDUCED RESISTANCE IN SOYBEAN AGAINST RUST USING A NITROGEN- AND CALCIUM-POLYPHENOLS COMPOUND AND A PHOSPHITE OF NICKEL AND POTASSIUM

Thesis submitted to the Graduate Program in Plant Pathology of the Universidade Federal de Viçosa in partial fulfillment of the requirements for the degree of *Doctor Scientiae*.

APPROVED: October 25, 2023.

Assent:

Bianca Apolônio Fontes

Bianca Apolônio Fontes

Author

Fabrício Ávila Rodrigues

Fabrício de Ávila Rodrigues

Advisor

I dedicate my thesis to God, my parents, Marisa and Wilson, my sister Mariana, my husband Lucas, and my grandparents Elvira, Osvaldo, Zilda, and Cici, for all the love, care, and support in my journey.

ACKNOWLEDGEMENTS

First, I would like to thank God for all the blessings and opportunities I have had throughout my life and for being my strength during this stage.

I want to express my sincere thanks to:

My mother, Marisa, my father, Wilson, and my sister, Mariana, for their love, support, trust, understanding, affection, friendship, and encouragement, and for not measuring efforts to make my dreams come true.

My husband Lucas, for all his love, friendship, support, help, care, encouragement, and for being my life partner.

My grandparents, Elvira, Zilda, Cici, and especially my grandfather Osvaldo, for all the love, help, encouragement, and advice and for believing I can overcome any challenge.

Professor Fabrício de Ávila Rodrigues for his guidance, attention, professionalism, and competence, and for helping me professionally and personally.

My colleagues at the Laboratory of Host-Pathogen Interaction, especially Leandro, for all their support, teaching, help, friendship, and contribution to this research.

UFV employees, especially Mr. Mário, Mr. Bruno, and Mrs. Sara.

The Federal University of Viçosa, for the opportunity to complete the postgraduate course.

The Department of Plant Pathology, Postgraduate Program in Plant Pathology, and the Laboratory of Host-Pathogen Interaction for supporting the development of this study and for providing me with all the conditions for my research.

This study was financed in part by the Coordenação de Aperfeiçoamento de Pessoal de Nível Superior – Brasil (CAPES) – Finance Code 001.

The Coordenação de Aperfeiçoamento de Pessoal de Nível Superior (CAPES) and the Conselho Nacional de Desenvolvimento Científico e Tecnológico (CNPq), for granting the scholarship.

BIOGRAPHY

BIANCA APOLÔNIO FONTES, daughter of Marisa Apolônio Fontes and Wilson José Fontes, was born on September 28, 1995, in Viçosa, Minas Gerais State. In May 2013, she started to study Agronomy at the Federal University of Viçosa (UFV). In July 2018, she obtained the title of Agronomist. From August 2018 to February 2019, she received training at the Plant Diagnostic Center at Louisiana State University. In February 2021, she obtained the *Master Scientiae* in Plant Pathology at Universidade Federal de Viçosa (UFV). In March 2021, she started the doctoral degree in the Plant Pathology Program at UFV under the guidance of Professor Fabrício de Ávila Rodrigues, defending her Thesis in October 2023.

ABSTRACT

FONTES, Bianca Apolônio, D.Sc., Universidade Federal de Viçosa, October, 2023. **Physiological, biochemical, and molecular aspects of induced resistance in soybean against rust using a nitrogenand calcium-polyphenols compound and a phosphite of nickel and potassium.** Adviser: Fabrício de Ávila Rodrigues.

Soybean rust (SR), caused by *Phakopsora pachyrhizi*, is an aggressive disease that severely reduces the production of soybean crops worldwide. The SR control has been done by spraying fungicides and using cultural practices (e.g., early sowing dates, early detection of the rust symptoms development, cultivars of early maturing, and 60 to 90 days without growing soybean). However, sustainable control methods are preferred nowadays. In this point of view, induced resistance using biotic and abiotic defense elicitors plays an important role in plant disease management. The present study investigated the potential of Cautha® [calcium (11.01%) and nitrogen (3.3%) complexed with polyphenols (10%)] and Blindage Ni® [potassium (20% K_2O, 280 g/L), nickel (0.5% Ni, 7 g/L), and phosphorous acid (500 g/L)] in displaying biochemical, molecular, and physiological resistance mechanisms against *P. pachyrhizi*. In the first study, plants were sprayed with water (control) or Cautha® (referred to as induced resistance [IR] stimulus after that) and inoculated or non-inoculated with *P. pachyrhizi*. The germination of urediniospores was reduced by 26% *in vitro* at the same dose of IR stimulus used to spray soybean plants. The rust severity and area under the disease progress curve lowered by 41% (at 15 days after inoculation) and 27%, respectively, for IR stimulus-sprayed plants compared to water-sprayed plants. The IR stimulus treatment greatly reduced the cellular damage caused by *P. pachyrhizi* infection in soybean tissues, maintained a great content of photosynthetic pigments, enhanced activities of defense-related enzymes, and built a robust antioxidative metabolism compared with the control treatment. In the second study, the factors investigated were water (control) or Blindage Ni® (referred to as induced resistance [IR] stimulus after that) inoculated or non-inoculated with *P. pachyrhizi*. *In vitro*, the urediniospores germination was reduced by 99% by IR stimulus. The soybean rust severity and area under the disease progress curve was decreased by 73% (at 15 days after inoculation) and 74%, respectively, in IR stimulus-sprayed plants compared to water-sprayed plants. The infected plants sprayed with IR stimulus maintain the proper functionality of photosynthetic apparatus and a good concentration of pigments. In addition, this treatment reduced the damage and lipid peroxidation in plant tissue, up-regulated the expression of several defense-related

genes in plants infected by *P. pachirhizi*, kept a great concentration of potassium and nickel in soybean tissues, and increased the concentrations of phenolics and lignin in contrast with the control plants. The results of the present study highlighted the positive role of both IR stimuli in activating defense mechanisms against *P. pachyrhizi* in soybean crop and reducing disease severity.

Keywords: Soybean rust. *Glycine max*. Plant defense mechanisms. Management of plant disease.

RESUMO

FONTES, Bianca Apolônio, D.Sc., Universidade Federal de Viçosa, October, 2023. **Aspectos fisiológicos, bioquímicos e moleculares da resistência induzida em soja contra ferrugem utilizando um composto de polifenóis contendo nitrogênio e cálcio e um fosfito de níquel e potássio.** Orientador: Fabrício Ávila Rodrigues

A ferrugem da soja (FS), causada por *Phakopsora pachyrhizi*, é uma doença agressiva que reduz severamente a produção da cultura da soja em todo o mundo. O controle da FS tem sido feito principalmente por meio de pulverização de fungicidas e uso de práticas culturais (por exemplo, semeadura precoce, detecção precoce do desenvolvimento de sintomas de ferrugem, cultivares de maturação precoce e período de 60 a 90 dias sem cultivo de soja), porém, métodos de controle sustentáveis são preferidos atualmente. Neste sentido, a resistência induzida pelo uso de elicitores de defesa bióticos e abióticos desempenha um papel importante no manejo de doenças de plantas. O presente estudo investigou o potencial de Cautha® [cálcio (11,01%) e nitrogênio (3,3%) complexados com polifenóis (10%)] e Blindage Ni® [níquel (0,5% Ni, 7 g/L) potássio (20% K2O, 280 g/L) e ácido fosforoso (500 g/L)] na ativação de mecanismos de resistência bioquímica, molecular e fisiológica contra *P. pachyrhizi*. No primeiro estudo, as plantas foram pulverizadas com água (controle) ou Cautha® (posteriormente denominado estímulo de resistência induzida [IR]) e inoculadas ou não com *P. pachyrhizi*. A germinação dos urediniósporos foi reduzida em 26% *in vitro* na mesma dose de estímulo IR utilizada na pulverização das plantas de soja. A severidade da ferrugem e a área abaixo da curva de progresso da doença reduziram em 41% (15 dias após a inoculação) e 27%, respectivamente, para plantas pulverizadas com estímulo IR em comparação com plantas pulverizadas com água. O tratamento com estímulo IR reduziu o dano celular causado pela infecção por *P. pachyrhizi* nos tecidos da soja, manteve uma adequada concentração de pigmentos fotossintéticos, aumentou a atividade de proteínas relacionadas à defesa e construiu um metabolismo antioxidante ainda mais robusto em comparação com o tratamento controle. No segundo estudo, os fatores investigados foram água (controle) ou Blindage Ni® (posteriormente denominado estímulo de resistência induzida [IR]) inoculados ou não inoculados com *P. pachyrhizi*. *In vitro*, a germinação dos urediniósporos foi reduzida em 99% pelo estímulo IR. A severidade da ferrugem da soja e a área abaixo da curva de progresso da doença diminuíram em 73% (15 dias após a inoculação) e 74%, respectivamente, nas plantas pulverizadas com estímulo IR em comparação com as plantas pulverizadas com água. As plantas infectadas pulverizadas com

estímulo IR mantiveram um funcionamento adequado do aparato fotossintético e uma boa concentração de pigmentos. Além disso, este tratamento reduziu os danos e a peroxidação lipídica nos tecidos das plantas, regulou positivamente a expressão de vários genes relacionados à defesa em plantas infectadas por *P. pachirhizi*, manteve grande concentração de potássio e níquel nos tecidos da soja e aumentou as concentrações de compostos fenólicos e lignina em contraste com as plantas controle. Os resultados encontrados no presente estudo destacaram o papel positivo tanto do estímulo IR em ativar mecanismos de defesa contra *P. pachyrhizi* na cultura da soja quanto na redução da severidade da doença.

Palavras-chave: Ferrugem da soja. *Glycine max*. Mecanismos de defesa das plantas. Manejo de doenças de plantas.

SUMMARY

CHAPTER I

A NITROGEN-AND CALCIUM-POLYPHENOLS COMPOUND AS AN OPTION FOR SOYBEAN RUST CONTROL

Abstract

Among soybean diseases, rust, caused by *Phakopsora pachyrhizi*, stands out as one of the most destructive. Resistance inducers may be a great alternative to reduce the yield losses caused by this disease from the perspective of more sustainable agriculture. In this study, plants were sprayed with water (control) or with Cautha® (referred to as induced resistance [IR] stimulus after that) and inoculated or non-inoculated with *P. pachyrhizi*. The urediniospores germination was significantly reduced by 22, 26, 19, and 25% at the rates of 2.5, 5, 10, and 20 mL IR stimulus/L, respectively. Rust severity was significantly reduced by 27, 19, 23, 25, and 41% at 7, 9, 11, 13, and 15 days after inoculation, respectively. The area under the disease progress curve significantly decreased by 27% for IR stimulus-sprayed plants compared to water-sprayed plants. For infected plants, foliar concentrations of Ca, N, Chl *a+b*, and carotenoids were higher for IR-stimulus sprayed plants than water-sprayed plants. Lower concentrations of malondialdehyde and reactive oxygen species (hydrogen peroxide and anion superoxide) indicated less cellular damage imposed by fungal infection, along with great activities of antioxidative enzymes (catalase, glutathione reductase, superoxide dismutase, and ascorbate peroxidase) helped to reduce rust symptoms faced by the infected and IR-stimulus sprayed plant. On top of that, these plants also showed great foliar concentrations of total soluble phenols and lignin as well as greater activities of defense-related enzymes (chitinase, β-1,3-glucanase, phenylalanine ammonia-lyase, peroxidase, polyphenoloxidase, and lipoxygenase). These results strongly support the potential of using this IR stimulus to increase soybean resistance against *P. pachyrhizi* and, at the same time, act directly against urediniospores germination.

Keywords: *Glycine max*· *Phakopsora pachyrhizi*· Antioxidative metabolism· Induced resistance· Plant defense· Photosynthesis.

Introduction

Soybean is one of the most valuable global crops grown worldwide due to the versatility of using the grains, with higher protein content, for animal feed, human consumption, oil extraction, and biofuel feedstock (Chen et al. 2012). Epidemics of soybean rust (SR), caused by the biotrophic fungus *Phakopsora pachyrhizi* H. Sydow & P. Sydow, is without a doubt one of the major threat to achieve higher yield in producer areas considering its greatest capacity to reduce photosynthesis due to intense leaf tissue necrosis and yellowing, plant defoliation, earlier maturation, reduced grain weight, and lower grains quality (Langenbach et al. 2016; Rios et al. 2018). In Brazil, the management of SR consists of using some cultural practices (e.g., early sowing dates, early-maturing cultivars, and a period of 60- to 90-days without growing soybean in the off-season to avoid early disease development) and fungicides application (Langenbach et al. 2016). However, the efficiency of the currently available fungicides may be affected by the variability in the pathogen population and their precise time and frequency of application (Mueller et al. 2009) without disregarding the risks imposed on human health and the environment. Management measures such as using soybean cultivars with resistance to practically all isolates of *P. pachyrhizi* are not spreadly used by the growers yet (Goellner et al. 2010; Kato and Soares 2022). Based on the current scenario where SR has caused great economic yield losses in several countries and the urgent need for more sustainable and effective management measures, the decision to use the resistance inducers can become an important and prioritized tool to mitigate the damage caused by *P. pachyrhizi* in the soybean production to complement some of the management methods recommended nowadays.

To defend themselves against infection by a plethora of pathogens, agronomic crops used their basal defense mechanisms (Dixon 1986; Kessmann et al. 1994; Kaur et al. 2022). Besides that, plants are prone to have their resistance induced by several types of abiotic and biotic elicitors (Zeier 2021). The phenomenon of induced resistance (IR) refers to the faster, more accurate, and efficient activation of the latent plant defense mechanisms to restrict the colonization of plant tissues by the pathogen, resulting in slower disease progress (Walters 2010). Acquired systemic resistance (SAR) and induced systemic resistance (ISR) are the two known types of IR used by plants to defend themselves against pathogens of different lifestyles strategically (Choudhary et al. 2007; Lyon et al. 2007; Lorenzetti et al. 2018; Zeier 2021). The SAR occurs systemically after the exposure of plants to synthetic or natural elicitors and involves the participation of salicylic acid (SA) and the pathogenesis of non-expressing protein 1 (*NPR1*) (Hammerschmidt 2009; Walters 2010). The SA is accumulated after pathogen

infection and binds to *NPR1* to induce the expression of genes that codify for pathogenesis-related proteins (Kesel et al. 2021). Several metabolites may be involved in long-distance signaling for the occurrence of SAR, such as azelaic acid, dehydroabietinal, SA methyl ester, glycerol-3-phosphate, and pipecolic acid (Shah and Zeier 2013; Kesel et al. 2021; Zeier 2021). Although SA-mediated resistance is effective against a wide range of pathogens, it is known that SAR is generally more effective against biotrophic and hemibiotrophic pathogens (Hammerschmidt 2009; Llorens et al. 2017). On the other hand, ISR is induced by the colonization of plant roots by plant growth-promoting rhizobacteria with the participation of jasmonic acid (JA) and ethylene (ET) (Pieterse et al. 2000; Pieterse and Van Loon 2007; Vlot et al. 2021). In general, the intensity of diseases caused by necrotrophic pathogens is more prone to be reduced in plants exhibiting ISR (Zeier 2021). Interestingly, SA or JA/ET-mediated signaling pathways are not spatially separated in plant tissues facing pathogens infection considering their possible overlap or interconnection, at both antagonistic and synergistic levels, for a prompted activation of host defense reactions (Kesel et al. 2021; Vlot et al. 2021). The potential of using different IR stimuli to reduce SR severity in both field and greenhouse conditions (e.g., cell wall extract of *Saccharomyces cerevisiae*, *Bacillus subtilis*, thaxtomin A from the *Streptomyces scabies*, *Metarhizium* spp., saccharin, harpin protein-derived peptides, phosphite combined with free amino acids, copper-polyphenolic compound, hexanoic acid, azelaic acid, nickel, and silicon) has been described in the literature (Cruz et al. 2020; Einhardt et al. 2020; Paula et al. 2021; Picanço et al. 2022; Otolakoski et al. 2023; Rodrigues et al. 2023).

Considering the destructive potential of SR on soybean fields and the lack of suitable effective management measures against this disease, the present study raised the hypothesis that a compound made of a mixture of nitrogen, calcium, and polyphenols could potentiate the defense responses of soybean plants against *P. pachyrhizi* infection. This hypothesis was tested at the physiological and biochemical levels by profoundly analyzing the photosynthetic apparatus, the antioxidant metabolism, and the host defense responses of plants non-sprayed or sprayed with this compound that were challenged or not with *P. pachyrhizi*.

Material and Methods

In vitro assays

Different volumes of a stock solution (40 ml/L) of Cautha® [calcium (11.01% and 148.6 g/L) and nitrogen (3.3% and 44.55 g/L) complexed with plant-derived pool of polyphenols (10%); FertGlobal, Larderello, Italy] were mixed with 1 ml of *P. pachyrhizi* urediniospores suspension (10^5 urediniospores/ml) to obtain solutions of Cautha® with the final concentrations of 1.25, 2.5, 5, 10, and 20 mL/L. A 100 µL of urediniospores suspension mixed with the different concentrations of Cautha® solution was transferred to a glass slide and covered with a coverslip and also to a Petri dish containing 20 mL of agar-agar (AA) medium. A suspension of urediniospores without Cautha® solution corresponded to the control treatment. The suspension was homogeneously distributed over the AA medium using a Drigalski glass handle. The glass slides and the Petri dishes were transferred to a growth chamber (25°C and photoperiod of 12 h of light and 12 h of dark). Each glass slide and Petri dish received 5 µl of lactophenol after 12 h to stop urediniospores germination. Using the bright field, one hundred urediniospores were randomly examined in each glass slide and Petri dish under a light microscope (Carl Zeiss AxioImager A1) at 40 × magnification. The images of the details for urediniospores germination were acquired digitally (model AxioCam HR, Germany; Axion Vision software v. 4.8.1.). Urediniospore with a germ tube larger than its diameter was considered germinated. The percentage of urediniospores germination was calculated for the replication of each treatment.

Plant growth

A total of six soybean seeds from cultivar DS5916IPRO (https://www.brevant.com.br), susceptible to *P. pachyrhizi*, were sown in each plastic pot containing 2 Kg of a 1:1 mixture of soil and substrate (Tropstrato, Vida Verde, Mogi Mirim, SP, Brazil). After germination, a total of four seedlings were left per pot. Plants in each pot were fertilized weekly with 100 mL of nutrient solution prepared according to Picanço et al. (2022). Deionized water was used to prepare the nutrient solution. Plants were grown in a greenhouse (temperature of 25 ± 2°C, relative humidity of 70 ± 5%, and natural photosynthetically active radiation (PAR) of 952 ± 18 µmol photons m^{-2} s^{-1} measured at midday) and watered daily.

Foliar spray of soybean plants with Cautha®

Soybean plants (V4 growth stage; ≈ 30 days after seedlings emergence) were sprayed with a solution of Cautha® (5 ml/L, 5 ml of solution per plant) using a VL Airbrush atomizer (Paasche Airbrush Co., Chicago, IL, USA). This treatment will be referred to as induced resistance (IR) stimulus after that, according to the criteria proposed by Kesel et al. (2021). The IR stimulus solution was prepared using deionized water. Plants sprayed with deionized water served as the control treatment.

Inoculation of soybean plants with *P. pachyrhizi*

At 48 hours after being sprayed with IR stimulus or water, plants were inoculated with a suspension of 10^5 urediniospores of *P. pachyrhizi*/ml prepared with gelatin (0.5% wt/vol) and Tween 80 (25 µl/L) by using a VL Airbrush atomizer. After inoculation, plants were kept in a mist chamber at 25°C for 16 h under darkness. After this period, plants were transferred to a greenhouse (temperature of 25 ± 2°C, relative humidity of 75 ± 5%, and natural PAR of 935 ± 22 µmol photons m^{-2} s^{-1} measured at midday) until the end of the experiment. Plants non-inoculated with *P. pachyrhizi* were kept in different mist chamber and greenhouse benches under the same environmental conditions mentioned above.

Experimental design

For the in vitro assays, the experiment was arranged in a completely randomized design with six treatments (control and five IR stimulus concentrations) with six and ten replications for the glass slide and Petri dish assays, respectively. Each replication corresponded to one glass slide or a Petri dish. A 2 × 2 factorial experiment, consisting of plants sprayed with water (control) or IR stimulus and non-inoculated or inoculated with *P. pachyrhizi*, was arranged in a completely randomized design with five replications per evaluation time to assess rust severity as well to determine the concentration of photosynthetic pigments and the foliar concentrations of Ca and N. Leaf samples for the histochemical and biochemical assays were obtained from another 2 × 2 factorial experiment with the same factors and replications described above. All experiments were repeated once.

Assessment of soybean rust severity

At 7, 9, 11, 13, and 15 days after inoculation (dai) of soybean plants with *P. pachyrhizi*, the severity of soybean rust was evaluated in the leaflets of the second and third leaves (from base to top) of each plant per replication of each treatment (four replications, 16 plants, and 96 leaflets per experiment) using the diagrammatic scale proposed by Franceschi et al. (2020). The

area under disease progress curve (AUDPC) for each leaflet per leaf of each plant from the replications of each treatment was calculated using the trapezoidal integration of disease progress curves according to Shaner and Finney (1977). At 15 dai, the second and third leaves of each plant per replication of each treatment were collected and scanned at 600 dpi resolution, and the images were processed using the software QUANT (Fagundes-Nacarath et al. 2018) to obtain the values of final soybean rust severity.

Determination of foliar N and Ca concentrations

The foliar Ca and N concentrations were determined according to Mesquita et al. (2019) with a few modifications. At 15 dai, the leaflets of the second and third leaves (from base to top) of each plant per replication of each treatment (four replications, 16 plants, and 96 leaflets per experiment) were collected, washed in deionized water, and dried in a drying oven with forced ventilation for two days. The foliar Ca and N concentrations were determined by nitric-perchloric digestion and inductively coupled plasma-optical emission spectrometry (ICP-OES).

Determining photosynthetic pigments concentration

Five leaf discs (1 cm^2 each) obtained from the leaflets of the second leaf (from base to top) of each plant per replication of each treatment (four replications, 16 plants, and 64 leaflets) were collected from both non-inoculated and inoculated plants at 7, 11, and 15 dai. The discs were immersed in glass tubes containing 5 ml of saturated dimethyl sulfoxide solution and calcium carbonate (5 g/L) and kept in the dark at room temperature for 24 h. The absorbances of the extracts were read at 480, 649, and 665 nm to determine the concentrations of Chl *a*, Chl *b*, and carotenoids, according to Picanço et al. (2021).

Histochemical detection of lipid peroxidation, membrane damage, hydrogen peroxide (H_2O_2), and superoxide anion radical ($O_2^{\bullet-}$)

At 15 dai, the leaflets of the second leaf (from base to top) of each plant per replication of each treatment (four replications, 8 plants, and 24 leaflets) were collected from both non-inoculated and inoculated plants. Lipid peroxidation and membrane damage in the leaflets were visualized using Schiff and Evans' blue reagents, respectively (Tistama et al. 2012; Awasthi et al. 2018). The leaflets were randomly transferred to glass vials containing 50 mL of either Schiff (10% v/v prepared in deionized water) or Evans's blue (0.025% wt/v prepared in 100 μM of $CaCl_2$, pH 5.6) reagents (five leaflets per glass vial for each reagent) during 2 and 12 h, respectively. For H_2O_2 detection, leaflets were randomly placed in glass vials (five leaflets per glass vial)

containing 25 mL of 3,3′-diaminobenzidine tetrahydrochloride solution (1 mg/mL) (Sigma-Aldrich, São Paulo, Brazil) and kept in the dark at 25ºC for 12 h. For $O_2^{\bullet-}$ detection, leaflets were randomly placed in glass vials (five leaflets per glass vial) containing 50 mL of nitro blue tetrazolium (0.1%) solution (Sigma-Aldrich, São Paulo, Brazil) prepared in potassium phosphate buffer (10 mM, pH 6.8) during 24 h. The leaflets were cleared in boiling aqueous ethanol (80%) for 80 min until pink, blue, brown, and blue spots were visualized in the leaflets, confirming the occurrence of lipid peroxidation, membrane damage, H_2O_2, and $O_2^{\bullet-}$, respectively.

Biochemical assays

At 1, 3, 5, 10, and 15 dai, the second and third leaves (from base to top) of each plant per replication of each treatment (four replications, 16 plants, and 96 leaflets per experiment) were collected from both non-inoculated and inoculated plants. Leaf samples were kept in liquid nitrogen during sampling and stored at -80ºC until further analysis.

Malondialdehyde (MDA) concentration: oxidative damage in the leaflet tissues was estimated based on the concentration of total 2-thiobarbituric acid (TBA) reactive substances and expressed as equivalents of MDA (Cakmak and Horst 1991). Leaflet tissue (0.1 g) was ground into a fine powder using a vibration ball mill (Retsch, Haan, Germany) with liquid nitrogen and homogenized in 2 ml of 0.1% (w/v) trichloroacetic acid (TCA) solution in an ice bath. The homogenate was centrifuged at 12,000 *g* for 15 min at 4°C. After centrifugation, a total of 250 µl of the supernatant was reacted with 750 µl of TBA solution (0.5% in 20% TCA) for 60 min in a boiling water bath at 95°C. After this period, the reaction was stopped in an ice bath. The samples were centrifuged at 10,000 *g* for 10 min, and the specific absorbance was determined at 532 nm. The non-specific absorbance was estimated at 600 nm and subtracted from the specific absorbance value. The extinction coefficient of 155 mM^{-1} cm^{-1} (Heath and Packer 1968) was used to calculate the MDA concentration.

Concentrations of H_2O_2 and $O_2^{\bullet-}$: leaflet tissue (0.1 g) was ground into a fine powder described above and homogenized in 2 ml of 0.1% (w/v) of TCA. The homogenate was centrifuged at 12,000 *g* for 15 min at 4°C. The supernatant was added to a reaction mixture containing 10 mM potassium buffer (pH 7.0) and 1 M of iodide solution and incubated for 10 min. The H_2O_2 concentration was determined based on the oxidized product formed at 390 nm (Velikova et al. 2000). A standard curve of H_2O_2 (Sigma-Aldrich, São Paulo, Brazil) was used

to determine H_2O_2 concentration. Leaflet tissue (0.1 g) was ground as described above and homogenized in 2 ml of a solution containing 100 mM sodium phosphate buffer (pH 7.2) and 1 mM sodium diethyldithiocarbamate. The homogenate was centrifuged at 22,000 *g* for 20 min at 4°C, and the supernatant was used to determine $O_2^{\bullet-}$ concentration, according to Chaitanya and Naithani (1994).

Activities of defense-related enzymes: (0.2 g) was ground into a fine powder as described above and the fine powder was homogenized in 2 ml of a solution containing 50 mM potassium phosphate buffer (pH 6.8), 1 mM EDTA, 1 mM phenylmethylsulfonyl fluoride (PMSF), and 2% (w/v) polyvinylpyrrolidone (PVP) following centrifugation at 12,000 *g* for 15 min at 4°C. The supernatant was used to determine chitinase (CHI) (EC 3.2.1.14), *β*-1,3-glucanase (GLU) (EC 3.2.1.39), phenylalanine ammonia-lyase (PAL) (EC 4.3.1.5), peroxidase (POX) (EC 1.11.1.7), polyphenoloxidase (PPO), and lipoxygenase (LOX) (EC 1.13.11.12) activities. The CHI activity was determined by adding the crude enzyme extract to a reaction mixture containing 50 mM sodium acetate buffer (pH 5.0) and 0.1 mM *p*-nitrophenyl-β-*D*-*N*-*N'*-diacetylchitobiose (Harman et al. 1993). The reaction mixture was incubated in a water bath at 37°C for 2 h, and the reaction was determined by adding 0.2 M sodium carbonate. The sodium carbonate was added to the control samples soon after adding the crude enzyme extract to the reaction mixture. The absorbance of the product released by CHI was measured at 410 nm. The 7×103 mM^{-1} cm^{-1} extinction coefficient was used to calculate CHI activity. The GLU activity was determined after adding the crude enzyme extract to a reaction mixture containing 50 mM sodium acetate buffer (pH 5.0) and laminarin (1 mg/mL) (Lever 1972). The reaction mixture was incubated in a water bath for 30 min at 45°C. Afterward, this mixture was added to a reaction mixture of dinitrosalicylic acid (DNS). This reaction mixture was then incubated in a water bath for 10 min at 90°C and then cooled in an ice bath until it reached 25°C. The absorbance was measured at 540 nm. A similar procedure was used for the control samples, except that the first incubation was excluded. The crude enzyme extract reacted with a reaction mixture containing 25 mM Tris-HCl buffer (pH 8.8) and 25 mM L-phenylalanine for PAL activity. The reaction mixture was incubated at 40°C for 3 h. For the control samples, the extract was replaced by the Tris-HCl buffer. The reaction was stopped by adding 6 N HCl. The absorbance of *trans*-cinnamic acid derivatives was recorded at 290 nm. The extinction coefficient of 100 M^{-1} cm^{-1} was used to calculate PAL activity (Guo et al. 2007). The POX activity was assayed by determining the pyrogallol oxidation proposed by Kar and Mishra (1976). The reaction started after adding the crude enzyme extract to a reaction mixture

containing 25 mM potassium phosphate (pH 6.8), 20 mM pyrogallol, and 20 mM H_2O_2. The POX activity was determined by the absorbance of colored purpurogallin recorded for 1 min at 420 nm at 25°C. The extinction coefficient of 2.47 mM^{-1} cm^{-1} (Chance and Maehley 1955) was used to calculate POX activity. The PPO activity was determined using the same procedure as POX, but H_2O_2 was omitted from the reaction mixture. The LOX activity was determined by adding the crude enzyme extract to a reaction mixture containing 50 mM sodium phosphate buffer (pH 6.5) and 50 μM sodium linoleate. The reaction mixture was incubated at 25°C, and the absorbance of the product released by LOX for 1 min was measured at 234 nm. The extinction coefficient of 25000 M^{-1} cm^{-1} was used to calculate LOX activity (Axelrod et al. 1981). The activities of these enzymes were expressed on a protein basis, and the protein concentration was determined according to Bradford (1976).

Concentrations of total soluble phenols (TSP) and lignin-thioglycolic acid (LTGA) derivatives: leaflet tissue (0.1 g) was ground into a fine powder as described above and homogenized in 1 mL of 80% (v/v) methanol solution. The crude extract was shaken at 300 rpm at 25°C for 2 h and the mixture was centrifuged at 17,000 *g* for 30 min. 26 The TSP concentration was determined in the methanolic extract, and the pellet was used to determine the LTGA derivatives concentration according to Tatagiba et al. (2014).

Activities of antioxidant enzymes: leaflet tissue (0.2 g) was ground into a fine powder described above. The fine powder was homogenized in 2 ml of a solution containing 50 mM of potassium phosphate buffer (pH 6.8), 0.1 mM EDTA, 1 mM PMSF, and 2% (w/v) PVP and centrifuged at 12,000 *g* for 15 min at 4°C. The supernatant was used as the crude enzyme extract to determine superoxide dismutase (SOD) (EC 1.15.1.1), ascorbate peroxidase (APX) (EC 1.11.1.11), catalase (CAT) (EC 1.11.1.6), and glutathione reductase (GR) (EC 1.8.1.7) activities. The SOD activity was determined by measuring its ability to photochemically reduce nitroblue tetrazolium (NBT), as described by Beauchamp and Fridovich (1971). The reaction was initiated by adding the crude enzyme extract to a mixture containing 50 mM potassium phosphate buffer (pH 7.8), 14 mM methionine, 75 μM NBT, 0.1 mM EDTA, and 2 μM riboflavin. Samples were light-exposed for 7 min and the production of formazan blue, resulting from the photoreduction of NBT, was measured at 560 nm with a spectrophotometer (Giannopolitis and Ries 1977). Samples kept in the dark for 7 min served as a blank. One unit of SOD was defined as the amount of enzyme necessary to inhibit NBT photoreduction by 50%. The APX activity assay followed that described by Nakano and Asada (1981). The crude

enzyme extract was added to a mixture containing 50 mM phosphate buffer (pH 7.0), 0.5 mM ascorbic acid, and 0.1 mM H_2O_2. The rate of ascorbate oxidation was measured by recording the absorbance at 290 nm for 1 min. The extinction coefficient of 2.8 mM^{-1} cm^{-1} (Nakano and Asada 1981) was used to calculate APX activity. The CAT activity was determined by adding the crude enzyme extract to a reaction mixture containing 50 mM potassium phosphate buffer (pH 7.0) and 20 mM H_2O_2. The determination of CAT activity was based on the rate of H_2O_2 decomposition measured in the spectrophotometer at 240 nm for 1 min at 25°C (Cakmak and Marschner 1992). An extinction coefficient of 36 M^{-1} cm^{-1} was used to calculate CAT activity (Anderson et al. 1995). To determine GR activity, the reaction was started after the addition of the crude enzyme extract to a mixture containing 50 mM potassium phosphate (pH 7.8), 1 mM oxidized glutathione (GSSG), and 0.75 mM NADPH prepared in 0.5 mM Tris-HCl buffer (pH 7.5) according to Carlberg and Mannervik (1985). The decrease in absorbance was determined at 340 nm for 1 min at 30°C. The extinction coefficient of 6.22 mM^{-1} cm^{-1} was used to calculate GR activity (Foyer and Halliwell 1976). The activities of these enzymes were expressed on a protein basis, being the protein concentration determined according to Bradford (1976).

Data analysis

Data from urediniospores germination were subjected to analysis of variance (ANOVA), and means were compared by Tukey´s test ($P \leq 0.05$). For other variables and parameters, data were subjected to ANOVA and means for control and IR stimulus treatments, as well as for non-inoculated and inoculated plants, were compared by *F* test ($P \leq 0.05$). Before ANOVA, data were checked for normality and homogeneity of variance. The procedures described by Moore and Dixon (2015) were followed to combine the data from the variables and parameters evaluated from the repeated experiments. The Minitab Statistical software was used for the statistical analysis (Minitab, Inc., 2021). Data from all variables and parameters obtained from control and IR stimulus treatments for non-inoculated and inoculated plants at 15 dai were used for principal component analysis (PCA) using the software R (R Core Team, 2022).

Results

Analysis of variance

The effects of IR stimulus and control (water) treatments [named as products (P)] on urediniospores germination were analyzed by one-way ANOVA. The factor P was significant ($P < 0.001$) for the germination of urediniospores. The response of all variables and parameters to P, plant inoculation (PI), and the P × PI interaction was analyzed by a two-way ANOVA. The factors P and PI, as well as the P × PI interaction, were significant ($P \leq 0.05$) for most of the variables and parameters studied (Table 1).

Germination of urediniospores in vitro

The germinated urediniospores of *P. pachyrhizi* showed thin and shorter germ tubes when exposed to the rates of 2.5 and 5 mL/L of the IR stimulus compared to the rate of 1.25 mL/L of the IR stimulus and in the absence of IR stimulus (control treatment) (Fig. 1A). Urediniospores germination were inhibited by the IR stimulus at the rates of 10 and 20 mL/L compared to the control treatment (Fig. 1G). Urediniospores germination was significantly reduced by 22, 26, 19, and 25%, respectively, for the rates of 2.5, 5, 10, and 20 mL/L of IR stimulus compared to the control treatment (Fig. 1B).

Rust symptoms and severity, as well as AUDPC

Necrotic lesions containing many uredinia were abundant on the leaflets of plants from the control treatment in contrast to the leaflets of plants sprayed with the IR stimulus (Fig. 2A-B). Rust severity was significantly reduced by 27, 19, 23, 25, and 41%, respectively, at 7, 9, 11, 13, and 15 dai for plants sprayed with IR stimulus compared to plants from the control treatment (Fig. 2C). The AUDPC significantly decreased by 27% for IR stimulus-sprayed plants compared to plants from the control treatment (Fig. 2D).

Foliar concentrations of Ca and N

Foliar concentrations of Ca and N for non-inoculated plants were significantly higher (28 and 26%, respectively) for IR stimulus treatment compared to the control treatment (Fig. 3A and C). For inoculated plants, foliar concentrations of Ca and N were significantly higher (54 and 25%, respectively) for IR stimulus treatment compared to the control treatment (Fig. 3B and

D). There was no significant difference between non-inoculated and inoculated plants for foliar concentrations of Ca and N regardless of IR stimulus or control treatments (Fig. 3A-D).

Photosynthetic pigments concentration

For the control treatment, concentrations of Chl *a*+*b* (33, 23, and 60% at 7, 11, and 15, respectively) and carotenoids (18 and 54% at 7 and 15 dai, respectively) were significantly lower for inoculated plants in comparison to non-inoculated plants (Fig. 4A-D). For IR stimulus treatment, concentrations of Chl *a*+*b* and carotenoids (15 and 17%, respectively, at 11 dai) were significantly higher, while the concentrations of Chl *a*+*b* and carotenoids (27 and 35%, respectively, at 15 dai) were significantly lower for inoculated plants compared to non-inoculated plants (Fig. 4 A-D). The concentration of Chl *a*+*b* for non-inoculated plants was significantly lower by 13% at 11 dai for IR stimulus treatment compared to the control treatment (Fig. 4A). Concentration of carotenoids for non-inoculated plants was not affected by any of the treatments regardless of the evaluation time (Fig. 4C). For inoculated plants, concentrations of Chl *a*+*b* (31, 30, and 86% at 7, 11, and 15 dai, respectively) and carotenoids (16 and 36% at 11 and 15 dai, respectively) were significantly higher for IR stimulus treatment compared to the control treatment (Fig. 4B and D).

Histochemical detection of lipid peroxidation, membrane damage, H_2O_2, and $O_2^{\bullet-}$

The spray of IR stimulus did not cause any physiological perturbation to the leaflets of non-inoculated plants based on the absence of staining for lipid peroxidation, membrane damage, H_2O_2, and $O_2^{\bullet-}$ compared to the leaflets of plants from the control treatment (Fig. 5A-D). Lipid peroxidation, membrane damage, and depositions of H_2O_2 and $O_2^{\bullet-}$ (brown and blue colors, respectively) were less intense in the leaflets of plants sprayed with the IR stimulus in contrast to the leaflets of plants from the control treatment (Fig. 5A-D).

Concentrations of MDA, H_2O_2 and $O_2^{\bullet-}$

For control treatment, the concentrations of MDA (48, 71, 60, 19, and 121% at 1, 3, 5, 10, and 15 dai, respectively), H_2O_2 (29, 24, 40, 79, and 34% at 1, 3, 5, 10, and 15 dai, respectively), and $O_2^{\bullet-}$ (55, 147, 216, 56, and 182% at 1, 3, 5, 10, and 15 dai, respectively) were significantly higher for inoculated plants compared to non-inoculated plants (Fig. 6A-F). For IR stimulus treatment, the concentration of MDA was significantly higher by 24% at 1 dai and significantly lower by 31% at 3 dai for inoculated plants compared to non-inoculated plants. The concentration of H_2O_2 (0.8% at 3 dai) was significantly lower, while the concentration of $O_2^{\bullet-}$

(20, 34, and 112% at 1, 3, and 15 dai, respectively) was significantly higher for inoculated plants compared to non-inoculated plants (Fig. 6A-F).

For non-inoculated plants, the concentration of MDA was significantly higher by 18% at 5 dai for IR stimulus treatment compared to the control treatment (Fig. 6A). Concentrations of H_2O_2 and $O_2^{\bullet-}$ for non-inoculated plants were not affected by any of the treatments regardless of evaluation time (Fig. 6C and E). For inoculated plants, the concentrations of MDA (33, 58, 27, 28, and 45% at 1, 3, 5, 10, and 15, respectively), H_2O_2 (25, 24, 29, 23, and 26% at 1, 3, 5, 10, and 15 dai, respectively), and $O_2^{\bullet-}$ (37, 34, 29, 41, and 41% at 1, 3, 5, 10, and 15 dai, respectively) were significantly lower for IR stimulus treatment in comparison to the control treatment (Fig. 6B, D, and F).

Concentrations of TSP and LTGA derivatives

There was no significant change in TSP concentration for control treatment regardless of plant inoculation and evaluation time (Fig. 7A and B). The concentration of LTGA derivatives for control treatment was significantly lower by 28% at 15 dai for inoculated plants compared to non-inoculated plants (Fig. 7C and D). For IR stimulus treatment, the concentrations of TSP (30% at 1dai) and LTGA derivatives (66, 44, 52, and 61% at 1, 5, 10, and 15 dai, respectively) were significantly higher for inoculated plants in comparison to non-inoculated plants (Fig. 7A-D).

The treatments did not affect TSP and LTGA derivatives concentrations for non-inoculated plants regardless of evaluation time (Fig. 7A and C). Concentrations of TSP (41, 44, 51, and 33% at 1, 5, 10, and 15 dai, respectively) and LTGA derivatives (94, 44, 51, 30, and 82% at 1, 3, 5, 10, and 15 dai, respectively) for inoculated plants were significantly higher for IR stimulus treatment compared to the control treatment (Fig. 7B and D).

Activities of antioxidant enzymes

For control treatment, SOD (0.6, 12, and 2% at 1, 3, and 10 dai, respectively), APX (139, 114, and 93% at 1, 5, and 15 dai, respectively), CAT (61% at 15 dai), and GR (65% at 15 dai) activities were significantly higher while the activities of APX (34% at 10 dai), CAT (14% at 3 dai), and GR (84% at 10 dai) were significantly lower for inoculated plants compared to non-inoculated plants (Fig. 8A-H). For IR stimulus treatment, SOD (31, 51, 47, 109, and 99% at 1, 3, 5, 10, and 15 dai, respectively), APX (177, 7, 29, and 934% at 1, 3, 10, and 15 dai, respectively), CAT (40, 225, 156, 137, and 124% at 1, 3, 5, 10, and 15 dai, respectively), and

GR (42% at 3 dai) activities were significantly higher while the activity of GR (39.67% at 10 dai) was significantly lower for inoculated plants compared to non-inoculated plants (Fig. 8A-H).

The activity of SOD for non-inoculated plants was not affected by any of the treatments regardless of the evaluation time (Fig. 8A). The APX activity was significantly higher (80 and 101% at 1 and 5 dai, respectively) and significantly lower (34 and 65% at 10 and 15 dai, respectively) for IR stimulus treatment compared to the control treatment (Fig. 8C). The activities of CAT (4 and 31% at 3 and 15 dai, respectively) and GR (20% at 15 dai) were significantly higher for IR stimulus treatment compared to the control treatment (Fig. 8E and G). For inoculated plants, SOD (37, 34, 59, 122, and 154% at 1, 3, 5, 10, and 15 dai, respectively), APX (108, 27, 29, and 88% at 1, 3, 10, and 15 dai, respectively), CAT (89, 173, 101, 104, and 81% at 1, 3, 5, 10, and 15 dai, respectively), and GR (48 and 335% at 3 and 10 dai, respectively) activities were significantly higher for IR stimulus treatment in comparison to the control treatment (Fig. 8B, D, F, and H).

Activities of defense-related enzymes

For control treatment, GLU (101 and 98% at 3 and 10 dai, respectively), PPO (11% at 3 dai), and LOX (106, 36, and 39% at 3, 5, and 15 dai, respectively) activities were significantly higher while the activities of GLU (63% at 1 dai), PAL (51% at 3 dai), and PPO (12% at 15 dai) were significantly lower for inoculated plants compared to non-inoculated plants (Fig. 9C-K). For IR stimulus treatment, CHI (137, 35, 86, and 48% at 3, 5, 10, and 15 dai, respectively), GLU (300, 115, and 126% at 1, 3, and 10 dai, respectively), PAL (147, 188, 130, and 287% at 1, 5, 10, and 15 dai, respectively), POX (59, 126, 55, and 95% at 3, 5, 10, and 15 dai, respectively), PPO (94, 121, 41, 87, and 64% at 1, 3, 5, 10, and 15 dai, respectively), and LOX (143, 273, 124, 103, and 252% at 1, 3, 5, 10, and 15 dai, respectively) activities were significantly higher for inoculated plants in comparison to non-inoculated plants (Fig. 9A-K).

Activities of CHI, GLU, and PPO for non-inoculated plants were not affected by any of the treatments regardless of evaluation time (Fig. 9A, C, and G). The PAL activity was significantly lower by 14% at 3 dai, while PPO and LOX activities were significantly higher (24 and 20%, respectively, at 5 dai) for IR stimulus treatment compared to the control treatment (Fig. 9I and K). For inoculated plants, CHI (169, 36, and 48% at 3, 10, and 15 dai, respectively), GLU (190 and 78% at 1 and 10 dai, respectively), PAL (102, 97, 156, 123, and 223% at 1, 3, 5, 10, and 15 dai, respectively), POX (88, 78, 46, and 83% at 1, 5, 10, and 15 dai, respectively), PPO (39, 84, 68, and 103% at 1, 5, 10, and 15 dai, respectively), and LOX (108, 182, 99, 48,

and 158% at 1, 3, 5, 10, and 15 dai, respectively) activities were significantly higher for IR stimulus treatment compared to the control treatment (Fig. 9B, D, F, H, J, and L).

PCA analysis

Four clusters were generated (NI and I plants separately for control and IR stimulus treatments) based on the cluster analysis with complete linkage and Pearson distance. One principal component (PC) explained most of the data variation (PC1 = 50.2% and PC2 = 43.1%) (Fig. 10). The PC1 indicated positive scores for severity, AUDPC, Y(NO), Ca, N, LTGA derivatives, $O_2^{\bullet-}$, and activities of defense-related and antioxidative enzymes (SOD, APX, CAT, GR, CHI, GLU, PAL, POX, PPO, and LOX) while negative scores were obtained for Chl *a*+*b*, Car, TSP, MDA, and H_2O_2. For PC2, positive scores were obtained for Ca, N, Chl *a*+*b*, Car, LTGA derivatives, SOD, CHI, and PPO while negative scores occurred for severity, AUDPC, TSP, MDA, H_2O_2, $O_2^{\bullet-}$, APX, CAT, GR, GLU, PAL, POX, and LOX (Fig. 10).

Discussion

Considering the current scenario of global agriculture that needs to produce more food and fiber to feed a rapidly growing population (OECD/FAO, 2023), the growers will demand more efficient and sustainable practices. Therefore, using resistance inducers may become a remarkable option for the integrated management of diseases that cause great yield losses and affect the economy (Reglinski et al., 2023). The present study aimed to investigate the effect of applying an IR stimulus on the biochemical and physiological outcomes in the soybean-*P. pachyrhizi* interaction. Soybean plants sprayed with the IR stimulus showed reduced SR symptoms and less fungal colonization of leaf tissues (less cellular damage) biochemically supported by the lower MDA, H_2O_2, and $O_2^{\bullet-}$ concentrations. The IR stimulus investigated in the present study showed a direct effect against the germination of urediniospores of *P. pachyrhizi in vitro*. It is known that some IR stimuli such as azelaic acid, acibenzolar-S-methyl, hexanoic acid, compounds containing Ca, and a copper-polyphenolic compound can have a more robust and direct antifungal activity against pathogens *in vitro* (Paula et al. 2021; Rodrigues et al. 2023a,b). Interestingly, IR stimuli are efficient in boosting the resistance of soybean plants facing *P. pachyrhizi* infection despite being able to exert an antifungal activity (Langenbach et al. 2016; Paula et al. 2021; Rodrigues et al. 2023a,b; Siah et al. 2018).

Plants enhance their foliar content of nutrients after being sprayed with or growing in soil amended with compounds formulated with different forms and concentrations of nutrients (Cruz et al. 2020; Debona et al. 2015; Einhardt et al. 2020a; Fernández and Brown 2013; Hawerroth et al. 2023; Otolakoski et al. 2023; Picanço et al. 2021). Some crops (e.g., banana, basil, potato, rice, strawberry, and wheat) supplied with some compounds containing Ca and N, either through soil amendment or foliar spray, showed increased resistance against diseases (e.g., downy mildew, early blight, gray mold, leaf blast, and Banana Xanthomonas wilt) due to an increased foliar concentration of these two macronutrients (Abou-El-Hassan et al, 2020; Debona et al. 2017; Elad et al. 2021; Elmer 2023; Mandour et al. 2019; Reekie and Punja 2023; Wang et al. 2022). In the present study, the foliar spray of the IR stimulus significantly enhanced the foliar concentrations of Ca and N for non-infected or infected plants. An adequate N content in plant tissues directly affects the biosynthesis of photosynthetic pigments, considering the involvement of this macronutrient in the tetrapyrroles biosynthesis and in the function of some important cellular constituents (e.g., amino acids, hormones, phenolics, phytoalexins, and proteins) that play a major role in several biochemical processes (Elmer 2023). Furthermore, Ca contributes to the proper functioning of the photosynthetic apparatus since this

macronutrient is found in the chloroplasts and helps to maintain the stability and aggregation of chlorophylls in the antenna complex, regulates the stomata aperture as well as the electron transport and the ATP synthesis besides helping in the strengthening of the cell wall (Reekie and Punja 2023). In this regard, the higher foliar concentrations of Ca and N in IR stimulus-sprayed plants certainly contributed to preserving the concentration of Chl *a*+*b* in the diseased leaflets of IR stimulus-sprayed plants.

Pathogen infection negatively impairs the integrity of the photosynthetic apparatus of the plants by decreasing the concentration of photosynthetic pigments (Aucique-Pérez et al. 2014; Dias et al. 2018; Einhardt et al. 2020b; Rios et al. 2018 Silva et al. 2023; Silveira et al. 2015). The Chl *a*+*b* and carotenoids are intrinsically associated with photosynthesis for being responsible for light absorption and the successive energy transport to the centers of reaction where the photochemical phase of photosynthesis takes place (Taiz and Zeiger 2006). In the present study, lower photosynthetic pigments concentration due to great SR (e.g., intense coalescence of necrotic lesions and yellowing of leaf tissues) severity occurred for plants non-sprayed with the IR stimulus. In contrast, infected plants sprayed with the IR stimulus displayed enhanced concentration of photosynthetic pigments (Chl *a*+*b* at 7, 11, and 15 dai and carotenoid at 11 and 15 dai) that immensely helped to maintain the integrity of the photosynthetic apparatus. Some reports highlighted the positive role of IR stimulus spray in preserving the pool of photosynthetic pigments in leaf tissues of soybean plants infected with *P. pachyrhizi* (Einhardt et al. 2020b; Picanço et al. 2022; Rodrigues et al. 2023b).

During the infection process of pathogens, the stressed plant tissues accumulate reactive oxygen species (ROS) [e.g., H_2O_2, singlet oxygen ($^1O_2$), $O_2^{\bullet-}$, and hydroxyl radical (OH)] (Das and Roychoudhury 2014; Kaur et al. 2022). The excess of ROS produced causes the oxidative stress of cells with significant damage to nucleic acids, lipids, proteins, and some metabolites (Das and Roychoudhury 2014; Demidchik 2015; Farooq et al. 2019; Kaur et al. 2022; Mohammad et al. 2021; Segal and Wilson 2018; Wang et al.2019; Xie et al. 2019). In the present study, infected plants non-sprayed with the IR stimulus displayed enhanced concentrations of H_2O_2 and $O_2^{\bullet-}$, following histochemical confirmation, due to higher rust severity and intense damage in the infected leaf tissues. Histochemical analysis of soybean leaflets infected by *P. pachyrhizi* showed great depositions of H_2O_2 and $O_2^{\bullet-}$ (Einhardt et al. 2020b; Picanço et al. 2022; 2023; Rodrigues et al. 2023a,b). To scavenge the excess of ROS, an effective enzymatic system in the cell wall, symplast, and plasma membrane occurs in plant tissues infected by pathogens (Das and Roychoudhury 2014; Sharma et al. 2012; You and Chan 2015). Among the antioxidant enzymes, SOD converts $O_2^{\bullet-}$ to H_2O_2 and O_2, while CAT, POX,

and APX act in the reduction of the pool of H_2O_2 (Das and Roychoudhury 2014). The GR is also used to remove the excess of H_2O_2 by promoting the reduction of GSSG to GSH using NADPH as a reductant (Das and Roychoudhury 2014; Sharma et al. 2012). In the present study, infected plants sprayed with IR stimulus exhibited higher SOD, APX, CAT, and GR activities than non-sprayed infected plants. On top of that, the great activities of these enzymes contributed directly to keeping the lower concentrations of ROS in IR stimulus-sprayed plants infected by *P. pachyrhizi* and consequently attenuating the oxidative stress at the cellular level. Conversely, infected plants non-sprayed with the IR stimulus displayed lower activities of CAT, POX, APX, and GR during the time course evaluated, explaining the higher H_2O_2 and $O_2^{\bullet-}$ concentrations. In contrast to the present study findings, Rodrigues et al. (2023b) reported an increase in the POX, CAT, APX, and GR activities in soybean plants infected by *P. pachyrhizi* infection.

The pool of MDA is a great biochemical marker to measure the cellular damage due to lipids peroxidation caused by pathogen infection (Mittler 2002; Mohammadi et al. 2021). In the present study, the concentration of MDA was higher for infected plants non-sprayed with the IR stimulus in contrast to the infected plants sprayed with the IR stimulus, which biochemically confirms the less stress imposed by ROS in the lesser damaged infected leaf tissues. Picanço et al. (2022) reported a lower concentration of MDA in soybean leaves infected by *P. pachyrhizi* after being sprayed with a phosphite combined with free aminoacids.

It is well-established in the literature that plants can display diverse defense strategies of biochemical nature [e.g., production of soluble phenolics, flavonoids, and phytoalexins, deposition of papillae and lignin in the cell wall, and expression of genes coding for pathogenesis-related proteins (glucanases, chitinases, phenylalanine ammonia-lyase, peroxidase, poliphenoloxidade, and lipoxygenase)] (Durrant and Dong 2004; Kaur et al.2022; Sharma et al. 2011). The production of soluble phenolics and their subsequent use for lignin production following deposition in the plant cell wall requires higher PAL activity that catalyzes the deamination of L-phenylalanine to yield *trans*-cinnamic acid and other related phenolics in the phenylpropanoid pathway (Fortunato et al. 2015; Hossain et al. 2018; Kaur et al. 2022; Kumar et al. 2020). The colonization of soybean tissues by *P. pachyrhizi* is impaired by antimicrobial phenolics (Lygin et al. 2009). Furthermore, TSP and LTGA derivatives were able to restrict the colonization of plant tissues by pathogens of different lifestyles (Einhardt et al. 2020a; Fortunato et al. 2015; Kumar et al. 2020; Rodrigues et al. 2023a; Silveira et al. 2020). An increase in PAL activity in infected leaflet tissues of IR stimulus-sprayed plants during the time course evaluated is another piece of biochemical evidence for the potentiation of soybean

resistance gained by using this IR stimulus. In the present study, plants sprayed with IR stimulus showed increased POX and PPO activities at earlier and later stages of *P. pachyrhizi* infection. Higher activities of these enzymes can also be directly linked with an increased concentration of TSP and LTGA derivatives, considering their involvement in the polymerization of phenolics towards lignin production and the production of more toxic compounds such as the quinones (Gajewska and Sklodowska 2007; Lattanzio et al. 2006). As expected, TSP (at 1, 5,10, and 15 dai) and LTGA derivatives (at all evaluation times) concentrations were higher for infected leaflet tissues of IR stimulus-sprayed plants, reinforcing the interplay of PAL, POX, and PPO activities and phenolics production for the increased resistance of these plants. Considering the key role played by lignification of leaflet tissues of soybean plants to reduce SR symptoms (Lygin et al. 2009), the enhanced concentrations of TSP and LTGA derivatives played a pivotal role in the enhanced resistance of plants against *P. pachyrhizi* infection. Soybean plants infected by *P. pachyrhizi* also increased phenolics and lignin production in response to different IR stimuli (Paula et al. 2021; Picanço et al. 2021; 2022; Rodrigues et al. 2023a,b).

In plant tissues infected by fungal pathogens, CHI and GLU promote the hydrolysis of chitin and β-1,3-glucan, respectively, which will remarkably affect their colonization and further reproduction (Shetty et al. 2009). In the present study, CHI (at 3, 10, and 15 dai) and GLU (at 1 and 10 dai) activities were higher for infected plants sprayed with IR stimulus, confirming their importance to hamp the colonization of leaflet tissues by *P. pachyrhizi*. Interestingly, CHI and GLU are more important pathogenesis-related proteins in plants developing SAR (Durrant and Dong 2004). A faster increase in GLU activity was noticed in the leaflets of soybean plants supplied with nickel and infected by *P. pachyrhizi* with lower SR severity (Einhardt et al. 2020a). The oxidation of polyunsaturated fatty acids in plant tissues originates oxylipins through the action of LOX and the subsequent production of jasmonic acid that is involved in ISR (Kaur et al. 2022; Porta and Rocha-Sosa 2002; Vlot et al. 2021). Surprisingly, soybean plants displayed greater LOX activity regardless of being infected by *P. pachyrhizi*. For IR stimulus-sprayed plants, LOX activity was higher for non-inoculated plants (at 1, 3, and 5 dai) and at both earlier and advanced stages of *P. pachyrhizi* infection. This finding agrees with the study carried out by Rodrigues et al. (2023b) that reported up-regulation of *LOX* at 5 dai on leaflets of soybean plants sprayed with IR stimulus in response to *P. pachyrhizi* infection.

Based on the findings of the present study, it is possible to conclude that a calcium and nitrogen-polyphenolic compound triggered the defense of soybean plants against *P. pachyrhizi* infection. The reduced SR symptoms were a result of a better nutrition status (higher foliar

levels of N and Ca), less cellular damage, greater activities of defense enzymes along with more production of phenolics and lignin, and a robust antioxidative metabolism gained by spraying the soybean plants with the IR stimulus. Based on the PCA analysis, the cluster inoculated IR stimulus-sprayed plants were placed apart from other clusters (inoculated and non-inoculated plants for control treatment as well as non-inoculated IR stimulus treatment), indicating, therefore, the positive effect of the IR stimulus in the outcome of the variables and parameters deeply investigated in this study. Thinking about sustainable agriculture and the need for practical options for soybean rust management, the findings obtained in the present study encourage the possibility of using this IR stimulus to reduce the yield losses caused by SR and to reduce the excessive use of fungicides that increase the production cost and the serious risks imposed to humans and the environment.

References

Abou-El-Hassan S, Metwaly HA, Ali AM (2020) Efficiency of potassium and calcium compounds in gel formula to control early blight disease, improve productivity, and shelf life of potato. Egyptian Journal of Agricultural Research 98:154-168

Anderson LA, Johnson AK, Simms MD, Willingham TR (1995) Comparative analysis of catalases: spectral evidence against heme-bound water for the solution enzymes. FEBBS Letters 370:97-100

Aucique-Pérez CE, Rodrigues FA, Moreira WR, DaMatta FM (2014) Leaf gas exchange and chlorophyll *a* fluorescence in wheat plants supplied with silicon and infected with *Pyricularia oryzae*. Phytopathology 104:143-149

Awasthi JP, Saha B, Chowardhara B, Devi SS, Borgohain P, Panda SK (2018) Qualitative analysis of lipid peroxidation in plants under multiple stress through schiff's reagent: a histochemical approach. Bio-Protocol 8:2807-2807

Axelrod B, Cheesbrough TM, Laakso S (1981) Lipoxygenase from soybeans: EC 1.13. 11.12 Linoleate: oxygen oxidoreductase. In: Methods in Enzymology, vol. 71, pp. 441-451. Academic Press.

Beauchamp C, Fridovich I (1971) Superoxide dismutase: improved assays and an assay applicable to acrylamide gels. Analytical Biochemistry 44:276-287

Bradford MM (1976) A rapid and sensitive method for the quantitation of microgram quantities of protein utilizing the principle of protein-dye binding. Analytical Biochemistry 72:248-254

Cakmak I, Horst WJ (1991) Effect of aluminum on lipid peroxidation, superoxide dismutase, catalase, and peroxidase activities in root tips of soybean (*Glycine max*). Physiologia Plantarum 83:463-468

Cakmak I, Marschner H (1992) Magnesium deficiency and high light intensity enhance activities of superoxide dismutase, ascorbate peroxidase, and glutathione reductase in bean leaves. Plant Physiology 98:1222-1227

Carlberg I, Mannervik B (1985) Glutathione reductase. Methods in Enzymology 113:484-490

Chaitanya KSK, Naithani SC (1994) Role of superoxide lipid peroxidation and superoxide dismutase in membrane perturbation during loss of variability in seeds of *Shorea robusta*. New Phytologist 126:623-627

Chance B, Maehley AC (1955) Assay of catalases and peroxidases. Methods in Enzymology 2:764-775

Chen KI, Erh MH, Su NW, Liu WH, Chou CC, Cheng KC (2012) Soyfoods and soybean products: from traditional use to modern applications. Applied Microbiology and Biotechnology 96:9-22

Choudhary DK, Prakash A, Johri BN (2007) Induced systemic resistance (ISR) in plants: mechanism of action. Indian Journal of Microbiology 47:289-297

Cruz MFA, Pinto MO, Barros EG, Rodrigues FA (2020) Differential gene expression in soybean infected by *Phakopsora pachyrhizi* in response to acibenzolar-S-methyl, jasmonic acid and silicon. Journal of Phytopathology 168:571-580

Das K, Roychoudhury A (2014) Reactive oxygen species (ROS) and response of antioxidants as ROS-scavengers during environmental stress in plants. Frontiers in Environmental Science 2:53

Debona D, Cruz MF, Rodrigues FA (2017) Calcium-triggered accumulation of defense-related transcripts enhances wheat resistance to leaf blast. Tropical Plant Pathology 42:309-314

Debona D, Rodrigues FA, Rios JA, Martins SCV, Pereira LF, DaMatta FM (2014) Limitations to photosynthesis in leaves of wheat plants infected by *Pyricularia oryzae*. Phytopathology 104:34-39

Demidchik V (2015) Mechanisms of oxidative stress in plants: from classical chemistry to cell biology. Environmental and Experimental Botany 109:212-228

Dias CS, Araujo L, Chaves JAA, DaMatta FM, Rodrigues FA (2018) Water relation, leaf gas exchange and chlorophyll *a* fluorescence imaging of soybean leaves infected with *Colletotrichum truncatum*. Plant Physiology and Biochemistry 127:119-128

Dixon RA (1986) The phytoalexin response: elicitation, signaling and control of host gene expression. Biological Reviews 61:239-291

Durrant WE, Dong X (2004) Systemic acquired resistance. Annual Review of Phytopathology 42:185-209

Einhardt AM, Ferreira S, Hawerroth C, Valadares SV, Rodrigues FA (2020) Nickel potentiates soybean resistance against infection by *Phakopsora pachyrhizi*. Plant Pathology 69:849-859

Einhardt AM, Ferreira S, Souza GM, Mochko AC, Rodrigues FA (2020) Cellular oxidative damage and impairment on the photosynthetic apparatus caused by Asian soybean rust on soybeans are alleviated by nickel. Acta Physiologiae Plantarum 42:1-13

Elad Y, Kleinman Z, Nisan Z, Rav-David D, Yermiyahu U (2021) Effects of calcium, magnesium and potassium on sweet basil downy mildew (*Peronospora belbahrii*). Agronomy 11:688

Elmer WH (2023) Nitrogen and plant disease. In: Datnoff LE, Elmer WH, Rodrigues FA (Eds.) Mineral and Plant Nutrition. The American Phytopathological Society, St. Paul. pp. 47-74

Fagundes-Nacarath IRF, Debona D, Brás VV, Silveira PR, Rodrigues FA (2018) Phosphites attenuate *Sclerotinia sclerotiorum*-induced physiological impairments in common bean. Acta Physiologiae Plantarum 40:1-14

Farooq MA, Niazi AK, Akhtar J, Farooq M, Souri Z, Karimi N, Rengel Z (2019) Acquiring control: The evolution of ROS-Induced oxidative stress and redox signaling pathways in plant stress responses. Plant Physiology and Biochemistry 141:353-369

Fortunato AA, Debona D, Bernardeli AM, Rodrigues FA (2015) Defence-related enzymes in soybean resistance to target spot. Journal of Phytopathology 163:731-742

Foyer CH, Halliwell B (1976) The presence of glutathione and glutathione reductase in chloroplasts: a proposed role in ascorbic acid metabolism. Planta 133:21-25

Franceschi VT, Alves KS, Mazaro SM, Godoy CV, Duarte HSS, Ponte EMD (2019) A new standard diagram set for assessment of severity of soybean rust improves accuracy of estimates and optimizes resource use. Plant Pathology 69:495-505

Fridovich I (1972) Superoxide radical and superoxide dismutase. Accounts of Chemical Research 5:321-326

Gajewska E, Skłodowska M (2007) Effect of nickel on ROS content and antioxidative enzyme activities in wheat leaves. Biometals 20:27-36

Giannopoilitis CN, Ries SK (1977) Superoxide dismutases: purification and quantitative relationship with water soluble protein in seedlings. Plant Physiology 59:315-318

Glazebrook J (2005) Contrasting mechanisms of defense against biotrophic and necrotrophic pathogens. Annual Review of Phytopathology 43:205-227

Goellner K, Loehrer M, Langenbach C, Conrath UWE, Koch E, Schaffrath U (2010) *Phakopsora pachyrhizi*, the causal agent of Asian soybean rust. Molecular Plant Pathology 11:169-177

Guo Y, Liu L, Bi Y (2007) Use of silicon oxide and sodium silicate for controlling *Trichothecium roseum* postharvest rot in Chine cantaloupe (*Cucumis melo* L.). International Journal of Food Science Technology 42:1012-1018

Hammerschmidt R (2009) Systemic acquired resistance. Advances in Botanical Research 51:173-222

Harman GE, Hayes CK, Lorito M, Broadway RM, Di Pietro A, Peterbauer C, Tronsmo A (1993) Chitinolytic enzymes of *Trichoderma harzianum*, purification of chitobiosidase and endochitinase. Phytopathology 83:313-318

Hawerroth C, Einhardt AM, Fontes BA, Brás VV, Valadares SV, Rodrigues FA (2023) Nickel enhances rice resistance against *Bipolaris oryzae* infection. Plant and Soil (in press)

Heath RL, Packer L (1968) Photoperoxidation in isolated chloroplasts I. Kinetics and stoichiometry of fatty acid peroxidation. Archives of Biochemistry and Biophysics 125:189-198

Hossain Z, Pillai BVS, Gruber MY, Yu M, Amyot L, Hannoufa A (2018) Transcriptome profiling of *Brassica napus* stem sections in relation to differences in lignin content. BMC Genomics 19:1-16

Kar M, Mishra D (1976) Catalase, peroxidase, and polyphenoloxidase activities during rice leaf senescence. Plant Physiology 57:315-319

Kato M, Soares RM (2022) Field trials of a *Rpp*-pyramided line confirm the synergistic effect of multiple gene resistance to Asian soybean rust (*Phakopsora pachyrhizi*). Tropical Plant Pathology 47:222-232

Kaur S, Samota MH, Choudhary M, Choudhary M, Pandey AK, Sharma A, Thakur J (2022) How do plants defend themselves against pathogens - Biochemical mechanisms and genetic interventions. Physiology and Molecular Biology of Plants 28:485-504

Kesel J, Conrath U, Flors V, Luna E, Mageroy MH, Mauch-Mani B, Pastor V, Pozo MJ, Pieterse CMJ, Ton J, Kyndt T (2021) The induced resistance lexicon: do's and don'ts. Trends in Plant Science 26:685-691

Kessmann H, Staub T, Ligon JIM, Oostendorp M, Ryals J (1994) Activation of systemic acquired disease resistance in plants. European Journal of Plant Pathology 100:359-369

Kumar A, Singh S, Gaurav AK, Srivastava S, Verma JP (2020) Plant growth-promoting bacteria: biological tools for the mitigation of salinity stress in plants. Frontiers in Microbiology 11:1216

Lamb C, Dixon RA (1997) The oxidative burst in plant disease resistance. Annual Review of Plant Biology 48:251-275

Langenbach C, Campe R, Beyer SF, Mueller AN, Conrath U (2016) Fighting Asian soybean rust. Frontiers in Plant Science 7:797

Lattanzio V, Lattanzio VM, Cardinali A (2006) Role of phenolics in the resistance mechanisms of plants against fungal pathogens and insects. Phytochemistry: Advances in Research 661:23-67

Lever M (1972) A new reaction for colorimetric determination of carbohydrates. Analytical Biochemistry 47:273-279

Llorens E, García-Agustín P, Lapeña L (2017) Advances in induced resistance by natural compounds: towards new options for woody crop protection. Scientia Agricola 74:90-100

Lorenzetti E, Stangarlin JR, Kuhn OI, Portz RL (2018) Indução de resistência à *Macrophomina phaseolina* em soja tratada com extrato de alecrim. Summa Phytopathologica 44:45-50

Lygin AV, Li S, Vittal R, Widholm JM, Hartman GL, Lozovaya VV (2009) The importance of phenolic metabolism to limit the growth of *Phakopsora pachyrhizi*. Phytopathology 99:1412-1420

Lyon G (2007) Agents that can elicit induced resistance. In: Walters D, Newton A, Lyon G (Eds). Induced resistance for plant defense: A sustainable approach to crop protection. Blackwell Publishing. pp. 9-23

Mandour MA, Metwaly HA, Ali AM (2019) Effect of foliar spray with amino acids, citric acid, some calcium compounds and mono-potassium phosphate on productivity, storability and controlling gray mould of strawberry fruits under sandy soil conditions. Zagazig Journal of Agricultural Research 46:985-997

Mesquita GL, Tanaka FAO, Zambrosi FCB, Chapola R, Cursi D, Habermann G, Massola Junior NS, Ferreira VP, Gaziola SA, Azevedo RA (2019) Foliar application of manganese increases sugarcane resistance to orange rust. Plant Pathology 68:1296-1307

Mittler R (2002) Oxidative stress, antioxidants and stress tolerance. Trends in Plant Science 7:405-410

Mohammadi MA, Cheng Y, Aslam M, Jakada BH, Wai MH, Ye K, Qin Y (2021) ROS and oxidative response systems in plants under biotic and abiotic stresses: revisiting the crucial role of phosphite triggered plants defense response. Frontiers in Microbiology 12:631318

Moore KJ, Dixon PM (2015) Analysis of combined experiments revisited. Agronomy Journal 107:763-771

Mueller TA, Miles MR, Morel W, Marois JJ, Wright DL, Kemerout RC, Levy C, Hartman GL (2009) Effect of fungicide and timing of application on soybean rust severity and yield. Plant Disease 93:243-248

Nakano Y, Asada K (1981) Hydrogen peroxide is scavenged by ascorbate-specific peroxidase in spinach chloroplasts. Plant and Cell Physiology 22:867-880

OECD/FAO (2023), OECD-FAO Agricultural Outlook 2023-2032, OECD Publishing, Paris. Available at: https://doi.org/10.1787/08801ab7-en. Accessed on September 25, 2023

Otolakoski MG, Viegas BG, Bagio BZ, Blum MMC, Suzana-Milan CS, Huzar-Novakowiski J (2023) Reduction of the severity of Asian soybean rust with foliar application of silicon dioxide. Crop Protection 173:106387

Paula S, Holz S, Souza DHG, Pascholati SF (2021) Potential of resistance inducers for soybean rust management. Canadian Journal of Plant Pathology 43:298-307

Picanço BBM, Ferreira S, Fontes BA, Oliveira LM, Silva BN, Einhardt AM, Rodrigues FA (2021) Soybean resistance to *Phakopsora pachyrhizi* infection is barely potentiated by boron. Physiological and Molecular Plant Pathology 115:101668

Picanço BB, Silva BN, Rodrigues FA (2022) Potentiation of soybean resistance against *Phakopsora pachyrhizi* infection using phosphite combined with free amino acids. Plant Pathology 71:1496-1510

Picanço BB, Silva BN, Rodrigues FA (2023) Soybean leaf age influences the infection process of *Phakopsora pachyrhizi*. Physiological and Molecular Plant Pathology 102069

Pieterse CM, Van Pelt JA, Ton J, Parchmann S, Mueller MJ, Buchala AJ, Van Loon LC (2000) Rhizobacteria-mediated induced systemic resistance (ISR) in Arabidopsis requires sensitivity to jasmonate and ethylene but is not accompanied by an increase in their production. Physiological and Molecular Plant Pathology 57:123-134

Pieterse CM, Van Loon LC (2007) Signalling cascades involved in induced resistance. Induced resistance for plant defence: a sustainable approach to crop protection 65-88

Porta H, Rocha-Sosa M (2002) Plant lipoxygenases. Physiological and molecular features. Plant Physiology 130:15-21

Reekie H, Punja ZK (2023) Calcium and plant disease. In: Datnoff LE, Elmer WH, Rodrigues FA (Eds.) Mineral and Plant Nutrition. The American Phytopathological Society, St. Paul. pp. 141-165

Reglinski T, Havis N, Rees HJ, de Jong H (2023) The practical role of induced resistance for crop protection. Phytopathology 113:719-731

Rios VS, Rios JA, Aucique-Pérez CE, Silveira PR, Barros AV, Rodrigues FA (2018) Leaf gas exchange and chlorophyll *a* fluorescence in soybean leaves infected by *Phakopsora pachyrhizi*. Journal of Phytopathology 166:75-85

Rodrigues FCT, Araujo MUP, Silva BN, Fontes BA, Rodrigues FA (2023) A copper-polyphenolic compound as an alternative for the control of Asian soybean rust. Tropical Plant Pathology 48:469-483

Rodrigues FCT, Silveira PR, Cacique IS, Oliveira LM, Rodrigues FA (2023) Azelaic and hexanoic acids-inducing resistance in soybean against *Phakopsora pachyrhizi* infection. Plant Pathology 72:1034-1047

Segal LM, Wilson RA (2018) Reactive oxygen species metabolism and plant-fungal interactions. Fungal Genetics and Biology 110:1-9

Shah J, Zeier J (2013) Long-distance communication and signal amplification in systemic acquired resistance. Frontiers in Plant Science 4:30

Sharma P, Jha AB, Dubey RS, Pessarakli M (2012) Reactive oxygen species, oxidative damage, and antioxidative defense mechanism in plants under stressful conditions. Journal of Botany

Sharma N, Sharma KP, Gaur RK, Gupta VK (2011) Role of chitinase in plant defense. Asian Journal of Biochemistry 6:29-37

Shaner G, Finney RE (1977) The effect of nitrogen fertilization on the expression of slow-mildewing resistance in Knox wheat. Phytopathology 67:1051-1056

Shetty NP, Jensen JD, Knudsen A, Finnie C, Geshi N, Blennow A, Jørgensen HJL (2009) Effects of β-1,3-glucan from *Septoria tritici* on structural defence responses in wheat. Journal of Experimental Botany 60:4287-4300

Siah A, Magnin-Robert M, Randoux B, Choma C, Rivière C, Halama P, Reignault P (2018) Natural agents inducing plant resistance against pests and diseases. Natural Antimicrobial Agents 121-159

Silva BN, Picanço BBM, Hawerroth C, Silva LC, Rodrigues FA (2022) Physiological and biochemical insights into induced resistance on tomato against septoria leaf spot by a phosphite combined with free amino acids. Physiological and Molecular Plant Pathology 120:101854

Silveira PR, Nascimento KJT, Andrade CCL, Bispo WMS, Oliveira JR, Rodrigues FA (2015) Physiological changes in tomato leaves arising from *Xanthomonas gardneri* infection. Physiological and Molecular Plant Pathology 92:130-138

Silveira PR, Aucique-Pérez CE, Cruz MFA, Rodrigues FA (2021) Biochemical and physiological changes in maize plants supplied with silicon and infected by *Exserohilum turcicum*. Journal of Phytopathology 169:393-408

Taiz L, Zeiger E (2006) Secondary metabolites and plant defense. Plant Physiology 4:315-344

Tatagiba SD, Rodrigues FA, Filippi MCC, Silva GB, Silva LC (2014) Physiological responses of rice plants supplied with silicon to *Monographella albescens* infection. Journal of Phytopathology 162:596-606

Tistama R, Mawaddah PAS, Ade-Fiprinil LUBIS, Junaidi J (2019) Physiological status of high and low metabolism *Hevea* clones in the difference stage of tapping panel dryness. Biodiversitas Journal of Biological Diversit 20(1)

Van Loon LC (1997) Induced resistance in plants and the role of pathogenesis-related proteins. European Journal of Plant Pathology 103:753-765

Velikova V, Yordanov I, Edreva A (2000) Oxidative stress and some antioxidant systems in acid rain-treated bean plants: Protective role of exogenous polyamines. Plant Science 151:59-66

Vlot AC, Sales JH, Lenk M, Bauer K, Brambilla A, Sommer A, Chen Y, Wenig M, Nayem S (2021) Systemic propagation of immunity in plants. New Phytologist 229:1234-1250

Walters DR (2010) Induced resistance: destined to remain on the sidelines of crop protection? Phytoparasitica 38:1-4

Wang Y, Ji D, Chen T, Li B, Zhang Z, Qin G, Tian S (2019) Production, signaling, and scavenging mechanisms of reactive oxygen species in fruit–pathogen interactions. International Journal of Molecular Sciences 20:2994

Wang G, Wang J, Han X, Chen R, Xue X (2022) Effects of spraying calcium fertilizer on photosynthesis, mineral content, sugar-acid metabolism and fruit quality of Fuji apples. Agronomy 12: 2563

Xie X, He Z, Chen N, Tang Z, Wang Q, Cai Y (2019) The roles of environmental factors in regulation of oxidative stress in plant. BioMed Research International Article ID 9732325

You J, Chan Z (2015) ROS regulation during abiotic stress responses in crop plants. Frontiers in Plant Science 6:1092

Zeier J (2021) Metabolic regulation of systemic acquired resistance. Current Opinion in Plant Biology 62:102050

Tables and Figures

Table 1. Analysis of variance for the effects of products (P), plant inoculation (PI), and the interaction P × PI for urediniospores germination (UG), soybean rust (SR) severity, area under disease progress curve (AUDPC), foliar concentrations of calcium (Ca) and nitrogen (N), concentrations of total chlorophyll *a*+*b* (Chl *a*+*b*), carotenoids (Car), malondialdehyde (MDA), hydrogen peroxide (H_2O_2), superoxide anion radical ($O_2^{\bullet-}$), total soluble phenolics (TSP), and lignin-thioglycolic acid (LTGA) derivatives as well as the activities of defense [chitinase (CHI), *β*-1,3-glucanase (GLU), phenylalanine ammonia-lyase (PAL), peroxidase (POX), polyphenoloxidase (PPO), and lipoxygenase (LOX)] and antioxidant [superoxide dismutase (SOD), ascorbate peroxidase (APX), catalase (CAT), and glutathione reductase (GR)] enzymes.

Variables/Parameters	IR stimulus	PI	IR stimulus × PI
UG	**<0.001**	-	-
SR severity	**<0.001**	-	-
AUDPC	**<0.001**	-	-
Ca	**<0.001**	0.219	0.099
N	**<0.001**	0.648	0.058
Chl *a*+*b*	**0.011**	**<0.001**	**<0.001**
Car	0.422	**<0.001**	0.011
MDA	**<0.001**	**<0.001**	**<0.001**
H_2O_2	**<0.001**	**<0.001**	**<0.001**
$O_2^{\bullet-}$	**0.012**	**<0.001**	0.072
TSP	**<0.001**	**0.044**	**<0.001**
LTGA derivatives	**<0.001**	**<0.001**	**<0.001**
CHI	0.091	0.324	**<0.001**
GLU	**0.035**	**<0.001**	0.056
PAL	**<0.001**	**<0.001**	**<0.001**
POX	**<0.001**	**<0.001**	**<0.001**
PPO	**<0.001**	**<0.001**	**<0.001**
LOX	**0.018**	**<0.001**	**0.030**
SOD	**<0.001**	**<0.001**	**<0.001**
APX	0.652	**<0.001**	0.548

CAT	**<0.001**	**<0.001**	**0.003**
GR	**0.011**	0.164	0.233

Bold values are significant at $P \leq 0.05$.

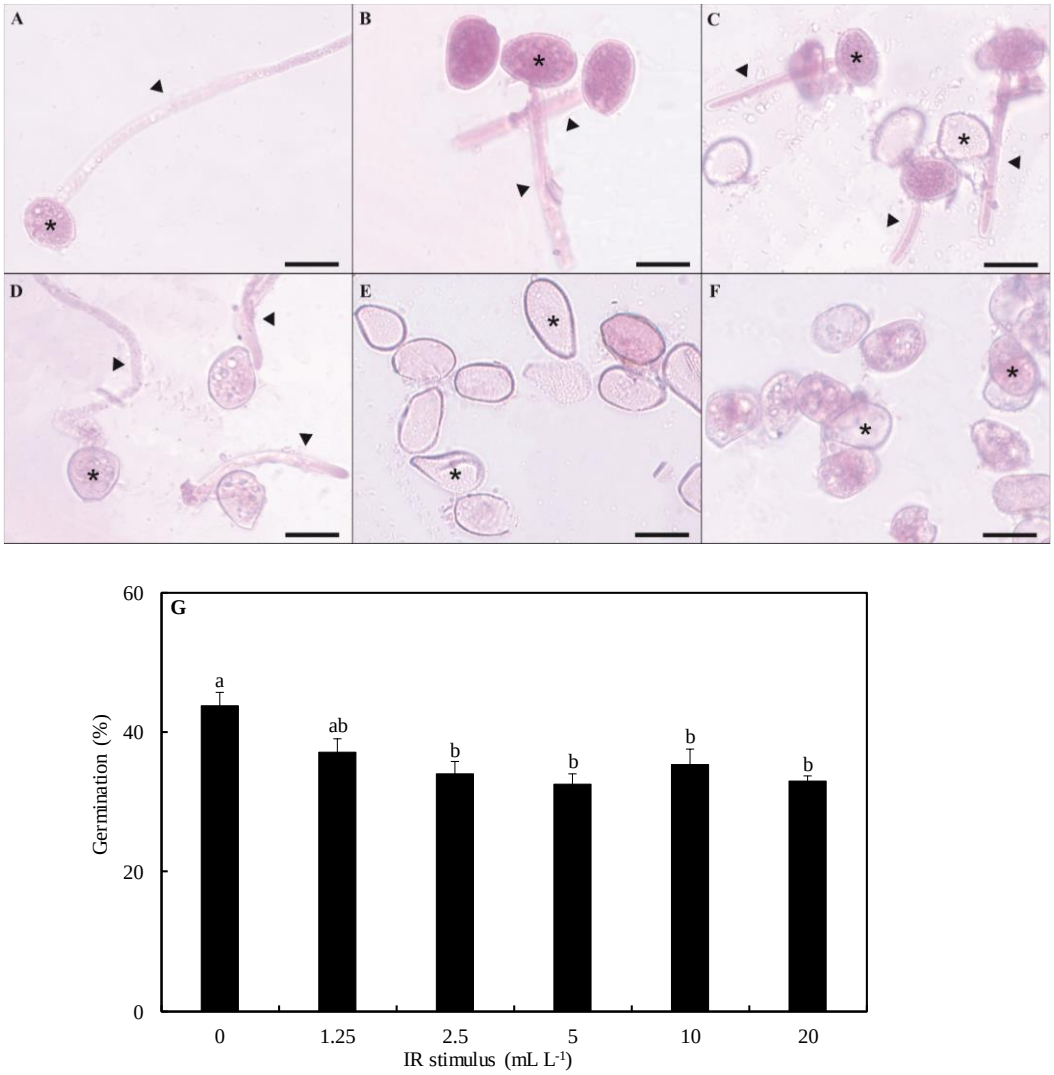

Figure 1. Aspects of the germination of *Phakopsora pachyrhizi* urediniospores in glass slides containing different rates of induced resistance (IR) stimulus (1.25, 2.5, 5, 10, and 20 mL L^{-1}, respectively, to B, C, D, E, and F). Control treatment corresponded to urediniospores suspension without IR stimulus (A). Scale bars = 25 µm. Urediniospore germination of *P. pachyrhizi* in Petri dishes containing agar-agar medium non-amended (control) or amended with different rates of IR stimulus. For each evaluation time, means from each treatment followed by different letters are significantly different ($P \leq 0.05$) according to Tukey's test. Bars represent the standard error of the means. Germ tube (▼) and urediniospores (*).

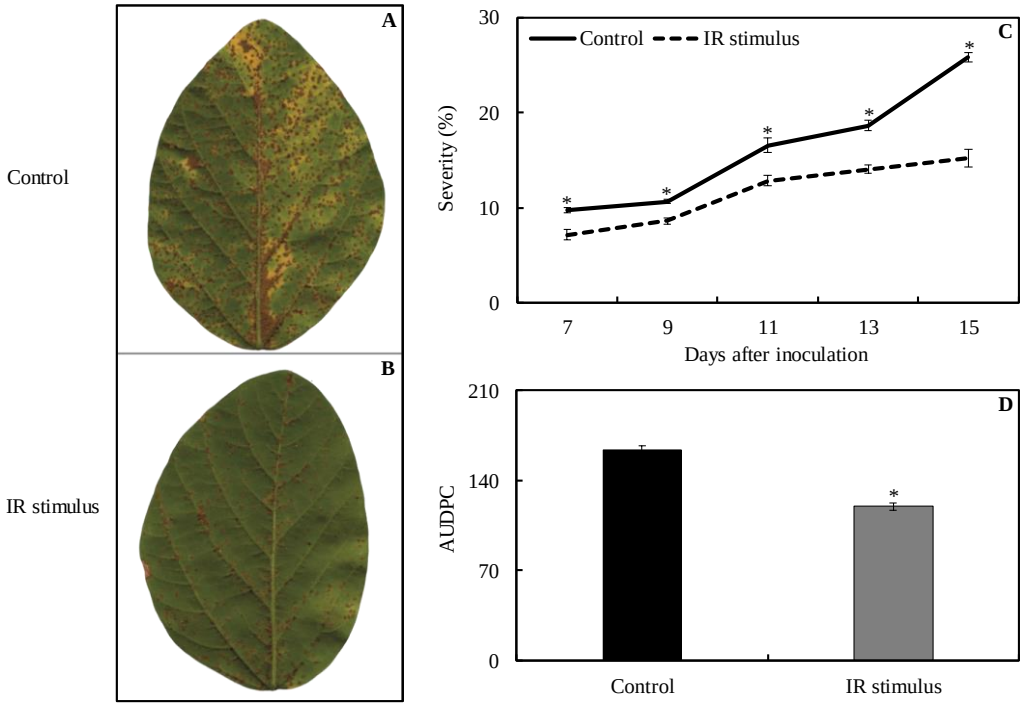

Figure 2. Symptoms (chlorosis and necrosis) (A and B) and severity (C) of soybean rust as well as area under disease progress curve (AUDPC) (D) for soybean plants sprayed with water (control) or with the induced resistance (IR) stimulus. Means for control and IR stimulus treatments, at each evaluation time (C), followed by an asterisk (*) or between these treatments followed by * (D) are significantly different ($P \leq 0.05$) according to the *F* test. Bars represent the standard error of the means. Data are from 15 days after inoculation of soybean plants with *Phakopsora pachyrhizi*.

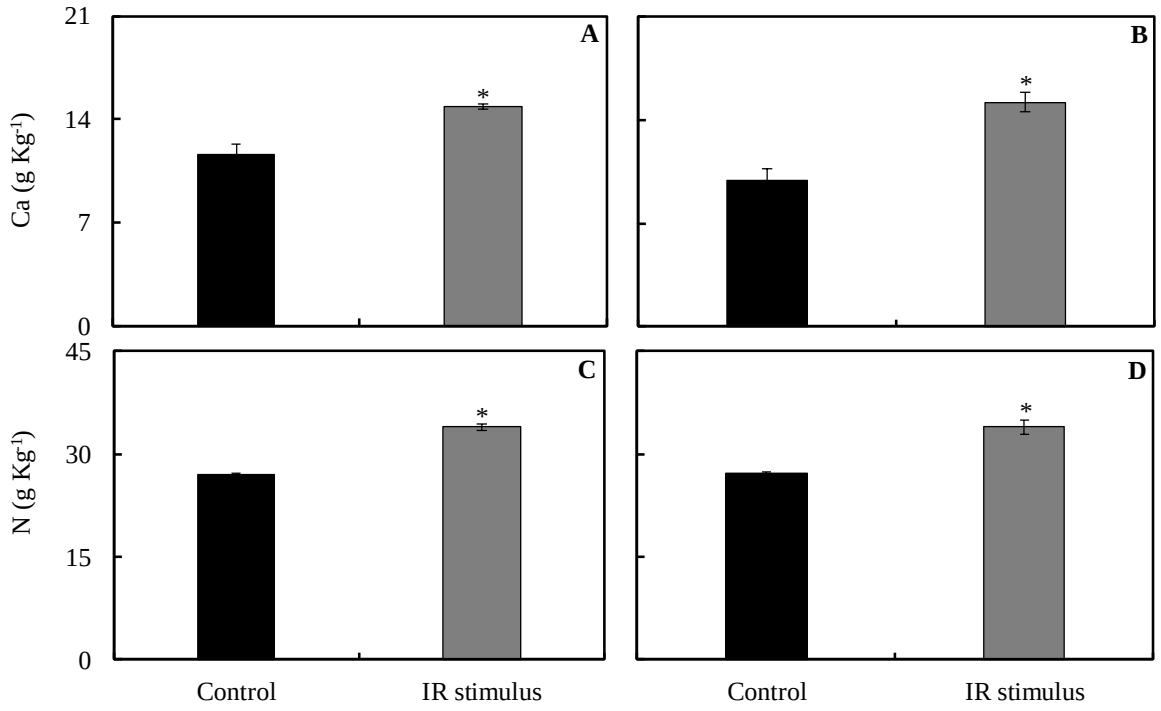

Figure 3. Foliar concentrations of calcium (Ca) and nitrogen (N) for soybean plants non-inoculated (NI) (A and C) or inoculated (I) (B and D) with *Phakopsora pachyrhizi* and sprayed with water (control) or with induced resistance (IR) stimulus. Means for control and IR stimulus treatments followed by an asterisk (*) and means for NI and I plants followed by an inverted triangle (▼) are significantly different ($P \leq 0.05$) according to the *F* test. Bars represent the standard error of the means.

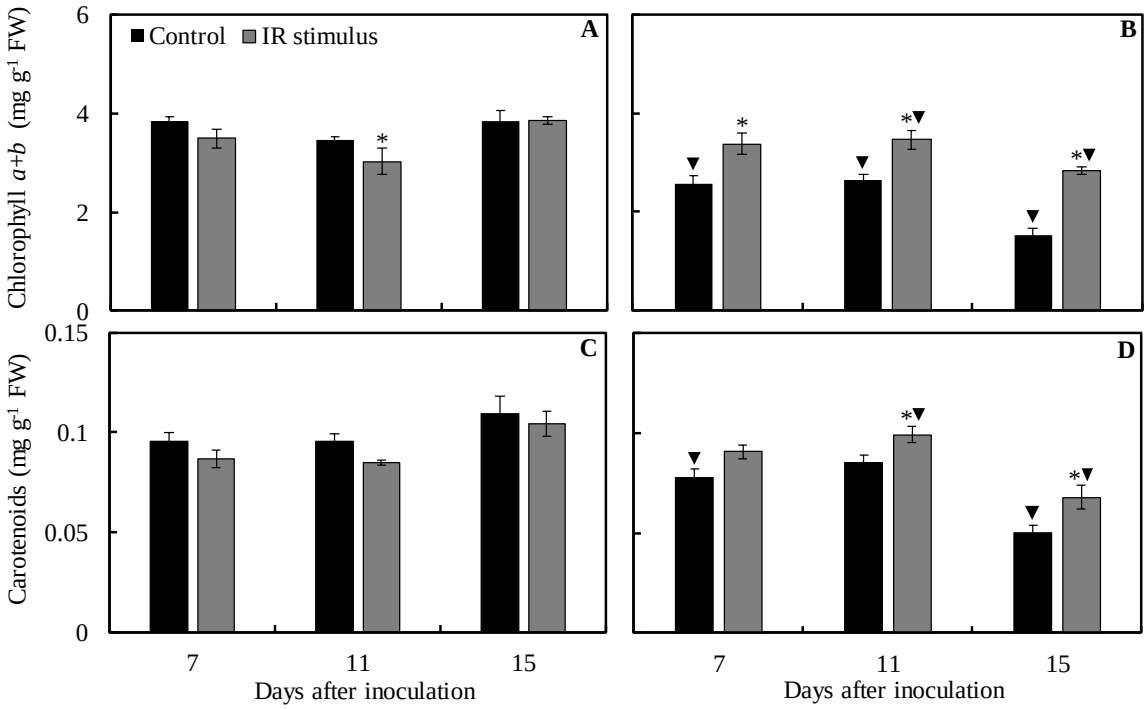

Figure 4. Concentrations of chlorophyll *a*+*b* (Chl *a*+*b*) (A and B) and carotenoids (C and D) determined in the leaflets of soybean plants sprayed with water (control) or with induced resistance (IR) stimulus and non-inoculated (NI) (A and C) or inoculated (I) (B and D) with *Phakopsora pachyrhizi*. Means for control and induced resistance (IR) stimulus treatments followed by an asterisk (*) and means from for NI and I plants followed by an inverted triangle (▼), at each evaluation time, are significantly different ($P \leq 0.05$) according to the *F* test. Bars represent the standard error of the means. FW = fresh weight.

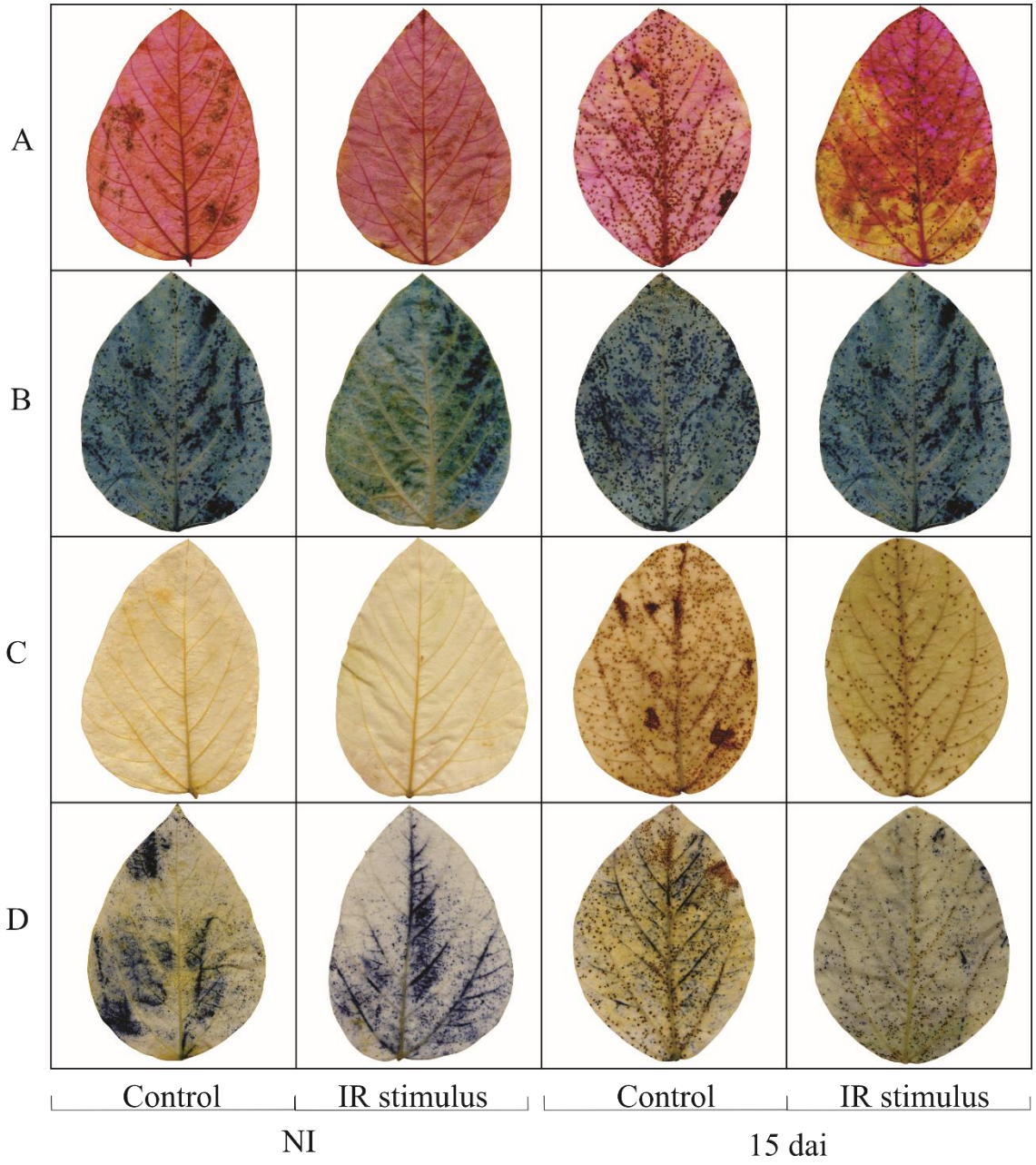

Figure 5. Histochemical detection of lipid peroxidation (A), membrane damage (B), hydrogen peroxide (C), and superoxide anion radical (D) on the leaflets of soybean plants non-inoculated (NI) or at 15 days after inoculation (dai) with *Phakopsora pachyrhizi* that were previously sprayed with water (control) or with the induced resistance (IR) stimulus.

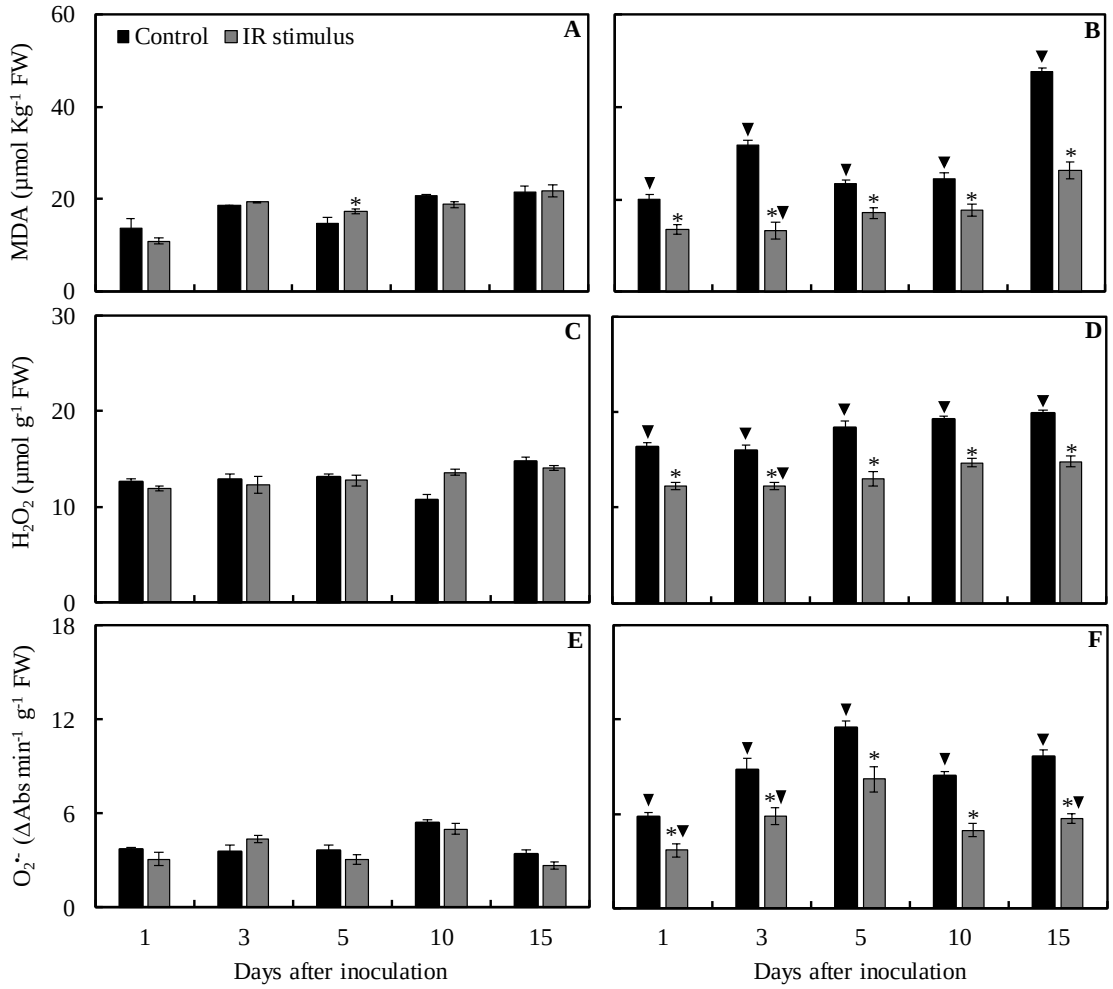

Figure 6. Concentrations of malondialdehyde (MDA) (A and B), hydrogen peroxide (H_2O_2) (C and D), and superoxide anion radical ($O_2^{\bullet-}$) (E and F) determined in the leaflets of soybean plants sprayed with water (control) or with induced resistance (IR) stimulus and non-inoculated (NI) (A, C, and E) or inoculated (I) (B, D, and F) with *Phakopsora pachyrhizi*. Means for control and IR stimulus treatments followed by an asterisk (*) and means for NI and I plants followed by an inverted triangle (▼), at each evaluation time, are significantly different ($P \leq 0.05$) according to the *F* test. Bars represent the standard error of the means. FW = fresh weight.

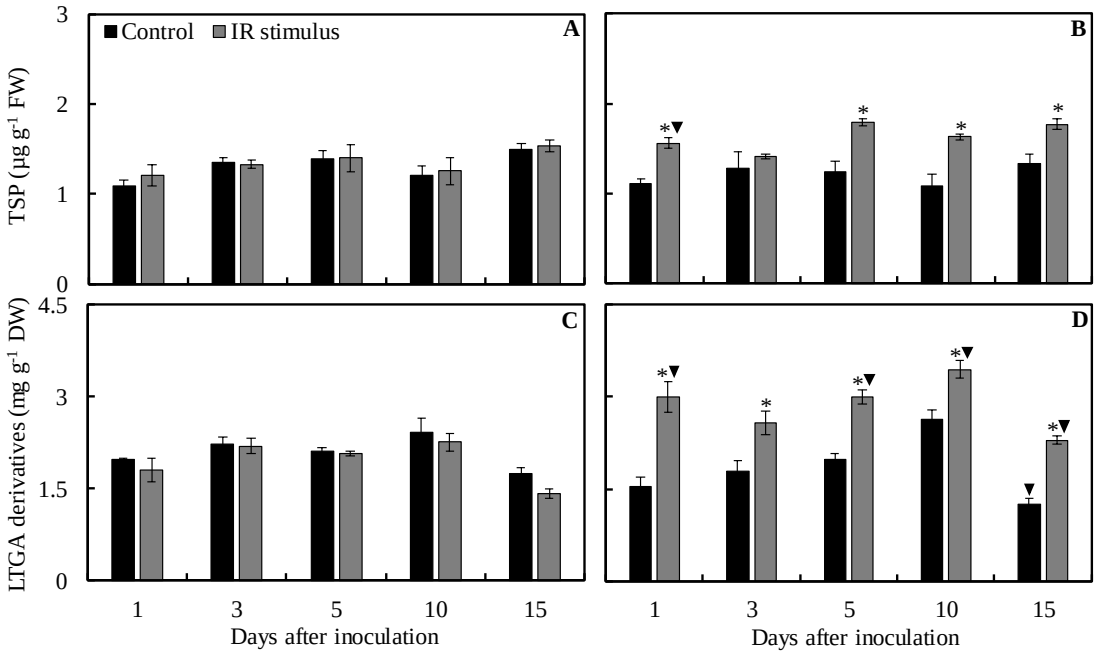

Figure 7. Concentrations of total soluble phenolics (TSP) and lignin-thioglycolic acid (LTGA) derivatives determined in the leaflets of soybean plants sprayed with water (control) or with induced resistance (IR) stimulus and non-inoculated (NI) (A and C) or inoculated (I) (B and D) with *Phakopsora pachyrhizi*. Means for control and IR stimulus treatments followed by an asterisk (*) and means for NI and I plants followed by an inverted triangle (▼), at each evaluation time, are significantly different ($P \leq 0.05$) according to the *F* test. Bars represent the standard error of the means. FW and DW = fresh weight and dry weight, respectively.

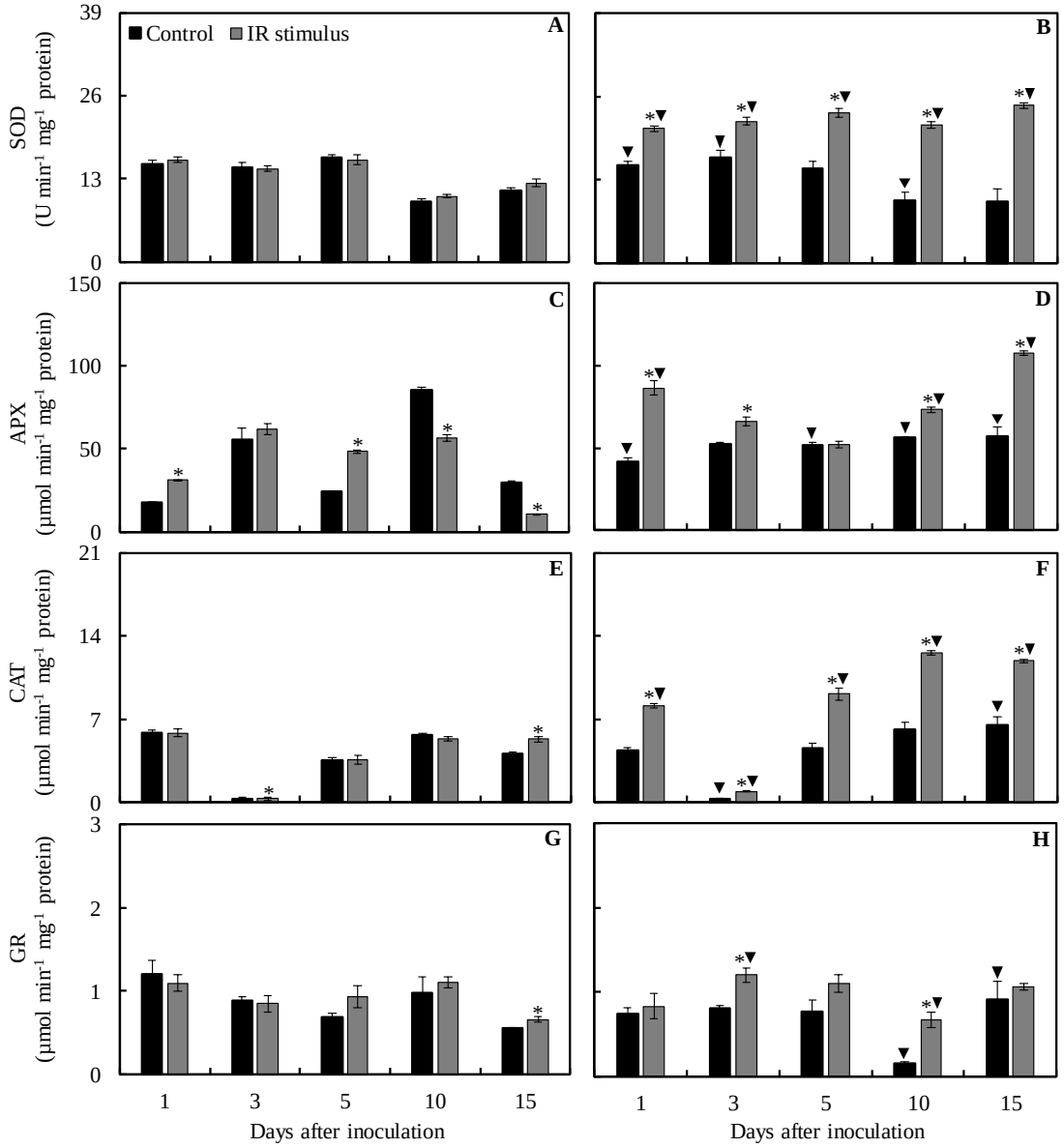

Figure 8. Activities of superoxide dismutase (SOD) (A and B), ascorbate peroxidase (APX) (C and D), catalase (CAT) (E and F), and glutathione reductase (GR) (G and H) determined on the leaflets of soybean plants non-inoculated (NI) (A, C, E, and G) or inoculated (I) (B, D, F, and H) with *Phakopsora pachyrhizi* and sprayed with water (control) or with induced resistance (IR) stimulus. Means for control and IR stimulus treatments followed by an asterisk (*) and means for NI and I plants followed by an inverted triangle (▼), at each evaluation time, are significantly different ($P \leq 0.05$) according to the *F* test. Bars represent the standard error of the means.

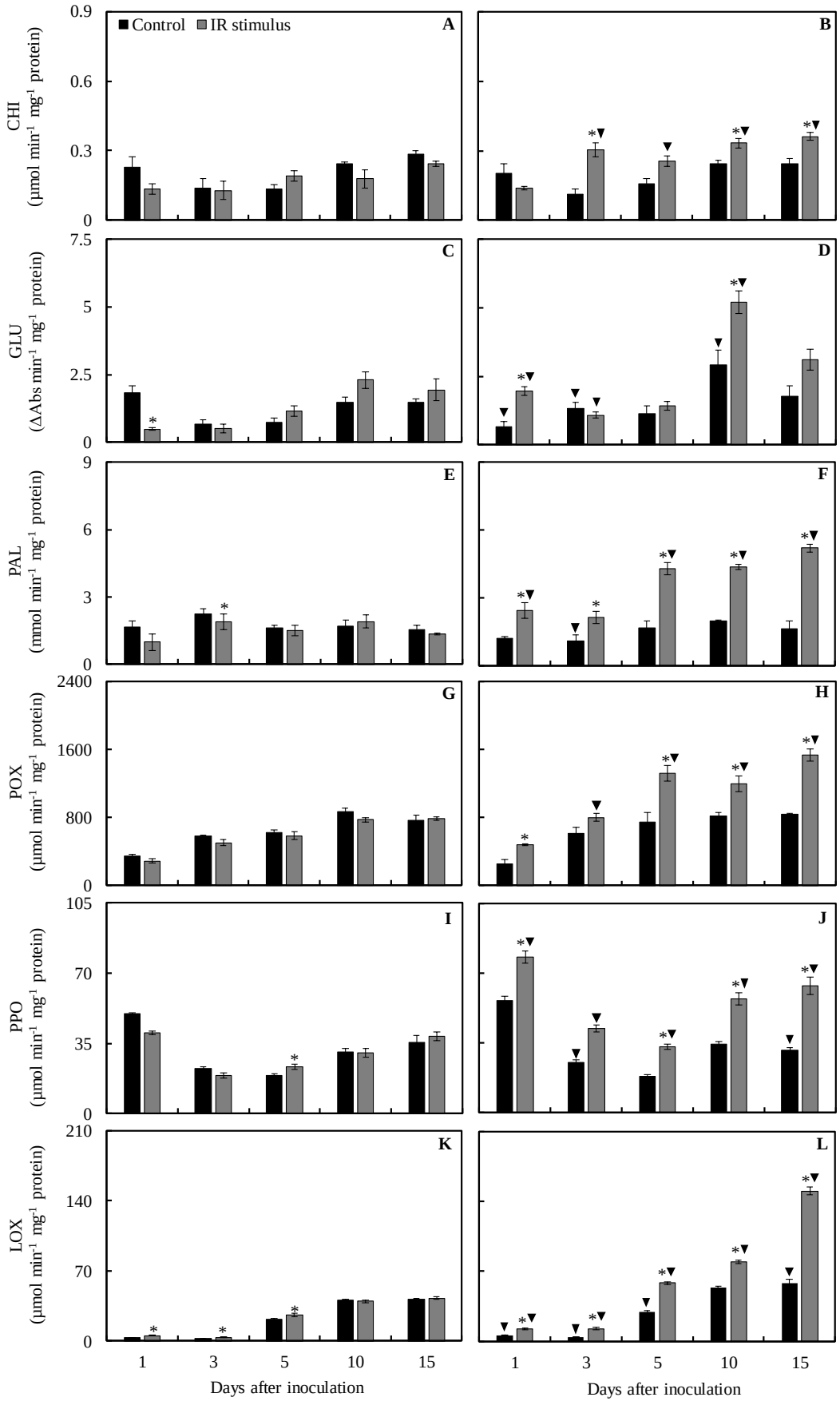
Control
IR stimulus
A
B
C
D
E
F
G
H
I
J
K
L
CHI (μmol min-1 mg-1 protein)
GLU (ΔAbs min-1 mg-1 protein)
PAL (mmol min-1 mg-1 protein)
POX (μmol min-1 mg-1 protein)
PPO (μmol min-1 mg-1 protein)
LOX (μmol min-1 mg-1 protein)
0.9
0.6
0.3
0
7.5
5
2.5
9
6
3
2400
1600
800
105
70
35
210
140
70
1
3
5
10
15
Days after inoculation
Days after inoculation

Figure 9. Activities of chitinase (CHI) (A and B), β-1,3-glucanase (GLU) (C and D), phenylalanine ammonia-lyase (PAL) (E and F), peroxidase (POX) (G and H), polyphenoloxidase (PPO) (I and J), and lipoxygenase (LOX) (K and L) determined on the leaflets of soybean plants non-inoculated (NI) (A, C, E, G, I, and K) or inoculated (I) (B, D, F, H, J, and L) with *Phakopsora pachyrhizi* and sprayed with water (control) or with induced resistance (IR) stimulus. Means for control and IR stimulus treatments followed by an asterisk (*) and means for NI and I plants followed by an inverted triangle (▼), at each evaluation time, are significantly different ($P \leq 0.05$) according to the *F* test. Bars represent the standard error of the means.

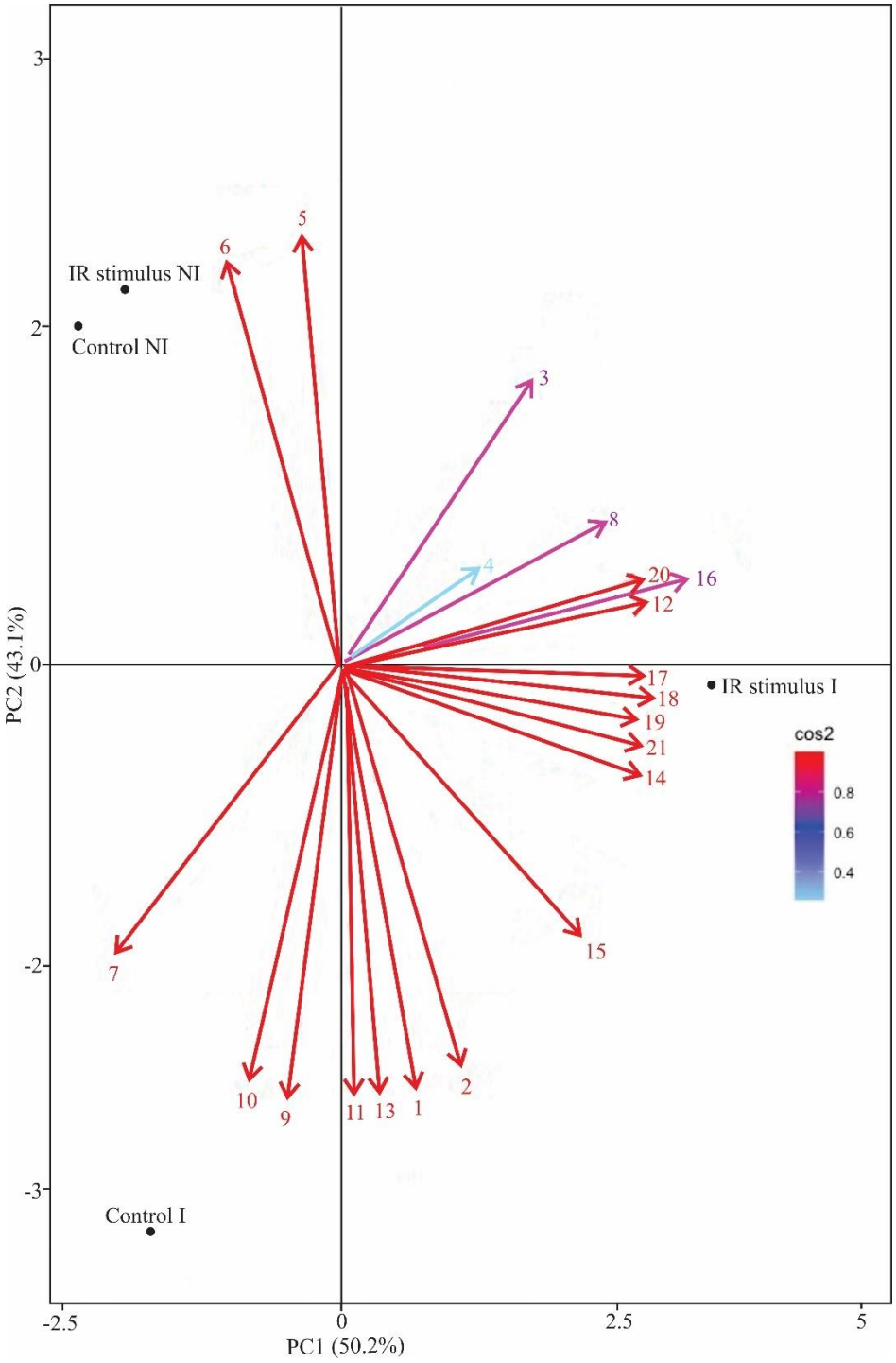
IR stimulus NI
Control NI
IR stimulus I
Control I
cos2
0.8
0.6
0.4
PC2 (43.1%)
PC1 (50.2%)
3
2
0
-2
-3
-2.5
0
2.5
5
1
2
3
4
5
6
7
8
9
10
11
12
13
14
15
16
17
18
19
20
21

Figure 10. Score plots and loading values in the principal component analysis (PCA) for variables and parameters evaluated in soybean plants sprayed with water (control) and with induced resistance (IR) stimulus and non-inoculated (NI) or inoculated (I) with *Phakopsora pachyrhizi*. Numbers in the PCA are as follow: severity (1), the area under disease progress curve (2), the concentration of foliar nutrients (3 and 4, respectively, to Ca and N), concentrations of photosynthetic pigments (5 and 6, respectively, to Chl *a*+*b* and carotenoids), metabolites (7, 8, 9, 10, and 11, respectively, to TSP, LTGA derivatives, MDA, H_20_2, and $O_2^{\bullet-}$), activities of antioxidant enzymes (12, 13, 14, and 15, respectively, to SOD, APX, CAT, and GR) and defense-related enzymes (16, 17, 18, 19, 20, and 21, respectively, to CHI, GLU, PAL, POX, PPO, and LOX). Groups were generated from cluster analysis with complete linkage and Pearson distance. Data from variables and parameters used in the PCA were obtained at 15 days for plants non-inoculated or inoculated with *P. pachyrhizi*.

CHAPTER II

FOLIAR SPRAY OF PHOSPHITE CONTAINING NICKEL AND POTASSIUM TO INDUCE SOYBEAN RESISTANCE AGAINST *Phakopsora pachyrhizi* INFECTION

Abstract

Soybean is considered one of the most profitable crops among the legumes grown worldwide, and the occurrence of rust epidemics, caused by *Phakopsora pachyrhizi*, has greatly contributed to significant yield losses and an abusive use of fungicides. Within this context, this study investigated the potential of using a phosphite of nickel (Ni) and potassium (K) (referred to as induced resistance [IR] stimulus) to induce soybean resistance against *P. pachyrhizi* infection. Plants were sprayed with water (control) or with IR stimulus and non-inoculated or inoculated with *P. pachyrhizi*. Urediniospores germination was greatly reduced by 99% by IR stimulus, with rates ranging from 2 to 15 mL/L *in vitro*. Rust severity was significantly reduced by 68-78% from 7 to 15 days after inoculation (dai). The area under the disease progress curve significantly decreased by 74% for IR stimulus-sprayed plants compared to water-sprayed plants. For inoculated plants, K and Ni foliar concentrations were significantly higher for IR stimulus treatment than for the control treatment. Infected plants sprayed with IR stimulus had their photosynthetic apparatus (great pool of photosynthetic pigments and lower values for some chlorophyll *a* fluorescence parameters) preserved, associated with less cellular damage (lower concentrations of malondialdehyde, hydrogen peroxide, and anion superoxide) and more production of phenolics and lignin than plants from the control treatment. In response to *P. pachyrhizi* infection, the defense-related genes (*PAL2.1*, *PAL3.1*, *CHIB1*, *LOX7*, *PR-1A*, *PR10*, *ICS1*, *ICS2*, *JAR*, *ETR1*, *ACS*, *ACO*, and *OPR3*) were up-regulated from 7 to 15 dai for IR stimulus-sprayed plants in contrast to plants from the control treatment. Collectively, these findings provide a global picture of the enhanced capacity of IR stimulus-sprayed plants to efficiently cope with fungal infection at both biochemical and physiological levels without discarding the direct effect of this IR stimulus on urediniospores germination.

Keywords *Glycine max*· *Phakopsora pachyrhizi*· Photosynthesis. Antioxidative metabolism· Plant defense· Induced resistance.

Introduction

Due to its highest content of protein and oil, soybean (*Glycine max* (L.) Merr.) became the most profitable crop grown worldwide and plays a pivotal role in livestock, human food, and biodiesel production (Sun et al. 2018). The biotrophic fungus *Phakopsora pachyrhizi* H. Sydow & P. Sydow, the causal agent of soybean rust (SR), is among the most destructive pathogens affecting soybean plants worldwide (Kelly et al. 2015; Paula et al. 2021). The infection process of this fungus starts with the deposition of urediniospores over the leaf surface, and, under favorable environmental conditions, their germination takes place to give rise to a germ tube from which an appressorium is formed to allow penetration into the epidermal cell (Goellner et al. 2010). Small yellowish-brown lesions, restricted by leaf veins, are formed mainly on the abaxial leaf surface due to a successful infection process (Goellner et al. 2010). On infected leaves, many necrotic lesions, with discreet chlorosis around them, formed on the leaflets cause premature defoliation and earlier plant organ maturation, resulting, therefore, in significant yield losses (Godoy et al. 2016; Goellner et al. 2010; Hartman et al. 2015).

In Brazil, the mManagement of SR is mainly achieved by intense sprays of fungicides composed of molecules with different modes of action along with the use of some cultural practices (e.g., preference for early-maturing cultivars, paying attention to the appearance of earlier rust lesions, adopting a period without growing soybean in the off-season, and following specific sowing date) (Godoy et al. 2016; Miles et al. 2007). Unfortunately, soybean cultivars exhibiting race-specific resistance or with higher levels of non-race resistance against SR are not being widely used by farmers yet (Langenbach et al. 2016; Kashiwa et al. 2020; Kato and Soares 2022). The lower sensibility of *P. pachyrhizi* populations to the current molecules in the fungicides has been an actual concern of many agricultural chemical companies and growers owing technified farms (Godoy et al. 2016; Miles et al. 2007).

Considering the occurrence of severe SR epidemics in each soybean growing season and the lack of effective control measures to slow disease progress rate, the use of resistance inducers may become a plausible alternative towards more sustainable agriculture. Induced resistance (IR) is a well-known phenomenon in plants after being stimulated by abiotic or biotic IR stimuli, resulting in a physiological state of greater defensive capacity (Durrant and Dong 2004; Llorens et al. 2007). Systemic acquired resistance (SAR) and induced systemic resistance (ISR) are the two types of IR taking place in plants countering infection by pathogens of different lifestyles (Choudhary et al. 2007; Kesel et al. 2021; Zeier 2021). The SAR involves a

rapid, systemic, and long-lasting defense response to impair the colonization of plant tissues by pathogens (Zeier 2021). The SAR is activated after plants are exposed to different IR stimuli and are closely linked to salicylic acid (SA) production and expression of pathogenesis-related (PR) proteins (Hammerschmidt 2009; Kesel et al. 2021). Several metabolites (e.g., azelaic acid, pipecolic acid, glycerol-3-phosphate, SA methyl ester, and dehydroabietinal) are involved in the SAR signaling pathway in plants (Dempsey and Klessig 2012; Shah and Zeier 2013) while ISR is activated by plant growth-promoting rhizobacteria or by some particular IR stimuli with the signaling pathway being mediated by jasmonic acid in collaboration with the ethylene (Choudhary et al. 2007; Vlot et al. 2020). The literature emphasizes the importance of using different IR stimuli (acibenzolar-S-methyl, harpin protein-derived peptides, nickel, silicon, *Bacillus subtilis*, saccharin, azelaic acid, hexanoic acid, salicylic acid, inorganic salts, phosphites) to induce the defense responses of plants aiming to obtain a satisfactory level of disease control in very profitable crops (Ahmed et al. 2023; Cruz et al. 2020; Einhardt et al. 2020; Paula et al. 2021; Reglinski et al. 2023; Rodrigues et al. 2023; Sood et al. 2023). The use of phosphites in soybean to control various diseases, including SR, is well documented in the literature (Einhardt et al. 2020; Novaes et al. 2019; Paula et al. 2021; Picanço et al. 2022). Under field conditions, soybean plants sprayed with potassium phosphite showed reduced SR severity and increased polyphenoloxidase activity and higher levels of genes expression such as *GmAOX2a* (encoding an alternative oxidase) and those encoding for PR proteins (*PR1*, *PR2*, *PR3*, *PR4*, *PR5*, and *PR8*) (Gill et al. 2018). Moreover, experiments carried out under greenhouse conditions showed the potential of formulations of phosphites containing copper, manganese, or potassium to potentiate soybean resistance against *P. pachyrhizi* infection as a result of increased activities of chitinase, phenylalanine ammonia-lyase, and β-1,3-glucanase (Bruzamarello et al. 2018; Paula et al. 2021; Picanço et al. 2022).

Considering the economic importance of soybean for the global economy and the major threat that SR may impose on food security, the present study hypothesized that the spray of soybean plants with an IR stimulus containing nickel and potassium phosphites could potentiate their resistance against *P. pachyrhizi* infection. This hypothesis was tested by performing several analyses at biochemical, physiological, and molecular levels that included the examination of the photosynthetic apparatus, the antioxidative metabolism, and the host defense responses in plants that were non-sprayed or sprayed with the IR stimulus and non-inoculated or inoculated with *P. pachyrhizi*.

Material and Methods

In vitro assay

Different volumes of a stock solution (80 ml/L) of Blindage Ni® [nickel (0.5% Ni, 7 g/L), potassium (20% K_2O, 280 g/L), and phosphorous acid (500 g/L); Unity Agro, Paraná, Brazil] were mixed with 1 mL of a suspension of *P. pachyrhizi* urediniospores (10^5 urediniospores/ml) to obtain the final concentrations of 2, 5, 7, 10, and 15 mL/L. A total of 100 µl of urediniospores suspension (10^5 urediniospores/ml) containing the different concentrations of Blindage® was transferred to a glass slide and covered with a coverslip. A suspension of urediniospores without Blindage® solution corresponded to the control treatment. The glass slides were transferred to a growth chamber (25°C and 12 h light/12 h dark photoperiod). Each glass slide received 5 µl of lactophenol after 12 h to help stop urediniospores germination. One hundred urediniospores were randomly examined in each glass slide under a light microscope (Carl Zeiss AxioImager A1) at 40 × magnification using the bright field. The images of the details for urediniospores germination were acquired digitally (model AxioCam HR, Germany; Axion Vision software v. 4.8.1.). Urediniospore with a germ tube larger than its diameter was considered germinated. The percentage of urediniospores germination was calculated for the replication of each treatment.

Growth of soybean plants

A total of six soybean seeds from cultivar DS5916IPRO (https://www.brevant.com.br), susceptible to *P. pachyrhizi*, were sown in each plastic pot containing 2 Kg of a 1:1 mixture of soil and substrate (Tropstrato, Vida Verde, Mogi Mirim, SP, Brazil). After germination, a total of four seedlings were left per pot. Plants in each pot were fertilized weekly with 100 mL of nutrient solution by Clark (1975), with some modifications, which consisted of: 1.04 mM $Ca(NO_3)_2 \cdot 4H_2O$, 1 mM NH_4NO_3, 0.8 mM KNO_3, 0.6 mM $MgSO_4 \cdot 7H_2O$, 0.069 mM KH_2PO_4, 0.931 mM KCl, 19 µM H_3BO_3, 2 µM $ZnSO_4 \cdot 7H_2O$, 7 µM $MnCl_2 \cdot 4H_2O$, 0.6 µM $Na_2MoO_4 \cdot 4H_2O$, 0.5 µM $CuSO_4 \cdot 5H_2O$, 90 µM $FeSO_4 \cdot 7H_2O$, and 90 mM ethylenediaminetetraacetic acid disodium (EDTA). Plants were grown in a greenhouse with temperature of 25 ± 2°C, relative humidity of 70 ± 5%, and natural photosynthetically active radiation (PAR) of 915 ± 12 µmol photons m^{-2} s^{-1} measured at midday.

Application of Blindage

Soybean plants (V4 growth stage; ≈ 30 days after seedlings emergence) were sprayed with Blindage® (7.5 ml/L, 5 ml of solution per plant) using a VL Airbrush atomizer (Paasche Airbrush Co., Chicago, IL, USA). According to the criteria proposed by Kesel et al. (2021), this treatment will be called IR stimulus. The IR stimulus solution was prepared using deionized water. Plants sprayed with water served as the control treatment.

Plant inoculation with *P. pachyrhizi*

At 48 hours after being sprayed with water or IR stimulus, plants were inoculated with a suspension of 10^5 urediniospores of *P. pachyrhizi*/ml prepared with gelatin (0.5% w/v) and Tween 80 (25 μL/L) by using a VL Airbrush atomizer. After inoculation, plants were kept in a mist chamber at 25°C for 16 h under darkness. After this period, plants were transferred to a greenhouse (temperature of 25 ± 2°C, relative humidity of 75 ± 5%, and natural PAR of 932 ± 20 μmol photons m^{-2} s^{-1} measured at midday) until the end of the experiments. Plants non-inoculated with *P. pachyrhizi* were kept in different mist chamber and greenhouse under the same environmental conditions.

Experimental design

For the in vitro assay, the experiment was arranged in a completely randomized design with six treatments (control and five concentrations of IR stimulus) with eight replications. A 2 × 2 factorial experiment, consisting of plants sprayed with water (control) and IR stimulus and non-inoculated or inoculated with *P. pachyrhizi*, was arranged in a completely randomized design with four replications per evaluation time to assess rust severity as well to determine the foliar concentrations of Ni and K. Another 2 × 2 factorial experiment with the same factors mentioned above and five replications was carried out to evaluate the fluorescence of chlorophyll *a* fluorescence parameters and to quantify the foliar concentration of pigments. Leaf samples for the histochemical, biochemical assays, and gene expression using quantitative real-time PCR were obtained from another 2 × 2 factorial experiment with the same factors described above and six replications. All experiments were repeated once.

Evaluation of ASR severity

The leaflets of the second and third leaves (from base to top) of each plant per replication of each treatment (four replications, 16 plants, and 96 leaflets per experiment) were used to evaluate SR severity according to the diagrammatic scale proposed by Franceschi et al. (2020) at 7, 9, 11, 13, and 15 days after inoculation (dai). The area under disease progress curve

(AUDPC) for each leaflet per leaf of each plant from the replications of each treatment was calculated using the trapezoidal integration of disease progress curves (Shaner and Finney 1977). At 15 dai, the second and third leaves of each plant per replication of each treatment were collected and scanned at 600 dpi resolution. The images were processed using the software QUANT (Fagundes-Nacarath et al. 2018) to obtain the values of final SR severity.

Determination of foliar nickel (Ni) and potassium (K) concentrations

The leaflets of the second and third leaves (from base to top) of each plant per replication of each treatment (four replications, 8 plants, and 32 leaflets per experiment) were collected at 15 dai, washed in deionized water, and dried in a drying oven with forced ventilation for two days. The foliar Ni and K concentrations were determined by nitric-perchloric digestion and inductively coupled plasma-optical emission spectrometry (ICP-OES).

Processing leaf samples for scanning electron microscopy (SEM)

Fragments (≈ 5 mm^2) were randomly obtained from the leaflets of the second and third leaves (from base to top) of each plant per replication of each treatment (four replications, 8 plants, and 48 leaflets) at 15 dai. The fragments were carefully transferred to glass vials containing 10 mL of fixative [3% (v/v) glutaraldehyde and 2% paraformaldehyde (v/v) in 0.1 M sodium cacodylate buffer (pH 7.2)], stored at 4°C for 10 days. Leaflet fragments were washed with sodium cacodylate buffer (0.1 M), dehydrated in ethanol, and subjected to critical point drying using CO_2 (model CPD 030, Hatfield, PA., USA). Four leaf fragments were mounted on aluminum stubs, sputter coated with gold (model FDU 010, Hatfield, PA, USA), and uredinia containing urediniospores of *P. pachyrhizi* were observed in an LEO SEM (model 1430VP, Jena, Thuringia, Germany) operating at 10 kV and a working distance of 15 mm.

Imaging and quantification of chlorophyll (Chl) *a* fluorescence parameters

The Imaging-PAM fluorometer and the Imaging Win software MAXI version (Heinz Walz GmbH, Effeltrich Germany) were used to obtain the images and parameters of Chl *a* fluorescence using the leaflets of the second leaf (from base to top) of each plant per replication of each treatment (four replications, 16 plants, and 32 leaflets) at 7, 11, and 15 dai. Leaflets of the second leaf from non-inoculated plants were also evaluated at these evaluation times. Plants were adapted to darkness for 30 min and then placed individually in a support at a distance of 18.5 cm from the CCD ("charge-coupled device") camera to obtain images at the resolution of 640 × 480 pixels. The leaflets were exposed to a light pulse intensity of 0.5 μmol m^{-2} s^{-1}, 100

μs, 1 Hz to obtain the initial fluorescence (F_0). Next, a saturating white light pulse of 2,400 μmol m^{-2} s^{-1} (10 Hz) was emitted for 0.8 s to determine the maximum fluorescence emission (F_m). Based on these initial measurements, the maximum PS II photochemical efficiency of dark-adapted leaflets was estimated through the variable-to-maximum Chl *a* fluorescence ratio as follows: $F_v/F_m = [(F_m - F_0)/F_m)]$. Next, the leaflets were exposed to actinic photon irradiance (100 μmol m^{-2} s^{-1}) for 300 s to obtain the steady-state fluorescence yield (F_s), after which a saturating white light pulse (2,400 μmol m^{-2} s^{-1}; 0.8 s) was applied to achieve the light-adapted maximum fluorescence ($F_{m'}$). The light-adapted initial fluorescence ($F_{0'}$) was estimated according to Oxborough and Baker (1997). Based on Kramer et al. (2004), the energy that was absorbed by the PS II for the following three yield components for dissipative processes was calculated as follows: the photochemical yield [$Y(II) = (F_{m'} - F_s)/F_{m'})$], the yield for dissipation by down-regulation [$Y(NPQ) = (F_s/F_{m'}) - (F_s/F_m)$], and the yield for other non-photochemical (non-regulated) losses [$Y(NO) = F_s/F_m$]. The apparent electron transport rate was calculated as ETR = Y(II) × PPFD × f × α according to Baker (2008). The parameters of Chl *a* fluorescence were determined on each leaflet (area of ≈ 0.5 cm^2) by selecting the circular option on the Imaging Win software.

Determining photosynthetic pigments concentration

Five leaf discs (1 cm^2 each) were obtained from the leaflets of the second and third leaves (from base to top) of each plant per replication of each treatment (four replications, 16 plants, and 64 leaflets) at 7, 11, and 15 dai. The discs were immersed in glass tubes containing 5 ml of saturated dimethyl sulfoxide solution and calcium carbonate (5 g/L), kept in the dark at room temperature for 24 h, and the absorbances of the extracts were read at 480, 649, and 665 nm to determine the concentrations of Chl *a*, Chl *b*, and carotenoids according to Picanço et al. (2021).

Histochemical detection of lipid peroxidation, membrane damage, hydrogen peroxide (H_2O_2), and superoxide anion radical ($O_2^{\bullet-}$)

The leaflets of the second leaf (from base to top) of each plant per replication of each treatment (four replications, 8 plants, and 24 leaflets) were collected from both non-inoculated and inoculated plants at 15 dai. Lipid peroxidation and membrane damage in the leaflets were visualized using Schiff and Evans' blue reagents, respectively (Awasthi et al. 2018; Tistama et al. 2012). The leaflets were randomly transferred to glass vials containing 50 mL of either Schiff (10% v/v prepared in deionized water) or Evans's blue (0.025% w/v prepared in 100 μM of $CaCl_2$, pH 5.6) reagents (five leaflets per glass vial for each reagent) during 2 and 12 h,

respectively. For H_2O_2 detection, leaflets were randomly placed in glass vials (five leaflets per glass vial) containing 25 mL of 3,3′-diaminobenzidine tetrahydrochloride solution (1 mg/mL) (Sigma-Aldrich, São Paulo, Brazil) and kept in the dark at 25ºC for 12 h. For $O_2^{\bullet-}$ detection, leaflets were randomly placed in glass vials (five leaflets per glass vial) containing 50 mL of nitro blue tetrazolium (0.1%) solution (Sigma-Aldrich, São Paulo, Brazil) prepared in potassium phosphate buffer (10 mM, pH 6.8) during 24 h. The leaflets were cleared in boiling aqueous ethanol (80%) for 80 min until pink, blue, brown, and blue spots were noticed, confirming the presence of lipid peroxidation, membrane damage, H_2O_2, and $O_2^{\bullet-}$, respectively.

Biochemical assays and gene expression using quantitative real-time PCR

The second and third leaves (from base to top) of each plant per replication of each treatment (four replications, 16 plants, and 96 leaflets per experiment) were collected at 1, 3, 5, 10, and 15 dai from both non-inoculated and inoculated plants. Leaf samples were kept in liquid nitrogen during sampling and stored at -80ºC until further analysis.

Malondialdehyde (MDA) concentration: oxidative damage in the leaflet tissues was estimated based on the concentration of total 2-thiobarbituric acid (TBA) reactive substances and expressed as equivalents of MDA (Cakmak and Horst 1991). Leaflet tissue (0.1 g) was ground into a fine powder using a vibration ball mill (Retsch, Haan, Germany) with liquid nitrogen and homogenized in 2 ml of 0.1% (w/v) trichloroacetic acid (TCA) solution in an ice bath. The homogenate was centrifuged at 12,000 *g* for 15 min at 4°C. After centrifugation, a total of 250 µl of the supernatant was reacted with 750 µl of TBA solution (0.5% in 20% TCA) for 60 min in a boiling water bath at 95°C. After this period, the reaction was stopped in an ice bath. The samples were centrifuged at 10,000 *g* for 10 min and the specific absorbance was determined at 532 nm. The non-specific absorbance was estimated at 600 nm and subtracted from the specific absorbance value. The extinction coefficient of 155 mM^{-1} cm^{-1} (Heath and Packer 1968) was used to calculate the MDA concentration.

Concentrations of H_2O_2 and $O_2^{\bullet-}$: leaflet tissue (0.1 g) was ground into a fine powder described above and homogenized in 2 ml of 0.1% (w/v) of TCA. The homogenate was centrifuged at 12,000 *g* for 15 min at 4°C. The supernatant was added to a reaction mixture containing 10 mM potassium buffer (pH 7.0) and 1 M of iodide solution and incubated for 10 min. The H_2O_2 concentration was determined based on the oxidized product formed at 390 nm (Velikova et al. 2000). A standard curve of H_2O_2 (Sigma-Aldrich, São Paulo, Brazil) was used

to determine H_2O_2 concentration. Leaflet tissue (0.2 g) was ground as described above and homogenized in 2 ml of a solution containing 100 mM sodium phosphate buffer (pH 7.2) and 1 mM sodium diethyldithiocarbamate. The homogenate was centrifuged at 22,000 *g* for 20 min at 4°C, and the supernatant was used to determine $O_2^{\bullet-}$ concentration, according to Chaitanya and Naithani (1994).

Concentrations of total soluble phenols (TSP) and lignin-thioglycolic acid (LTGA) derivatives: leaflet tissue (0.1 g) was ground into a fine powder as described above and homogenized in 1 mL of 80% (v/v) methanol solution. The crude extract was shaken at 300 rpm at 25°C for 2 h and the mixture was centrifuged at 17,000 *g* for 30 min. 26 The TSP concentration was determined in the methanolic extract and the pellet was used to determine the LTGA derivatives concentration according to Tatagiba et al. (2014).

Genes expression: leaflet tissue (75 mg) was ground into a fine powder as described above. The fine powder was used for RNA extraction using Trizol (Invitrogen®). Contamination by DNA was removed with RQ1 RNase-Free DNase (Promega). The quality and integrity of the RNA were verified by 1.2% agarose gel electrophoresis and the amount of RNA was measured in a Qubit fluorometer using Qubit RNA HS Assay Kit (Invitrogen, São Paulo, Brazil). Single-stranded cDNAs were synthesized by reverse transcription using 5 μg of total RNA with oligo(dT) primers in a final volume of 20 μL using the SuperScript First-Strand Synthesis System for RT-PCR (Invitrogen®). The qRT-PCR was performed on a Bio-Rad CFX Real-Time Thermal Cycler using SYBR Green PCR Master Mix according to the manufacturer's recommendations. All reactions were duplicated, and the relative expression values for each gene studied were calculated using the $2^{-\Delta\Delta Ct}$ method (Livak and Schmittgen 2001). Expression analysis of genes encoding for phenylalanine ammonia-lyase (*PAL2.1* and *PAL3.1*), chalcone isomerase (*CHIB1*), lipoxygenase (*LOX7*), pathogenesis-related protein 1 (*PR1-A*), pathogenesis-related protein 10 (*PR10*), isochorismate synthase (*ICS1* and *ICS2*), jasmonic acid-amino synthetase (*JAR*), ethylene receptor 1 (*ETR1*), 1-aminocyclopropane-1-carboxylic acid synthase (*ACS*), 1-aminocyclopropane-1-carboxylic acid oxidase (*ACO*), and 12-oxophytodienoic acid reductase 3 (*OPR3*) was performed using specific primer sequences (Table 1). Expression of *TEF-1α,* corresponding to the translation elongation factor 1α of *P. pachyrhizi*, was quantified to confirm the presence of the fungus in the leaflet tissues. The Ubiquitin-3 (*UBIQ*) and glyceraldehyde-3-phosphate dehydrogenase (*GAPDH*) genes were used as references for normalization, according to Mortel et al. (2007).

Data analysis

Data from urediniospores germination were subjected to analysis of variance (ANOVA), and means were compared by Tukey´s test ($P \leq 0.05$). For other variables and parameters, data were subjected to ANOVA, and comparisons between control and IR stimulus treatments, as well as between non-inoculated and inoculated plants, were made using the *F* test ($P \leq 0.05$). Data were checked for normality and homogeneity of variance before ANOVA. The procedures described by Moore and Dixon (2015) were followed to combine the data from the variables and parameters evaluated from the repeated experiments. The Minitab Statistical software was used for the statistical analysis mentioned above (Minitab, Inc., 2021). Data from all variables and parameters obtained from control and IR stimulus treatments for non-inoculated and inoculated plants at 15 dai were used for principal component analysis (PCA) using the software R (R Core Team, 2022).

Results

Analysis of variance

The effect of IR stimulus and control (water) treatments [named as products (P)] on urediniospores germination was analyzed by one-way ANOVA. The factor P was significant ($P < 0.001$) for urediniospores germination. The response of all variables and parameters to P, plant inoculation (PI), and the P × PI interaction was analyzed by a two-way ANOVA. The factors P and PI, as well as the P × PI interaction, were significant ($P \leq 0.05$) for most of the variables and parameters studied (Table 1).

Germination of urediniospores *in vitro*

The urediniospores of *P. pachyrhizi* did not germinate when exposed to the IR stimulus rates ranging from 2 to 15 mL/L compared to the control treatment (Fig. 1A-F). Urediniospores germination was significantly reduced by 99% for IR stimulus in the rates ranging from 2 to 15 mL/L compared to the control treatment (Fig. 2).

Rust symptoms and severity, AUDPC, and observations at the SEM

Necrotic lesions containing many uredinia were abundant on the leaflets of plants from control treatment in contrast to the leaflets of IR-stimulus sprayed plants (Fig. 3A-B). Rust severity was significantly reduced by 68, 70, 72, 78, and 73%, respectively, at 7, 9, 11, 13, and 15 dai for IR-stimulus sprayed plants compared to plants from the control treatment (Fig. 3C). The AUDPC significantly decreased by 74% for IR stimulus-sprayed plants compared to plants from the control treatment (Fig. 3D). The uredinia formed in the leaflets of IR-stimulus sprayed plants were smaller and more compact than those observed on the leaflets of plants from the control treatment (Fig. 4A-B). Many urediniospores were found inside the uredinia formed on the leaflets of plants from the control treatment (Fig. 4A).

Foliar concentrations of Ni and K

The foliar Ni concentration significantly increased for non-inoculated and inoculated plants sprayed with the IR stimulus compared to non-inoculated and inoculated plants from the control treatment (Fig. 5A-B). The foliar K concentration was significantly higher by 14 and 31%, respectively, for non-inoculated and inoculated plants sprayed with IR stimulus compared to non-inoculated and inoculated plants from the control treatment. For IR stimulus treatment, the

foliar concentration of K significantly increased by 19% for inoculated plants compared to non-inoculated plants (Fig. 5C-D).

Photosynthetic pigments concentration

For the control treatment, concentrations of Chl *a*+*b* (30 and 27% at 7 and 15 dai, respectively) and carotenoids (29, 32, and 32% at 7, 11, and 15 dai, respectively) were significantly lower for inoculated plants compared to non-inoculated plants (Fig. 6A-D). For IR stimulus treatment, concentrations of Chl *a*+*b* (23% at 11 dai) and carotenoids (22% at 11 dai) were significantly lower for inoculated plants in comparison to non-inoculated plants (Fig. 6A-D).

Concentration of Chl *a*+*b* for non-inoculated plants was significantly higher by 0.7% at 11 dai for IR stimulus treatment compared to the control treatment (Fig. 5A). Concentration of carotenoids for non-inoculated plants was not affected by any of the treatments regardless of the evaluation time (Fig. 6C). For inoculated plants, concentrations of Chl *a*+*b* (29, 71, and 23% at 7, 11, and 15 dai, respectively) and carotenoids (25 and 24% at 11 and 15 dai, respectively) were significantly higher for IR stimulus treatment in comparison to the control treatment (Fig. 6B and D).

Imaging and quantification of Chl *a* fluorescence parameters

There was no alteration on the images of Chl *a* fluorescence parameters for non-inoculated plants regardless of treatments and sampling times (Fig. 7). Remarkable damage to photosynthetic apparatus occurred for inoculated plants from control treatment compared to inoculated plants sprayed with IR stimulus at 15 dai based on the darker areas in the images corresponding to F_v/F_m, Y(II), Y(NPQ), and Y(NO) parameters (Fig. 7).

There was no significant difference for control treatment between non-inoculated and inoculated plants for F_v/F_m, regardless of the evaluation time. The values for Y(II) (17, 22, and 42% at 7, 11, and 15 dai, respectively), Y(NPQ) (26 and 30% at 11 and 15 dai, respectively), and ETR (21, 27, and 42% at 7, 11, and 15 dai, respectively) were significantly lower while the values for Y(NO) (28 and 48% at 11 and 15 dai, respectively) were significantly higher for inoculated plants in comparison to non-inoculated plants (Fig. 8A-J). There was no significant difference between non-inoculated and inoculated plants for IR stimulus treatment for Y(II) regardless of the evaluation time. The values for F_v/F_m (1.4% at 7 dai) and Y(NPQ) (28% at 15 dai) were significantly higher, while the values for Y(NO) (18% at 15 dai) and ETR (8% at 11 dai) were significantly lower for inoculated plants compared to non-inoculated plants (Fig. 8A-J).

For non-inoculated plants, there was no significant difference for any of the treatments regardless of the evaluation time (Fig. 8A, C, E, G, and I). For inoculated plants, the values for F_v/F_m (1% at 11 dai), Y(II) (21, 20, and 51% at 7, 11, and 15 dai, respectively), Y(NPQ) (19 and 92% at 11 and 15 dai, respectively), and ETR (22, 23, and 63% at 7, 11, and 15 dai, respectively) were significantly higher while the values for Y(NO) (27 and 46% at 11 and 15 dai, respectively) were significantly lower for IR stimulus treatment compared to the control treatment (Fig. 8B, D, F, H, and J).

Histochemical detection of lipid peroxidation, membrane damage, hydrogen peroxide (H_2O_2), and superoxide anion radical ($O_2^{\bullet-}$)

The spray of IR stimulus did not cause any physiological perturbation to the leaflets of non-inoculated plants, considering the absence of staining for lipid peroxidation, membrane damage, H_2O_2, and $O_2^{\bullet-}$ compared to leaflets of plants from the control treatment (Fig. 8A-D). Lipid peroxidation, membrane damage, and depositions of H_2O_2 and $O_2^{\bullet-}$ (brown and blue colors, respectively) were less intense in the leaflets of plants sprayed with the IR stimulus than on the leaflets of plants from the control treatment at 15 dai (Fig. 9A-D).

Concentrations of MDA, H_2O_2 and $O_2^{\bullet-}$

For the control treatment, concentrations of MDA (23, 38, 30, and 44% at 3, 5, 10, and 15 dai, respectively), H_2O_2 (29, 23, 18, and 21% at 1, 3, 5, and 10 dai, respectively), and $O_2^{\bullet-}$ (175, 239, and 86% at 3, 5, and 10 dai, respectively) were significantly higher for inoculated plants in comparison to non-inoculated plants (Fig. 10A-F). For IR stimulus treatment, concentrations of MDA (10% at 15 dai), H_2O_2 (31 and 17% at 1 and 10 dai, respectively), and $O_2^{\bullet-}$ (112 and 81% at 3 and 5 dai, respectively) were significantly higher while the concentration of $O_2^{\bullet-}$ (93% at 10 dai) was significantly lower for inoculated plants compared to non-inoculated plants (Fig. 10A-F).

The concentrations of MDA and H_20_2 for non-inoculated plants were not affected by any treatments regardless of the evaluation time. The concentration of $O_2^{\bullet-}$ was significantly lower by 47% at 1 dai and significantly higher by 40% at 5 dai for IR stimulus treatment compared to the control treatment (Fig. 10A, C, and E). For inoculated plants, the concentrations of MDA (42, 27, 24, 20, and 30% at 1, 3, 5, 10, and 15 dai, respectively), H_2O_2 (14, 14, 14, and 22% at 3, 5, 10, and 15 dai, respectively), and $O_2^{\bullet-}$ (58, 26, and 97% at 1, 5, and 10 dai, respectively) were significantly lower for IR stimulus treatment in comparison to the control treatment (Fig. 10B, D, and F).

Concentrations of TSP and LTGA derivatives

For the control treatment, concentrations of TSP (41% at 5 dai) and LTGA derivatives (16% at 10 dai) were significantly lower for inoculated plants in comparison to non-inoculated plants (Fig. 11C and D). For IR stimulus treatment, concentrations of TSP (46, 49, 23, and 30% at 3, 5, 10, and 15 dai, respectively) and LTGA derivatives (49, 42, and 18% at 3, 10, and 15 dai, respectively) were significantly higher while the concentration of LTGA derivatives (19% at 1 dai) was significantly lower for inoculated plants in comparison to non-inoculated plants (Fig. 11A-D).

The treatments did not affect TSP and LTGA derivatives concentrations for non-inoculated plants regardless of evaluation time (Fig. 11A and C). Concentrations of TSP (31, 103, 40, and 49% at 3, 5, 10, and 15 dai, respectively) and LTGA derivatives (37, 28, 41, and 40% at 3, 5, 10, and 15 dai, respectively) for inoculated plants were significantly higher for IR stimulus treatment compared to the control treatment (Fig. 11B and D).

Gene expression

Comparing control and IR stimulus treatments for non-inoculated plants: expressions of *PAL3.1* and *LOX7* for non-inoculated plants were not affected by any treatments regardless of the evaluation time. Expressions of *CHIB1*, *PR1-A*, *PR10*, and *ACS* at 1 dai; *PAL2.1*, *CHIB1*, *ICS1*, *ICS2*, *JAR*, *ACO*, and *OPR3* at 3 dai; *PR1-A*, *ICS1*, *ICS2*, and *ETR1* at 5dai; *PAL 2.1*, *ACS*, and *OPR3* at 10 dai; and *PR1-A*, *PR10*, *ICS1*, and *OPR3* at 15 dai were significantly higher while expressions of *ETR1* and *OPR3* at 1 dai as well as *CHIB1* and *ACO* at 10 dai were significantly lower for IR stimulus treatment compared to the control treatment (Fig. 12A-B).

Comparing control and IR stimulus treatments for inoculated plants: for inoculated plants, expressions of *PAL2.1*, *CHIB1*, *PR1-A*, *PR10*, *ICS2*, *JAR*, *ACS*, *ACO*, and *OPR3* at 1 dai; *PAL3.1*, *CHIB1*, *LOX7*, *PR-1A*, *PR10*, *ICS1*, *ICS2*, *ETR*, *ACS*, and *OPR3* at 3 dai; *PAL2.1*, *PAL3.1*, *CHIB1*, *LOX7*, *PR1-A*, *PR10*, *ICS1*, *ICS2*, *JAR*, *ETR*, *ACS*, *ACO*, and *OPR3* at 5 and 10 dai as well as *PAL2.1*, *PAL3.1*, *CHIB1*, *LOX7*, *PR1-A*, *PR10*, *ICS1*, *ICS2*, *JAR*, *ETR*, *ACS*, and *OPR3* at 15 dai were significantly higher while expressions of *JAR* at 3 dai and *TEF-1*α at all evaluation times were significantly lower for IR stimulus treatment in comparison to the control treatment (Fig. 12C-D).

Comparing non-inoculated and inoculated plants for control treatment: for control treatment, expressions of *PAL2.1*, *CHIB1*, and *PR10* at 1 dai; *PAL2.1*, *ICS2*, *JAR*, and *OPR3* at 3 dai; *PAL3.1*, *PR10*, *ICS1*, and *ICS2* at 5 dai as well as *LOX7*, *PR1-A*, and *PR10* at 15 dai were significantly higher for inoculated plants in comparison to non-inoculated plants. Conversely, expressions of *PAL3.1*, *LOX7*, *PR-1A*, *ICS1*, and *ETR* at 1 dai; *LOX7* and *PR1-A* at 3 dai; *JAR*, *ETR*, *ACS*, and *ACO* at 5 dai; *PAL3.1*, *LOX7*, *PR-1A*, *ICS1*, *JAR*, *ETR*, *ACS*, and *ACO* at 10 dai as well as *ETR*, *ACS*, and *ACO* at 15 dai were significantly lower for inoculated plants compared to non-inoculated plants (Fig. 12A-D).

Comparing non-inoculated and inoculated plants for IR stimulus treatment: for IR stimulus treatment, expressions of *PAL2.1*, *CHIB1*, *PR10*, *ICS2*, *JAR*, and *OPR3* at 1 dai; *PAL3.1*, *CHIB1*, *LOX7*, *PR10*, *ICS1*, *ICS2*, *ETR*, *ACS*, and *OPR3* at 3 dai; *PAL2.1*, *PAL3.1*, *CHIB1*, *LOX7*, *PR1-A*, *PR10*, *ICS1*, *ICS2*, *JAR*, *ETR*, and *OPR3* at 5 dai; *PAL2.1*, *CHIB1*, *LOX7*, *PR1-A*, *PR10*, *ICS1*, *ICS2*, *JAR*, *ETR*, *ACO*, and *OPR3* at 10 dai as well as *PAL2.1*, *PAL3.1*, *CHIB1*, *LOX7*, *PR1-A*, *PR10*, *ICS1*, *ICS2*, *JAR*, *ACS*, and *OPR3* at 15 dai were significantly higher for inoculated plants compared to non-inoculated plants. Conversely, expressions of *PAL3.1*, *ICS1*, and *ETR* at 1 dai; *ACO* at 3 and 15 dai as well as *PAL3.1* and *ACS* at 10 dai were significantly lower for inoculated plants in comparison to non-inoculated plants (Fig. 12A-D).

PCA analysis

Four clusters were generated (NI and I plants separately for control and IR stimulus treatments) based on the cluster analysis with complete linkage and Pearson distance. One principal component (PC) explained most data variation (PC1 = 61.3% and PC2 = 35.1%). The PC1 indicated negative scores for severity, AUDPC, Y(NO), MDA, H_2O_2, $O_2^{\bullet-}$, *ACO*, and *TEF-1*α while positive scores were obtained for Ni, K, Chl *a*+*b*, Car, F_v/F_m, Y(II), Y(NPQ), ETR, TSP, LTGA derivatives, and for the expression of some genes (*PAL2.1*, *PAL3.1*, *CHIB1*, *LOX7*, *PR-1A*, *PR10*, *ICS1*, *ICS2*, *JAR*, *ETR1*, *ACS*, and *OPR3*). For PC2, negative scores occurred for severity, AUDPC, K, Y(NO), TSP, MDA, H_2O_2, and for the expression of some genes (*PAL2.1*, *PAL3.1*, *CHIB1*, *LOX7*, *PR-1A*, *PR10*, *ICS1*, *ICS2*, *JAR*, *ETR1*, *ACS*, *OPR3*, and *TEF-1*α) while positive scores were obtained for Ni, Chl *a*+*b*, Car, F_v/F_m, Y(II), Y(NPQ), ETR, LTGA derivatives, $O_2^{\bullet-}$, and *ACO* (Fig. 13).

Discussion

Considering the low availability of soybean cultivars with race-specific resistance or even displaying the highest level of non-race-specific resistance that will impact some components of resistance (e.g., incubation period, latent period, infectious period) are available to growers besides the capacity of *P. pachyrhizi* to become more sensible to the currently used fungicides (Langenbach et al. 2016; Hao et al. 2023), the use of resistance inducers may become a great tool that could be used in an integrated rust management program. The present study brings biochemical, molecular, and physiological evidence for using the IR stimulus to boost soybean resistance against rust. Phosphites have great potential to induce plant defense reactions against pathogens causing a plethora of diseases besides having a direct effect against mycelial growth and spore germination (Havlin et al. 2021; Liu et al. 2023; Metha et al. 2022; Mohammadi et al. 2021). Interestingly, the IR stimulus used in this study was efficient in reducing the rust symptoms considering the lower severity, leaflet tissues colonized by *P. pachyrhizi* (less *TEF-1α* expression), and impaired reproduction noticed by the reduced number of uredinia containing a lower amount of urediniospores formed on the leaflets. In addition, the IR stimulus helped reduce the cellular damage provoked by fungal infection in the leaflets by decreasing the MDA, H_2O_2, and $O_2^{\bullet-}$ pool. The *in vitro* assay demonstrated the direct effect of the IR stimulus to reduce the germination of *P. pachyrhizi* urediniospores. It is known that some IR stimuli (e.g., acibenzolar-S-methyl, azelaic acid, copper-polyphenolic compound, hexanoic acid, nickel, and phosphites formulated with different nutrients) were able to inhibit mycelia growth or spore germination *in vitro* (Chaves et al. 2021; Einhardt et al. 2020; Fagundes-Nacarath et al. 2018; Gill et al. 2018; Hawerroth et al. 2023; Novaes et al. 2019; Oliveira et al. 2022; Paula et al. 2021; Rodrigues et al. 2023a,b). The germ-tube growth of urediniospores from *P. pachyrhizi* and *Puccinia emaculata* was greatly reduced by K phosphite *in vitro* (Gill et al. 2018). Guo et al. (2021) also reported that different rates of phosphite K inhibited the mycelial growth of *Phytophthora sojae in vitro*.

Plants can absorb and translocate a large amount of nutrients sprayed to their shoots and use them to improve the basic physiological process that will result in better growth and yield besides being used to mount defense reactions against pathogens infection (Fernández and Brown 2013; Mohammadi et al. 2021; Otolakoski et al. 2023; Wang et al., 2013). Cacique et al. (2017), Einhardt et al. (2020a,b), Hawerroth et al. (2023), and Oliveira et al. (2022) reported increased foliar concentrations of Ni and K for different crops in response to the foliar spray of products containing these nutrients. The present study noticed higher foliar concentrations of

Ni and K for infected and IR stimulus-sprayed plants. Higher foliar K concentration for infected and IR stimulus-sprayed plants helped to lower rust symptoms, considering the role played by this macronutrient in increasing the production of phenolics, improving photosynthesis (stomatal aperture and osmoregulation), co-factor of different enzymes, and synthesis of proteins (Amtmann and Srivastava 2023). On the other hand, Ni plays an important role in plant physiology for being associated with some enzymes (superoxide dismutase and catalase) that are important in scavenging some reactive oxygen species in stressed plant tissues besides having a direct effect against fungal growth and spore germination (Bock et al. 2023; Einhardt el al. 2020; Hawerroth et al. 2023; Oliveira et al. 2023). In the soybean-*phakopsora pachyrhizi* pathosystem, foliar spray of Ni reduced rust symptoms due to higher expression of defense-related genes (e.g., chalcone isomerase, phenylalanine ammonia-lyase and urease), great production of lignin, higher β-1,3-glucanase activity, less oxidative damage (lower MDA, H_2O_2, and $O_2^{\bullet-}$ concentrations) and less impairment of the photosynthetic apparatus (maintenance of Chl *a* fluorescence parameters and great pool of photosynthetic pigments) (Einhardt et al. 2020a,b).

Infection by pathogens of different lifestyles can seriously impair the functioning of the photosynthetic apparatus by reducing the pool of Chl *a*+*b* and carotenoids in plant tissues and negatively affecting the outcome of Chl *a* fluorescence parameters (Rios et al. 2018; Aucique-Pérez et al. 2020; Silva et al. 2023). There are in the literature several studies reporting the potential of different plant pathogens (e.g., *Bipolaris oryzae*, *Exserohilum turcicum*; *Phakopsora pachyrhizi*, *Pyricularia oryzae*; *Sclerotinia sclerotiorum*, and *Septoria lycopersici*) to impair the photosynthetic performance of their hosts drastically and, consequently, contributing for disease symptoms development (Aucique-Pérez et al. 2019, 2020; Chaves et al. 2021; Hawerroth et al. 2023; Oliveira et al. 2022; Picanço et al. 2022; Rios et al. 2018; Rodrigues et al. 2023a,b; Silva et al. 2022). In the present study, infection of soybean leaflets by *P. pachyrhizi* severely impaired the photosynthesis as pictured by an expressive alteration of Chl *a* fluorescence [lower values for F_v/F_m, Y(II), Y(NPQ), and ETR along with higher Y(NO) values] parameters and reduced pool of photosynthetic pigments (Chl *a*+*b* and carotenoids) suggesting the occurrence of photoinhibition, reduction in the conversion of photochemical energy, and severe damage on the PSII. Rios et al. (2018) highlighted the capacity of rust to significantly impair the photosynthetic apparatus of soybean plants significantly, considering the lower values obtained for F_v/F_m and Y(II) and the smooth increase in Y(NO). It is known that the application of some IR stimuli (e.g., acibenzolar-S-methyl, azelaic acid, hexanoic acid, products containing different nutrients mixed with polyphenolic

compounds, picolinic acid, and phosphites) can attenuate the damage in the photosynthetic process and the pool of pigments caused by pathogens infection (Aucique-Pérez et al. 2019; Chaves et al. 2021; Einhardt et al. 2020; Hawerroth et al. 2023; Oliveira et al. 2022; Picanço et al. 2022; Rodrigues et al., 2023a,b). Tomato plants infected by *Sclerotinia sclerotioum* and sprayed with manganese phosphite exhibited less impairment of the photosynthetic apparatus (increases in F_v/F_m, Y(II), and ETR values) and the preservation of Chl *a+b* and carotenoids in infected leaves (Chaves et al. 2021). In the present study, the spray of IR stimulus greatly alleviated the damage caused by *P. pachyrhizi* at the physiological level. The values of F_v/F_m, Y(II), Y(NPQ), and ETR significantly increased. In contrast, the Y(NO) values decreased in infected and IR stimulus-sprayed plants, confirming less photodamage, an efficient photochemical energy conversion, and high PSII preservation. Consistent with these findings, Picanço et al. (2022) reported great F_v/F_m, Y(II), and ETR values associated with reduced Y(NO) values for soybean plants sprayed with phosphite combined with free amino acids and infected by *P. pachyrhizi* which guaranteed less photodamage that kept an adequate functionality of the photosynthetic apparatus. The infection of soybean leaflets by *P. pachyrhizi* was negatively impacted with the spray of a cooper-polyphenolic compound along with the preservation of photosynthesis [higher Y(II) and ETR values linked with reduced Y(NPQ) and Y(NO) values] and associated pigments (Rodrigues et al. 2023b). The concentrations of Chl *a+b* (at earlier and late stages of rust progress) and carotenoids (at an advanced stage of rust progress) were kept higher for infected and IR stimulus-sprayed plants, highlighting its efficiency in keeping plants with more robust photosynthetic machinery.

The ROS, mainly H_2O_2 and $O_2^{\bullet-}$, is found in plant tissues of different crops infected by pathogens (Kaur et al. 2022). It is known that ROS can greatly impair cell physiology due to lipid peroxidation in the membranes as well as degradation of photosynthetic pigments, proteins, and nucleic acid (Aucique-Pérez et al. 2020; Farooq et al. 2019; Huang et al. 2019; Mohammadi et al. 2021). In some dicots, some types of phosphites promoted hormone signaling pathways or H_2O_2 production (Eshraghi et al. 2014; Gill et al. 2018). In the present study, the concentration and the histochemical accumulation of H_2O_2 and $O_2^{\bullet-}$, along with MDA, a lipid peroxidation marker, were great for infected leaflets of water-sprayed plants due to intensive rust symptoms. In contrast, infected and IR stimulus-sprayed plants displayed less oxidative stress based on lower H_2O_2, $O_2^{\bullet-}$, and MDA concentrations. According to Rodrigues et al. (2023), the histochemical localization ofH_2O_2 and $O_2^{\bullet-}$ in the leaflets of soybean plants infected by *P. pachyrhizi* sprayed with a copper-polyphenolic compound was weakly detected. Genes

involved in oxidoreductase activity (*AOX*) and the ROS pathway were strongly induced in switchgrass infected by *Puccinia emaculata* (Gill et al. 2018).

To cope with infection by pathogens of different lifestyles, plants developed a very efficient defense system that is formed by multilayered mechanisms and strategies (e.g., modification of cell wall composition, production of ROS, expression of various defense-related genes (*PR-1A*, *PR10*, *PAL2.1*, and *PAL3.1*), and high production of phenolics, flavonoids, and phytoalexins (Kaur et al. 2022). Phenolics and lignin precursors, originating from the phenylpropanoid pathway, are of pivotal importance for plant defense against pathogens due to their strong antimicrobial and antioxidant characteristics (Chowdhary et al. 2021; Kumar et al. 2022; Ninkuu et al. 2023; Pratyusha 2022; Yadav et al. 2020). A large body of studies highlights the importance of phenolics and lignin in reducing disease symptoms in plants sprayed with different IR stimuli (Hawerroth et al. 2023; Picanço et al. 2022; Rodrigues et al. 2023a; Silveira et al. 2021). In the present study, TSP and LTGA derivatives concentrations were greatly enhanced on infected leaflets of IR stimulus-sprayed plants, which greatly helped to boost their resistance against *P. pachyrhizi* infection. The spray of phosphite combined with free amino acids helped to increase the pool of TSP and LTGA derivatives in the leaflets of soybean plants infected by *P. pachyrhizi* (Picanço et al. 2022).

During SAR, a plethora of genes (e.g. *CHIB1*, *ICS1*, *ICS2*, *PAL1.1*, *PAL2.1*, *PR1*, and *PR2*) are promptly and strongly up-regulated with the involvement of SA and other molecules (Kaur et al. 2022; Shine et al. 2016; Siah et al. 2018). The SA originates from either phenylpropanoid or isochorismate pathways in which *PAL* and *ICS* play, respectively, an essential role in increasing the amount of this hormone (Kumar et al. 2020; Ninkuu et al. 2023; Vlot et al. 2020). In soybean, an array of molecules and IR stimuli (e.g., acibenzolar-S-methyl, azelaic acid, cooper-polyphenolic compound, hexanoic acid, jasmonic acid, nickel, phosphite combined with free amino acids, and silicon) were reported to efficiently stimulate the expression of many defense-related genes (*PAL2.1*, *PAL3.1*, *ICS1*, *ICS2*, *PR-1A*, *PR10*, and *CHIB1*) involved in SAR (Cruz et al. 2020; Einhardt et al. 2020; Paula et al. 2021; Picanço et al. 2022; Rodrigues et al. 2023a,b). In the present study, *PAL2.1* (at 3 and 10 dai), *ICS1* (at 3, 5, and 10 dai), and *ICS2* (at 3 and 5 dai) were up-regulated for non-infected and IR stimulus-sprayed plants, indicating elicitation of host defense reactions. On the other hand, *PAL2.1*, *PAL3.1*, *ICS1*, and *ICS2* were strongly up-regulated during the time course of *P. pachyrhizi* infection process in IR stimulus sprayed plants, indicating the role played by these genes for the increased resistance of soybean plants. The expression of the genes mentioned above was strongly linked to the great pool of TSP and LTGA derivatives noticed in infected leaflets of

IR-stimulus sprayed plants that displayed lower rust symptoms and fungus reproduction. The spray of soybean plants with phosphites formulated with copper and manganese increased PAL activity, which boosted their resistance against rust (Bruzamarello et al. 2018). The up-regulation of *PR* genes in response to pathogen infection plays an essential role in plant defense during SAR (Kaur et al. 2022; Santos and Franco 2023). The *PR1* is a molecular marker for SAR (Santos and Franco 2023; Zribi et al. 2021). In the present study, *PR-1A* and *PR10* were up-regulated for both non-infected and infected leaflets of IR stimulus-sprayed plants, confirming a rise in their basal resistance level. Interestingly, these genes were strongly up-regulated during the time course evaluated for the infected, and IR-stimulus sprayed plants may be linked to reduced rust severity. Soybean plants sprayed with potassium phosphite and infected by *P. pachyrhizi* displayed great *PR1* expression and less rust severity (Gill et al. 2018). In addition, Guo et al. (2021) reported more robust up-regulation of *PR1* in leaves, stems, and roots of soybean plants infected by *Phytophthora sojae* after spraying with K phosphite. Chalcone isomerase, encoded by *CHIB1,* participates in the flavonoid pathway, leading to the biosynthesis of different antimicrobial compounds against pathogens (Zhou et al. 2018). In the present study, *CHIB1* was up-regulated for non-infected and IR stimulus-sprayed plants only at 1 and 3 dai while for infected and IR-stimulus sprayed stronger up-regulated of this gene occurred during the entire time-course evaluated, confirming, therefore, the potential of this IR stimulus to boost soybean defense against *P. pachyrhizi* infection. Rodrigues et al. (2023a) also reported up-regulation of *CHIB1* in leaflets of soybean plants sprayed with a cooper-polyphenolic compound and infected or not with *P. pachyrhizi*.

Plants can express SAR or ISR in response to infection by pathogens from different lifestyles without discarding that crosstalk between them may also occur at some point on their signal transduction pathways (Aerts et al. 2020; Kaur et al. 2022; Kesel et al. 2021; Paula et al. 2021). Different variables [e.g., level of cultivar resistance, type of the IR stimulus (rate and time of application), and the lifestyle of the pathogen and its level of aggressiveness] may modulate the response of plants against pathogen infection in terms of which pathway to be activated if mediated by SA or JA/ET (Llorens et al. 2017; Siah et al. 2018; Vlot et al. 2021; Zeier 2021). In soybean-*P. pachyrhizi* interaction, several studies reported the activation of the JA/ET pathway by different types of IR stimuli (e.g., azelaic acid, calcium silicate, copper-polyphenolic compound, hexanoic acid, and jasmonic acid) (Cruz et al. 2020; Rodrigues et al. 2023a,b). In the present study, genes involved in the jasmonic acid (*JAR*, *LOX7*, and *OPR3*) and ethylene (*ETR1*, *ACS*, and *ACO*) pathways were strongly up-regulated in infected and IR stimulus-sprayed plants at earlier and advanced stages of fungal infection. This finding

confirms the participation of the JA/ET pathway in the soybean defense against rust for being exposed to the IR stimulus. On top of that, the IR stimulus-sprayed plants not infected by *P. pachyrhizi* displayed earlier up-regulation of *JAR*, *OPR3*, *ETR1*, *ACS*, and *ACO*, suggesting, therefore, their priming resistance of these plants. Gill et al. (2018) reported remarkable up-regulation of *OPR* in switchgrass infected by *P. emaculata* in response to K phosphite treatment. Tomato plants sprayed with phosphite combined with free amino acids and infected by *Septoria lycopersici* activated the JA/ET pathway (stronger expression of *ACO2*, *ACO3*, *ACO4*, *ACO5*, *LOX1.1*, *LOXB*, *LOXC*, and *PDF1.2*) and exhibited increased resistance against fungal infection (Silva et al. 2022). It is tempting to assume that the IR stimulus used in the present study was efficient in priming plants for both SA and JA/ET signaling pathways and, therefore, contributed to reducing rust severity. According to Rodrigues et al. (2023a), both SA and JA/ET pathways were involved in the resistance of soybean plants against *P. pachyrhizi* infection (great up-regulation of *URE*, *ICS2*, *CHIB1*, *PAL1.1*, *PAL2.1*, *PAL3.1*, *PR1-A*, *SABATH2*, *JAR1*, *PR10*, *MMP2*, *NAC19*, *ETR1*, and *OPR3*) after being elicited by hexanoic acid.

In conclusion, biochemical, molecular, and physiological evidence in this study shows the potential of using the phosphite of K and Ni to boost soybean resistance against rust. It was evidenced in the PCA analysis that infected and IR stimulus-sprayed plants displayed remarkable differences from the infected and water-sprayed plants, considering the outcome of all variables and parameters studies. In short, infected and IR stimulus-sprayed plants were more responsive against *P. pachyrhizi* infection based on the different sets of defense responses (earlier and stronger activation of genes involved in SA and JA/ET signaling pathways, lower cellular damage, more production of phenolics and lignin, preservation of the photosynthetic apparatus, and great foliar concentrations of K and Ni). Together, these results open the way for using this IR stimulus as an eco-friendly alternative in integrated rust management to decrease yield losses and improve grain quality.

References

Ahmed HF, Elnaggar S, Abdel-Wahed GA, Taha RS, Ahmad A, Al-Selwey WA, Seleiman MF (2023) Induction of systemic resistance in *Hibiscus sabdariffa* Linn to control root rot and wilt diseases using biotic and abiotic inducers. Biology 12:789

Aerts N, Pereira Mendes M, Van Wees SC (2021) Multiple levels of crosstalk in hormone networks regulating plant defense. The Plant Journal 105:489-504

Amtmann A, Srivastava AK (2023) Potassium and plant disease. In: Datnoff LE, Elmer WH, and Rodrigues FA (Eds.) Mineral and Plant Nutrition. The American Phytopathological Society, St. Paul. pp. 105-140

Aucique-Pérez CE, Resende RS, Neto LBC, Dornelas F, DaMatta FM, Rodrigues FA (2019) Picolinic acid spray stimulates the antioxidative metabolism and minimizes impairments on photosynthesis on wheat leaves infected by *Pyricularia oryzae*. Physiologia Plantarum 167:628-644

Aucique-Pérez CE, Resende RS, Martins AO, Silveira PR, Cavalcanti JHF, Vieira NM, Rodrigues FA (2020) How do wheat plants cope with *Pyricularia oryzae* infection? A physiological and metabolic approach. Planta 252:1-17

Awasthi JP, Saha B, Chowardhara B, Devi SS, Borgohain P, Panda SK (2018) Qualitative analysis of lipid peroxidation in plants under multiple stress through schiff's reagent: a histochemical approach. Bio-Protocol 8:2807-2807

Baker NR (2008) Chlorophyll fluorescence: a probe of photosynthesis *in vivo*. Annual Review of Plant Biology 59:89-113

Bock CH, Pisani C, Wood BW (2023) Nickel and plant disease. In: Datnoff LE, Elmer WH, Rodrigues FA (Eds.) Mineral nutrition and plant disease. APS Press, St. Paul. pp. 355-378

Bruzamarello J, Franceschi VT, Dalacosta NL, Gonçalves I, Mazaro SM, Reis E (2018) Potencial de fosfitos na indução da resistência em plantas de soja. Agronomic Crop Journal 27:263-273

Cacique IS, Bispo WMS, Araujo L, Aucique-Pérez CE, Rios JA, Silva LC, Rodrigues FA (2017) Potassium-modulated physiological performance of mango plants infected by *Ceratocystis fimbriata*. Bragantia 76:521-535

Cakmak I, Horst WJ (1991) Effect of aluminum on lipid peroxidation, superoxide dismutase, catalase, and peroxidase activities in root tips of soybean (*Glycine max*). Physiologia Plantarum 83:463-468

Chaitanya KSK, Naithani SC (1994) Role of superoxide lipid peroxidation and superoxide dismutase in membrane perturbation during loss of variability in seeds of *Shorea robusta*. New Phytologist 126:623-627

Chaves JAA, Oliveira LM, Silva LC, Silva BN, Dias CS, Rios JA, Rodrigues FA (2021) Physiological and biochemical responses of tomato plants to white mold affected by manganese phosphite. Journal of Phytopathology 169:149-167

Choudhary DK, Prakash A, Johri BN (2007) Induced systemic resistance (ISR) in plants: mechanism of action. Indian Journal of Microbiology 47:289-297

Choudhary KK, Singh, S, Agrawal M, Agrawal SB (2021) Role of jasmonic and salicylic acid signaling in plants under UV-B stress. In: Aftab, T., Yusuf, M. (eds) Jasmonates and Salicylates Signaling in Plants. Signaling and Communication in Plants. Springer, Cham.

Clark RB (1975) Characterization of phosphatase of intact maize roots. Journal of Agriculture and Food Chemistry 23:458-460

Cruz MFA, Pinto MO, Barros EG, Rodrigues FA (2020) Differential gene expression in soybean infected by *Phakopsora pachyrhizi* in response to acibenzolar-S-methyl, jasmonic acid and silicon. Journal of Phytopathology 168:571-580

Dempsey DMA, Klessig DF (2012) SOS-too many signals for systemic acquired resistance?. Trends in Plant Science 17:538-545

Durrant WE, Dong X (2004) Systemic acquired resistance. Annual Review of Phytopathology 42:185-209

Einhardt AM, Ferreira S, Hawerroth C, Valadares SV, Rodrigues FA (2020) Nickel potentiates soybean resistance against infection by *Phakopsora pachyrhizi*. Plant Pathology 69:849-859

Einhardt AM, Ferreira S, Souza GM, Mochko AC, Rodrigues FA (2020) Cellular oxidative damage and impairment on the photosynthetic apparatus caused by Asian soybean rust on soybeans are alleviated by nickel. Acta Physiologiae Plantarum 42:1-13

Eshraghi L, Anderson JP, Aryamanesh N, McComb JA, Shearer B, Hardy GE (2014) Defence signalling pathways involved in plant resistance and phosphite-mediated control of *Phytophthora cinnamomi*. Plant Molecular Biology Reporter 32:342-356

Fagundes-Nacarath IRF, Debona D, Brás VV, Silveira PR, Rodrigues FA (2018) Phosphites attenuate *Sclerotinia sclerotiorum*-induced physiological impairments in common bean. Acta Physiologiae Plantarum 40:1-14

Farooq MA, Niazi AK, Akhtar J, Farooq M, Souri Z, Karimi N, Rengel Z (2019) Acquiring control: The evolution of ROS-Induced oxidative stress and redox signaling pathways in plant stress responses. Plant Physiology and Biochemistry 141:353-369

Fernández V, Brown PH (2013) From plant surface to plant metabolism: the uncertain fate of foliar-applied nutrients. Frontiers in Plant Science 4:289

Franceschi VT, Alves KS, Mazaro SM, Godoy CV, Duarte HSS, Ponte EMD (2019) A new standard diagram set for assessment of severity of soybean rust improves accuracy of estimates and optimizes resource use. Plant Pathology 69:495-505

Gill US, Sun L, Rustgi S, Tang Y, Wettstein D, Mysore KS (2018) Transcriptome-based analyses of phosphite-mediated suppression of rust pathogens *Puccinia emaculata* and *Phakopsora pachyrhizi* and functional characterization of selected fungal target genes. Plant Journal 93:894-904

Godoy CV, Seixas CDS, Soares RM, Marcelino-Guimarães FC, Meyer MC, Costamilan LM (2016) Asian soybean rust in Brazil: past, present, and future. Pesquisa Agropecuária Brasileira 51:407-421

Goellner K, Loehrer M, Langenbach C, Conrath UWE, Koch E, Schaffrath U (2010) *Phakopsora pachyrhizi*, the causal agent of Asian soybean rust. Molecular Plant Pathology 11:169-177

Guo M, Li B, Xiang Q, Wang R, Liu P, Chen Q (2021) Phosphite translocation in soybean and mechanisms of *Phytophthora sojae* inhibition. Pesticide Biochemistry and Physiology 172:104757

Hammerschmidt R (2009) Systemic acquired resistance. Advances in Botanical Research 51:173-222

Hao Q, Yang H, Chen S, Qu Y, Zhang C, Chen L, Zhou X (2023) RNA-Seq and comparative transcriptomic analyses of asian soybean rust resistant and susceptible soybean genotypes provide insights into identifying disease resistance genes. International Journal of Molecular Sciences 24:13450

Hartman GL, Sikora EJ, Rupe JC (2015) Rust. In: Hartman GL, Rupe JC, Sikora EJ, Domier LL, Davis JA, Stefey KL (Ed.) Compendium of soybean diseases and pests. American Phytopathological Society, Saint Paul. p. 56-58

Havlin JL, Schlegel AJ (2021) Review of phosphite as a plant nutrient and fungicide. Soil Systems 5:52

Hawerroth C, Einhardt AM, Fontes BA, Brás VV, Valadares SV, Rodrigues FA (2023) Nickel enhances rice resistance against *Bipolaris oryzae* infection. Plant and Soil (in press)

Heath RL, Packer L (1968) Photoperoxidation in isolated chloroplasts I. Kinetics and stoichiometry of fatty acid peroxidation. Archives of Biochemistry and Biophysics 125:189-198

Huang H, Ullah F, Zhou DX, Yi M, Zhao Y (2019) Mechanisms of ROS regulation of plant development and stress responses. Frontiers in Plant Science 10:800

Kashiwa T, Muraki Y, Yamanaka N (2020) Near-isogenic soybean lines carrying Asian soybean rust resistance genes for practical pathogenicity validation. Scientific Reports 10:13270

Kato M, Soares RM (2022) Field trials of a *Rpp*-pyramided line confirm the synergistic effect of multiple gene resistance to Asian soybean rust (*Phakopsora pachyrhizi*). Tropical Plant Pathology 47:222-232

Kaur S, Samota MH, Choudhary M, Choudhary M, Pandey AK, Sharma A, Thakur J (2022) How do plants defend themselves against pathogens - Biochemical mechanisms and genetic interventions. Physiology and Molecular Biology of Plants 28:485-504

Kelly HY, Dufault NS, Walker DR, Isard SA, Schneider RW, Giesler LJ, Hartman GL (2015) From select agent to an established pathogen: the response to *Phakopsora pachyrhizi* (soybean rust) in North America. Phytopathology 105:905-916

Kesel J, Conrath U, Flors V, Luna E, Mageroy MH, Mauch-Mani B, Pastor V, Pozo MJ, Pieterse CMJ, Ton J, Kyndt T (2021) The induced resistance lexicon: do's and don'ts. Trends in Plant Science 26:685-691

Kramer DM, Johnson G, Kiirats O, Edwards GE (2004) New fluorescence parameters for the determination of QA redox state and excitation energy fluxes. Photosynthesis Research 79:209-218

Kumar S, Abedin MM, Singh AK, Das S (2020) Role of phenolic compounds in plant-defensive mechanisms. Plant Phenolics in Sustainable Agriculture 1:517-532

Langenbach C, Campe R, Beyer SF, Mueller AN, Conrath U (2016) Fighting Asian soybean rust. Frontiers in Plant Science 7:797

Lima IP, Bruzi AT, Botelho FBS, Zambiazzi EV, Soares IO, Zuffo AM (2015) Performance of conventional and transgenic soybean cultivars in the south and Alto Paranaiba regions of Minas Gerais, Brazil. American Journal of Plant Sciences 6:1385

Liu Y, Burke DJ, Medeiros JS, Carrino-Kyker SR, Burns JH (2023) Phosphite indirectly mediates protection against root rot disease via altering soil fungal community in *Rhododendron* species. Plant and Soil 1-12

Livak KJ, Schmittgen TD (2001) Analysis of relative gene expression data using real-time quantitative PCR and the $2^{-\Delta\Delta CT}$ method. Methods 25:402-408

Llorens E, García-Agustín P, Lapeña L (2017) Advances in induced resistance by natural compounds: towards new options for woody crop protection. Scientia Agricola 74:90-100

Mehta S, Kumar A, Achary VMM, Ganesan P, Patel A, Singh A, Reddy MK (2022) Antifungal and defense elicitor activity of potassium phosphite against fungal blast disease on ptxD-OE transgenic indica rice and its acceptor parent. Pesticide Biochemistry and Physiology 182:105026

Miles MR, Levy C, Morel W, Mueller T, Steinlage T, Rij N, Frederick RD, Hartman GL (2007) International fungicide efficacy trials for the management of soybean rust. Plant Disease 91:1450-1458

Mohammadi MA, Cheng Y, Aslam M, Jakada BH, Wai MH, Ye K, Qin Y (2021) ROS and oxidative response systems in plants under biotic and abiotic stresses: revisiting the crucial role of phosphite triggered plants defense response. Frontiers in Microbiology 12:631318

Moore KJ, Dixon PM (2015) Analysis of combined experiments revisited. Agronomy Journal 107:763-771

Mortel M, Recknor JC, Graham MA, Nettleton D, Dittman JD, Nelson RT, Godoy CV, Abdelnoor RV, Almeida AMR, Baum TJ, Whitham SA (2007) Distinct biophasic mRNA changes in response to Asian soybean rust infection. Molecular Plant-Microbe Interactions 20:887-899

Ninkuu V, Yan J, Fu Z, Yang T, Ziemah J, Ullrich MS, Zeng H (2022) Lignin and its pathway-associated phytoalexins modulate plant defense against fungi. Journal of Fungi 9:52

Novaes MIC, Debona D, Fagundes-Nacarath IRF, Brás VV, Rodrigues FA (2019) Physiological and biochemical responses of soybean to white mold affected by manganese phosphite and fluazinam. Acta Physiologiae Plantarum 41:1-16

Oliveira LM, Araujo MU, Silva BN, Chaves JA, Pinto LF, Silveira PR, Rodrigues FA (2022) Maize resistance to northern corn leaf blight is potentiated by nickel. Plant Pathology 71:262-278

Otolakoski MG, Viegas BG, Bagio BZ, Blum MMC, Suzana-Milan CS, Huzar-Novakowiski J (2023) Reduction of the severity of Asian soybean rust with foliar application of silicon dioxide. Crop Protection 173:106387

Paula S, Holz S, Souza DHG, Pascholati SF (2021) Potential of resistance inducers for soybean rust management. Canadian Journal of Plant Pathology 43:298-307

Picanço BBM, Ferreira S, Fontes BA, Oliveira LM, Silva BN, Einhardt AM, Rodrigues FA (2021) Soybean resistance to *Phakopsora pachyrhizi* infection is barely potentiated by boron. Physiological and Molecular Plant Pathology 115:101668

Picanço BB, Silva BN, Rodrigues FA (2022) Potentiation of soybean resistance against *Phakopsora pachyrhizi* infection using phosphite combined with free amino acids. Plant Pathology 71:1496-1510

Pratyusha, S (2022) Phenolics compounds in the plant development and defense: an overview. In: Plant Stress Physiology: Perspectives in Agriculture

Reglinski T, Havis N, Rees HJ, Jong H (2023) The practical role of induced resistance for crop protection. Phytopathology 113:719-731

Rios VS, Rios JA, Aucique-Pérez CE, Silveira PR, Barros AV, Rodrigues FA (2018) Leaf gas exchange and chlorophyll *a* fluorescence in soybean leaves infected by *Phakopsora pachyrhizi*. Journal of Phytopathology 166:75-85

Rodrigues FCT, Araujo MUP, Silva BN, Fontes BA, Rodrigues FA (2023) A copper-polyphenolic compound as an alternative for the control of Asian soybean rust. Tropical Plant Pathology 1-15

Rodrigues FCT, Silveira PR, Cacique IS, Oliveira LM, Rodrigues FA (2023) Azelaic and hexanoic acids-inducing resistance in soybean against *Phakopsora pachyrhizi* infection. Plant Pathology 72:1034-1047

Rosa CRE, Spehar CR, Liu JQ (2015) Asian soybean rust resistance: an overview. Journal of Plant Pathology and Microbiology 6:307

Santos C, Franco OL (2023) Pathogenesis-related proteins (PRs) with enzyme activity activating plant defense responses. Plants 12: 2226

Shah J, Zeier J (2013) Long-distance communication and signal amplification in systemic acquired resistance. Frontiers in Plant Science 4:30

Shaner G, Finney RE (1977) The effect of nitrogen fertilization on the expression of slow-mildewing resistance in Knox wheat. Phytopathology 67:1051-1056

Shine MB, Yang JW, El-Habbak M, Nagyabhyru P, Fu DQ, Navarre D, Kachroo A (2016) Cooperative functioning between phenylalanine ammonia lyase and isochorismate synthase activities contributes to salicylic acid biosynthesis in soybean. New Phytologist 212:627-636

Siah A, Magnin-Robert M, Randoux B, Choma C, Rivière C, Halama P, Reignault P (2018) Natural agents inducing plant resistance against pests and diseases. Natural Antimicrobial Agents 121-159

Silva BN, Picanço BBM, Hawerroth C, Silva LC, Rodrigues FA (2022) Physiological and biochemical insights into induced resistance on tomato against septoria leaf spot by a phosphite combined with free amino acids. Physiological and Molecular Plant Pathology 120:101854

Silva BN, Picanço BB, Martins SC, Rodrigues FA (2023) Impairment of the photorespiratory pathway on tomato leaves during the infection process of *Septoria lycopersici*. Physiological and Molecular Plant Pathology 125:102020

Silveira PR, Aucique-Pérez CE, Cruz MFA, Rodrigues FA (2021) Biochemical and physiological changes in maize plants supplied with silicon and infected by *Exserohilum turcicum*. Journal of Phytopathology 169:393-408

Sood D, Sharma M, Sharma A (2023) Abiotic resistance inducers for management of bacterial wilt in tomato (*Solanum lycopersicum* L.). Journal of Plant Pathology 105:481-491

Sun, J, Mooney H, Wu W, Tang H, Tong Y, Xu Z, Liu J (2018) Importing food damages domestic environment: Evidence from global soybean trade. Proceedings of the National Academy of Sciences 115:5415-5419

Tatagiba SD, Rodrigues FA, Filippi MCC, Silva GB, Silva LC (2014) Physiological responses of rice plants supplied with silicon to *Monographella albescens* infection. Journal of Phytopathology 162:596-606

Tistama R, Mawaddah PAS, Ade-Fiprinil LUBIS, Junaidi J (2019) Physiological status of high and low metabolism *Hevea* clones in the difference stage of tapping panel dryness. Journal of Biological Diversity 20

Velikova V, Yordanov I, Edreva A (2000) Oxidative stress and some antioxidant systems in acid rain-treated bean plants: Protective role of exogenous polyamines. Plant Science 151:59-66

Vlot AC, Sales JH, Lenk M, Bauer K, Brambilla A, Sommer A, Chen Y, Wenig M, Nayem S (2021) Systemic propagation of immunity in plants. New Phytologist 229:1234-1250

Wang M, Zheng Q, Shen Q, Guo S (2013) The critical role of potassium in plant stress response. International Journal of Molecular Sciences 14:7370-7390

Yadav V, Wang Z, Wei C, Amo A, Ahmed B, Yang X, Zhang X (2020) Phenylpropanoid pathway engineering: An emerging approach towards plant defense. Pathogens 9:312

Zeier J (2021) Metabolic regulation of systemic acquired resistance. Current Opinion in Plant Biology 62:102050

Zhou Y, Huang JL, Zhang XL, Zhu LM, Wang XF, Guo N, Xing H (2018) Overexpression of chalcone isomerase (CHI) increases resistance against *Phytophthora sojae* in soybean. Journal of Plant Biology 61:309-319

Zribi I, Ghorbel M, Brini F (2021) Pathogenesis related proteins (PRs): From cellular mechanisms to plant defense. Current Protein and Peptide Science 22:396-412

Table and Figures

Table 1. Primer sequences used to study the expression of the following genes: phenylalanine ammonia-lyase (*PAL2.1* and *PAL3.1*), chalcone isomerase (*CHI1B1*), lipoxygenase (*LOX7*), pathogenesis-related protein 1 (*PR-1A*), pathogenesis-related protein 10 (*PR10*), isochorismate synthase (*ICS1* and *ICS2*), jasmonic acid-amino synthetase (*JAR1*), ethylene receptor 1 (*ETR1*), 1-aminocyclopropane-1-carboxylic acid oxidase (*ACO*), 1-aminocyclopropane-1-carboxylic synthase (*ACS*), 12-oxophytodienoic acid reductase 3 (*OPR3*), glyceraldehyde 3-phosphate dehydrogenase (GAPDH), translation elongation factor 1α of *Phakopsora pachyrhizi* (*TEF-1α*), and Ubiquitin-3 (*UBIQ*) from soybean.

Genes	GenBank	Primer sense 5'-3'	Primer antisense 5'-3'
PAL2.1	*Glyma.10G058200*	ATCTCCCTCCACTCACCATA	GTTCAAGGGGTCATTAGCAC
PAL3.1	*Glyma.02G309300*	TGCTCTTCAGAAGGAAATGGT	GTTGCTGATTTAGGCAGTGT
CHI1B1	*Glyma.20G2416001*	GTTTCCCCTGCTTTGAAAGAGA	GGATTGGCCTCTAACTCTTTGAAG
LOX7	*Glyma.13G347800*	ACAAGCTAGGCACAACAAAA	TTGTTTCCTCCGATGATTCCAA
PR-1A	*Glyma.09G040500*	GCACTACACACAGGTCGTTTGG	CCTCCGTTATCACATGTCACTTTG
PR10	*Glyma.07G243651v4*	AAATCAACTCCCCTGTGGCTC	CCACCATTTCCCTCAACGTTT
ICS1	*Glyma.01G104100*	GAAACAGTACAGTCCCTGCT	TGTGGCTGGGAAAAGAAAAC
ICS2	*Glyma.03G070600*	GCAACATCCTCGTACCTCTT	CTCTCTGCAACCGTTCATTG
JAR1	*Glyma.07G057900*	AGCCGTATGGTTGTGTTGTTC	TGCAGCATTGGGATTGGAGT
ETR1	*Glyma.19g40090*	ATGGATGCCTTCAAGAAGTGG	GCACATATCTTCCCACAAGAGG
ACS	*Glyma.05g36250*	CTCTTAACCTTCATTCTTGCTAACC	TTGCTTCTGCTTCTTTGTATGC
ACO	*Glyma.14g05350*	CCAATGCGCCATTCCATTGTTG	TGAGGCTACGGACATTCTGGTC
OPR3	*Glyma.13G109800*	GTGTATCAGCCTGGTGGG	GTGTATCAGCCTGGTGGG
GAPDH	*Glyma.04G193500*	AAGGGTGGTGCAAAGAAGGT	TCTGGCTTGTACTCGTGCTC
TEF-1α	*Glyma.07G060900*	ATTCGAAGCCGGTATTTCTAAAG	CCACTTGGTTGTGTCCATCTTAT
UBIQ	*Glyma.20g141600*	TGTAATGTTGGATGTGTTCCC	GGGACACAATTGAGTTCAACA

Table 2. Analysis of variance for the effects of products (P), plant inoculation (PI), and the interaction P × PI for urediniospores germination (UG), soybean rust (SR) severity, area under disease progress curve (AUDPC), foliar nickel (Ni) and potassium (K) concentrations, concentrations of total chlorophyll *a*+*b* (Chl *a*+*b*) and carotenoids (Car), parameters of chlorophyll (Chl) *a* fluorescence [maximum PSII quantum efficiency (F_v/F_m), photochemical yield (Y(II)), yield for dissipation by down-regulation (Y(NPQ)), yield for other non-photochemical (non-regulated) losses (Y(NO)), and electron transport rate (ETR)], concentrations of total soluble phenolics (TSP), lignin-thioglycolic acid (LTGA) derivatives, malondialdehyde (MDA), hydrogen peroxide (H_2O_2), and superoxide ($O_2^{\bullet-}$) as well as the expression of genes coding for phenylalanine ammonia-lyase (*PAL2.1* and *PAL3.1*), chalcone isomerase (*CHI1B1*), lipoxygenase (*LOX7*), pathogenesis-related protein 1 (*PR-1A*), pathogenesis-related protein 10 (*PR10*), isochorismate synthase (*ICS1* and *ICS2*), jasmonic acid-amino synthetase (*JAR1*), ethylene receptor 1 (*ETR1*), 1-aminocyclopropane-1-carboxylic acid oxidase (*ACO*), 1-aminocyclopropane-1-carboxylic synthase (*ACS*), 12-oxophytodienoic acid reductase 3 (*OPR3*), and the translation elongation factor 1α of *Phakopsora pachyrhizi* (*TEF-1α*).

Variables/Parameters	IR stimulus	PI	IR stimulus × PI
UG	**<0.001**	-	-
SR severity	**<0.001**	-	-
AUDPC	**<0.001**	-	-
Ni	**<0.001**	0.975	0.975
K	**<0.001**	**0.010**	**0.044**
Chl *a*+*b*	**0.018**	**<0.001**	**0.007**
Car	**<0.001**	**<0.001**	**<0.001**
F_v/F_m	0.385	0.986	0.053
Y(II)	**<0.001**	**<0.001**	**<0.001**
Y(NPQ)	**<0.001**	**0.030**	**<0.001**
Y(NO)	**<0.001**	**0.004**	**<0.001**
ETR	**<0.001**	**<0.001**	**<0.001**
MDA	**<0.001**	**<0.001**	**<0.001**
H_2O_2	**<0.001**	**<0.001**	**0.029**
$O_2^{\bullet-}$	**0.026**	**0.006**	**0.021**
TSP	**0.006**	**0.013**	**<0.001**
LTGA derivatives	**<0.001**	0.572	**<0.001**
PAL2.1	**0.006**	**0.006**	**0.006**
PAL3.1	**<0.001**	0.102	0.099
CHIB1	**<0.001**	**<0.001**	**<0.001**
LOX7	**0.002**	**0.003**	**0.002**

PR-1A	**0.031**	**0.032**	**0.032**
PR10	**<0.001**	**<0.001**	**<0.001**
ICS1	**<0.001**	**0.013**	**0.014**
ICS2	**0.046**	**0.043**	**0.046**
JAR1	0.683	0.002	0.434
ETR1	**<0.001**	**<0.001**	**<0.001**
ACS	**<0.001**	0.075	**<0.001**
ACO	**<0.001**	0.289	**0.004**
OPR3	**<0.001**	**<0.001**	**<0.001**
TEF-1α	**<0.001**	-	-

Bold values are significant at $P \leq 0.05$.

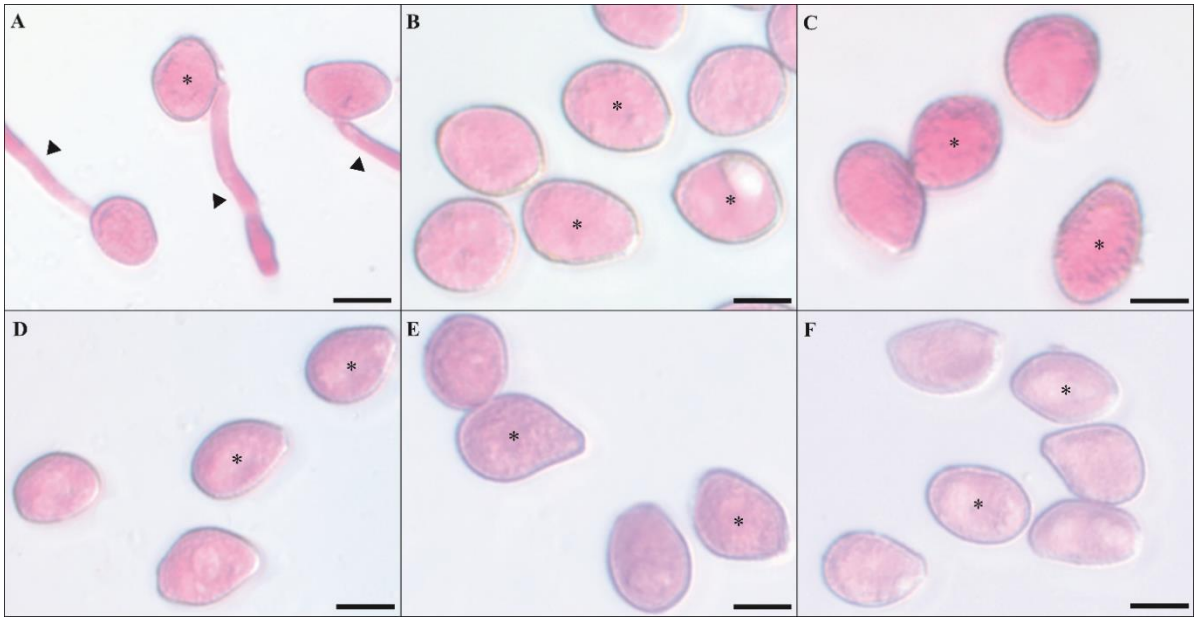

Figure 1. Aspects of the germination of *Phakopsora pachyrhizi* urediniospores in glass slides containing different rates of induced resistance (IR) stimulus (2, 5, 7, 10, and 15 mL L^{-1}, respectively to B, C, D, E, and F). Control treatment corresponded to urediniospores suspension without IR stimulus (A). Germ tube (▼) and urediniospores (*). Scale bars = 5 μm.

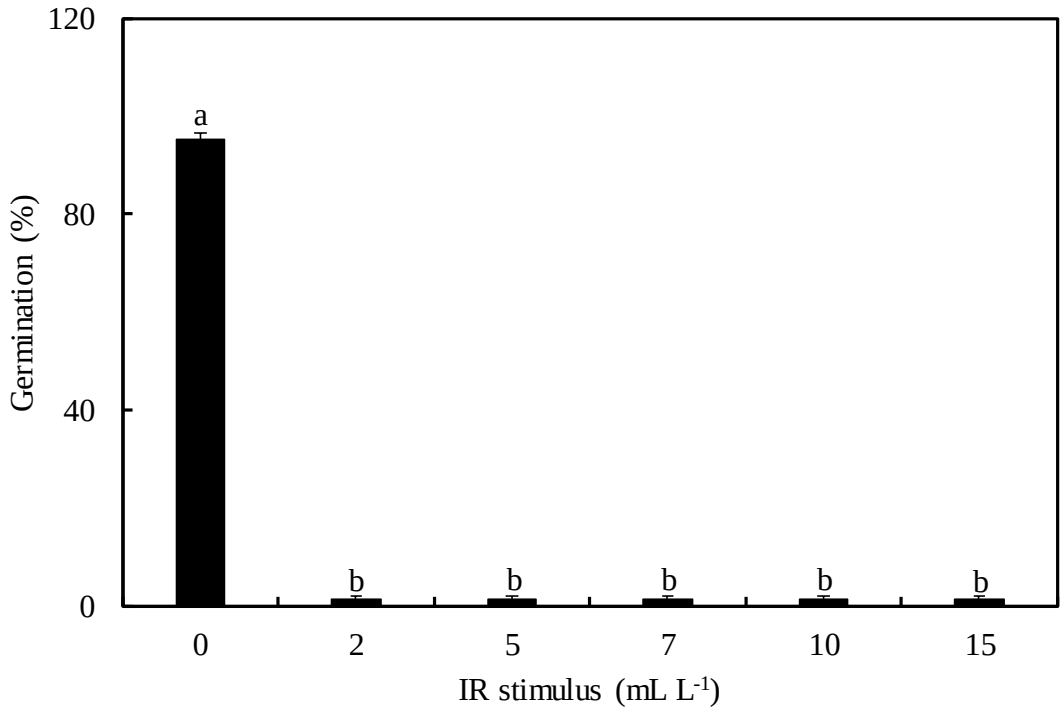

Figure 2. Urediniospore germination of *Phakopsora pachyrhizi* in Petri dishes containing agar-agar medium non-amended (control) or amended with different rates of IR stimulus. Means from each treatment followed by different letters are significantly different ($P \leq 0.05$) according to Tukey's test. Bars represent the standard error of the means.

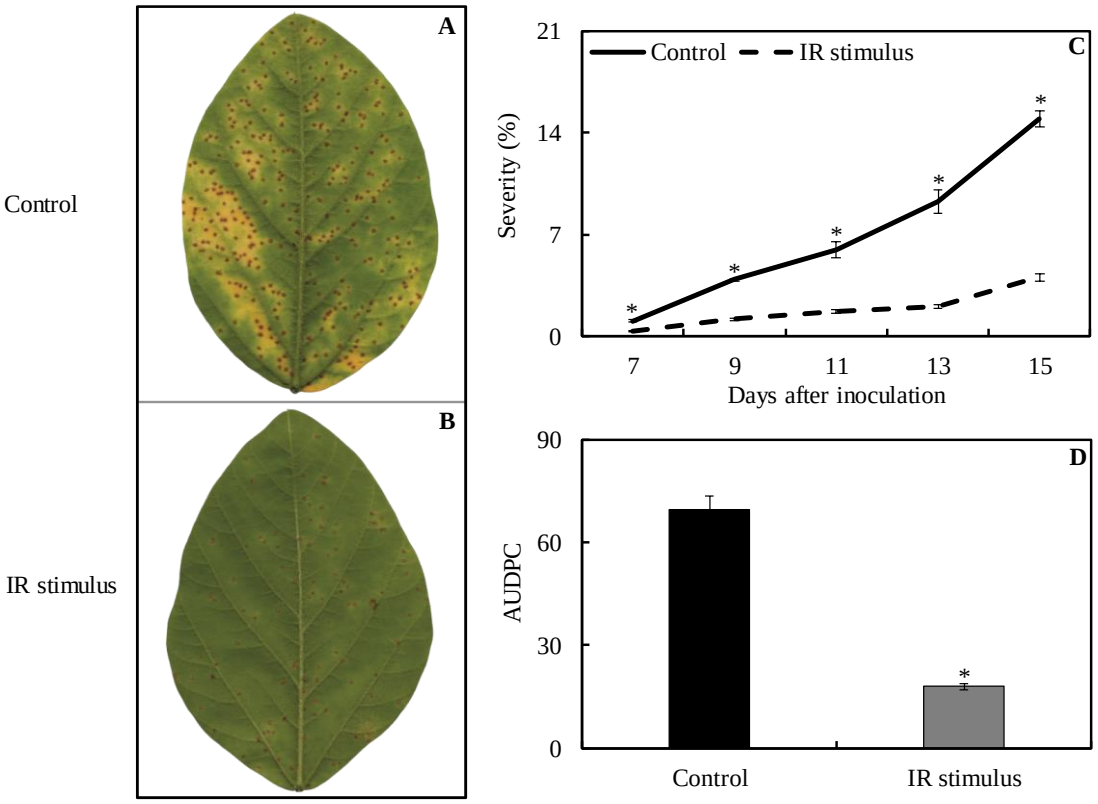

Figure 3. Symptoms (chlorosis and necrosis) (A and B) and severity (C) of soybean rust as well as area under disease progress curve (AUDPC) (D) for soybean plants sprayed with water (control) or with the induced resistance (IR) stimulus. Means for control and IR stimulus followed by an asterisk (*), at each evaluation time, (C) or between these treatments for AUDPC followed by * (D) are significantly different ($P \leq 0.05$) according to the *F* test. Bars represent the standard error of the means.

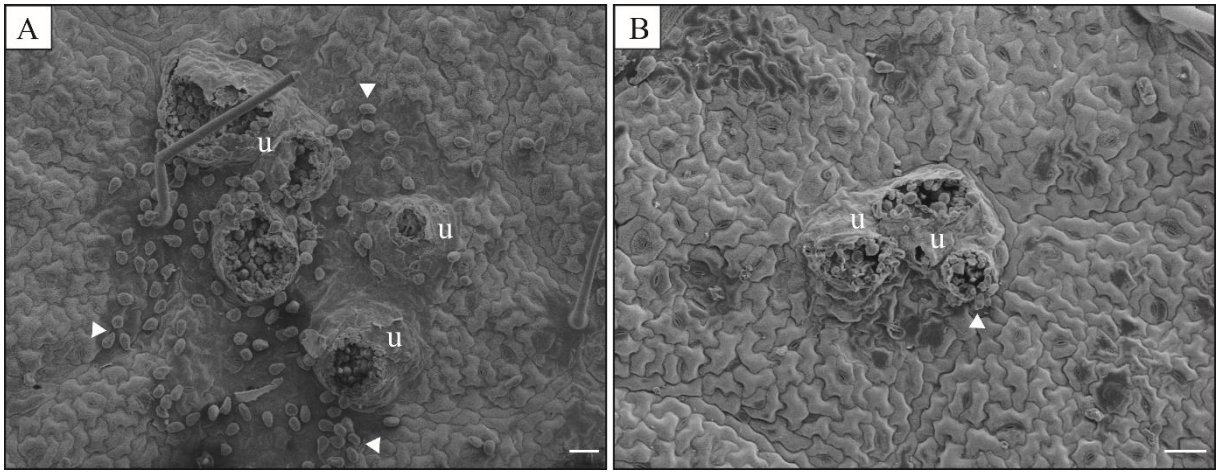

Figure 4. Scanning electron micrographs of the abaxial leaf surface of soybean plants at 15 days after inoculation with *Phakopsora pachyrhizi* and sprayed with water (control) (A) and induced resistance (IR) stimulus (B). Uredia (u) and urediniospores (arrowhead). Scale bars = 50 μm.

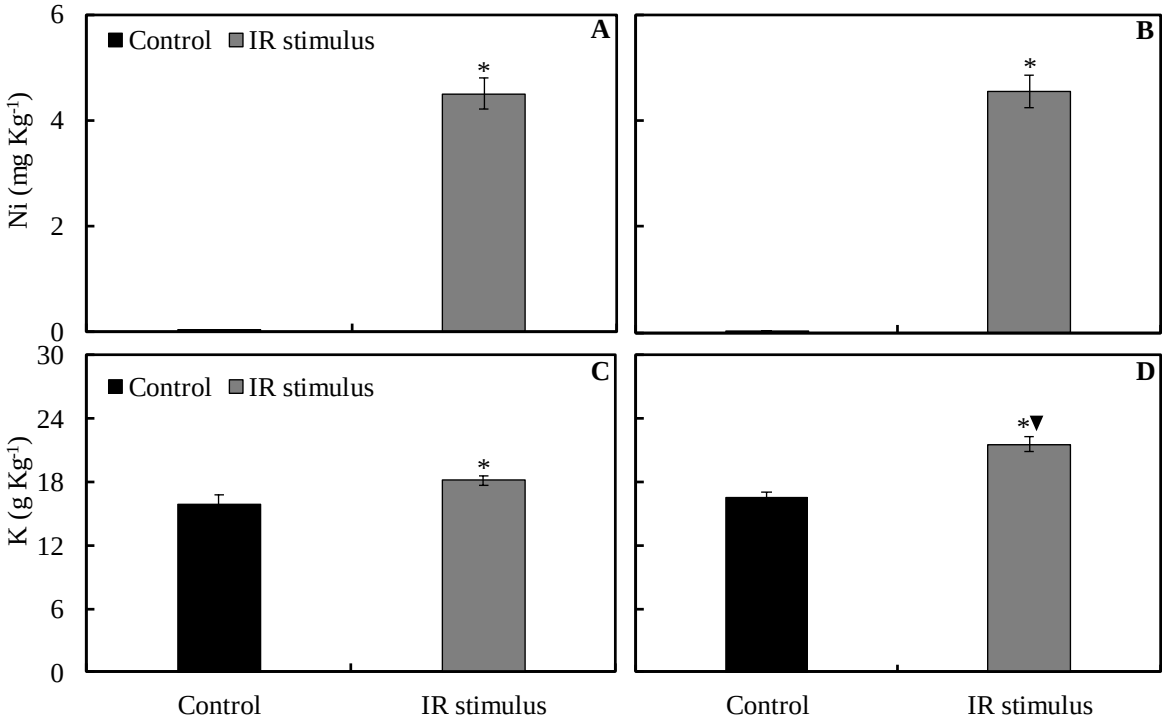

Figure 5. Foliar concentration of nickel (Ni) and potassium (K) for soybean plants non-inoculated (NI) (A) or inoculated (I) (B) with *Phakopsora pachyrhizi* and sprayed with water (control) or with induced resistance (IR) stimulus. Means for control and IR stimulus treatments followed by an asterisk (*) and means from for NI and I plants followed by an inverted triangle (▼) are significantly different ($P \leq 0.05$) according to the *F* test. Bars represent the standard error of the means.

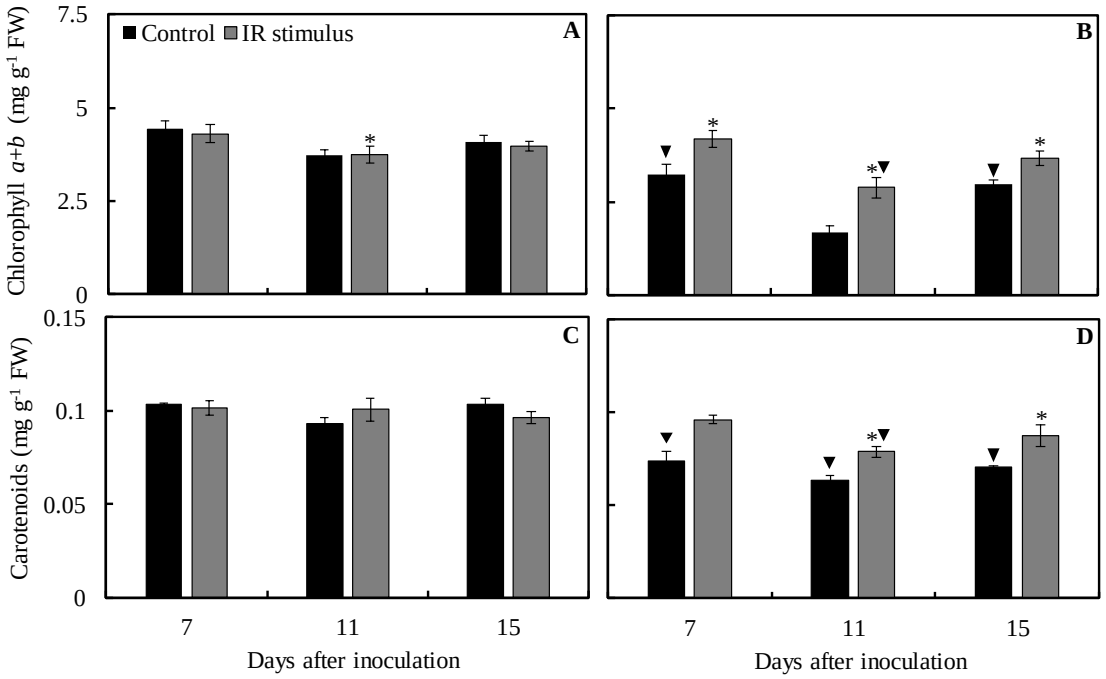

Figure 6. Concentrations of chlorophyll *a*+*b* (Chl *a*+*b*) (A and B) and carotenoids (C and D) determined in leaflets of soybean plants sprayed with water (control) or with induced resistance (IR) stimulus and non-inoculated (NI) (A and C) or inoculated (I) (B and D) with *Phakopsora pachyrhizi*. Means for control and induced resistance (IR) stimulus treatments followed by an asterisk (*) and means from for NI and I plants followed by an inverted triangle (▼), at each evaluation time, are significantly different ($P \leq 0.05$) according to the *F* test. Bars represent the standard error of the means. FW = fresh weight.

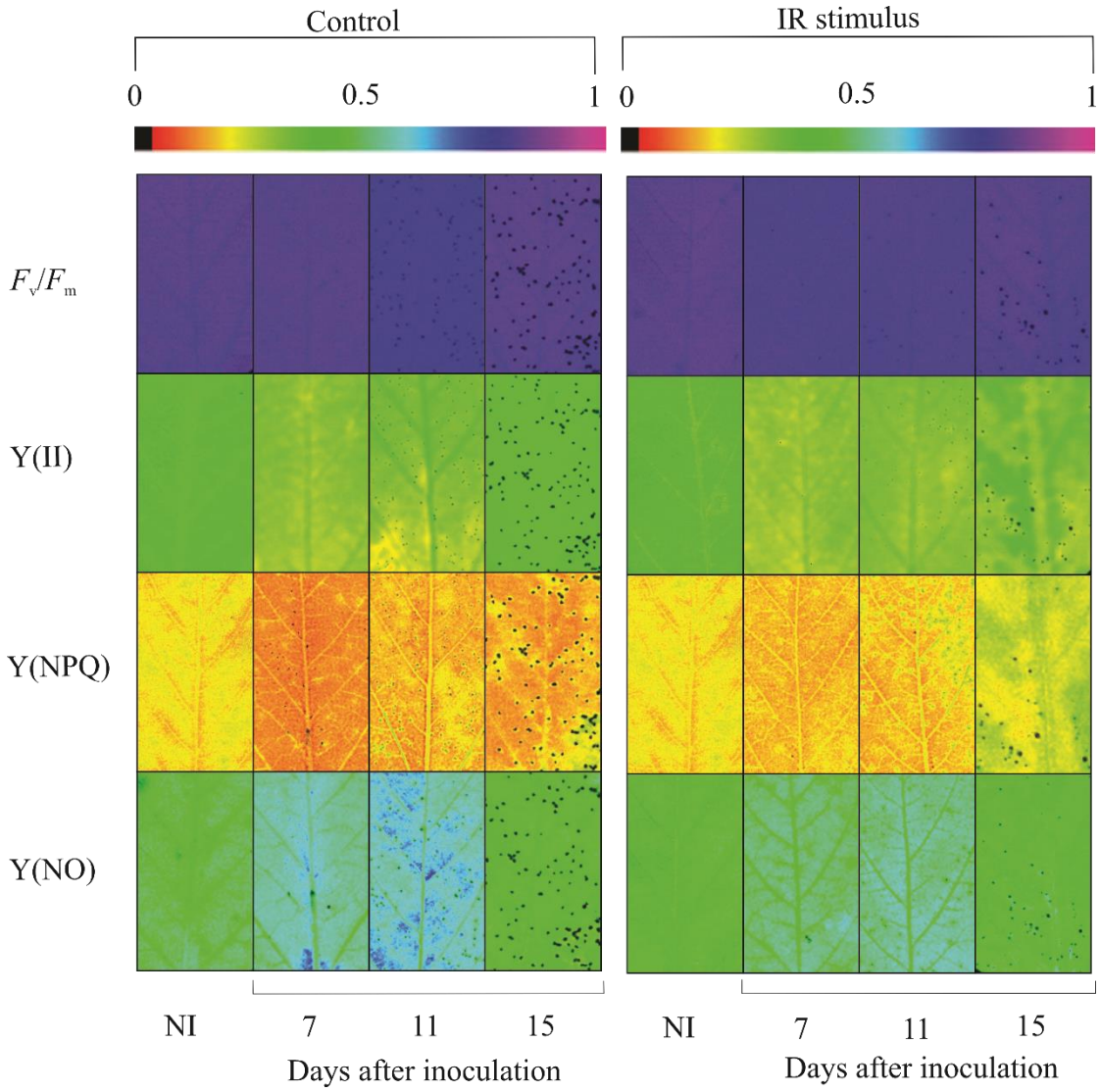

Figure 7. Quantification of chlorophyll *a* fluorescence parameters: maximum photosystem II quantum yield (F_v/F_m) (A and B), effective photosystem II quantum yield [Y(II)] (C and D), quantum yield of regulated energy dissipation [Y(NPQ)] (E and F), quantum yield of non-regulated energy dissipation [Y(NO)] (G and H) and electron transport rate (ETR) (I and J) in leaflets of soybean plants sprayed with water (control) and with induced resistance (IR) stimulus and non-inoculated (NI) (A, C, E, G, and I) or inoculated (I) (B, D, F, H, and J) with *Phakopsora pachyrhizi*. Means for control and IR stimulus treatments followed by an asterisk (*) and means for NI and I plants followed by an inverted triangle (▼), at each evaluation time, are significantly different ($P \leq 0.05$) according to the *F* test. Bars represent the standard error of the means.

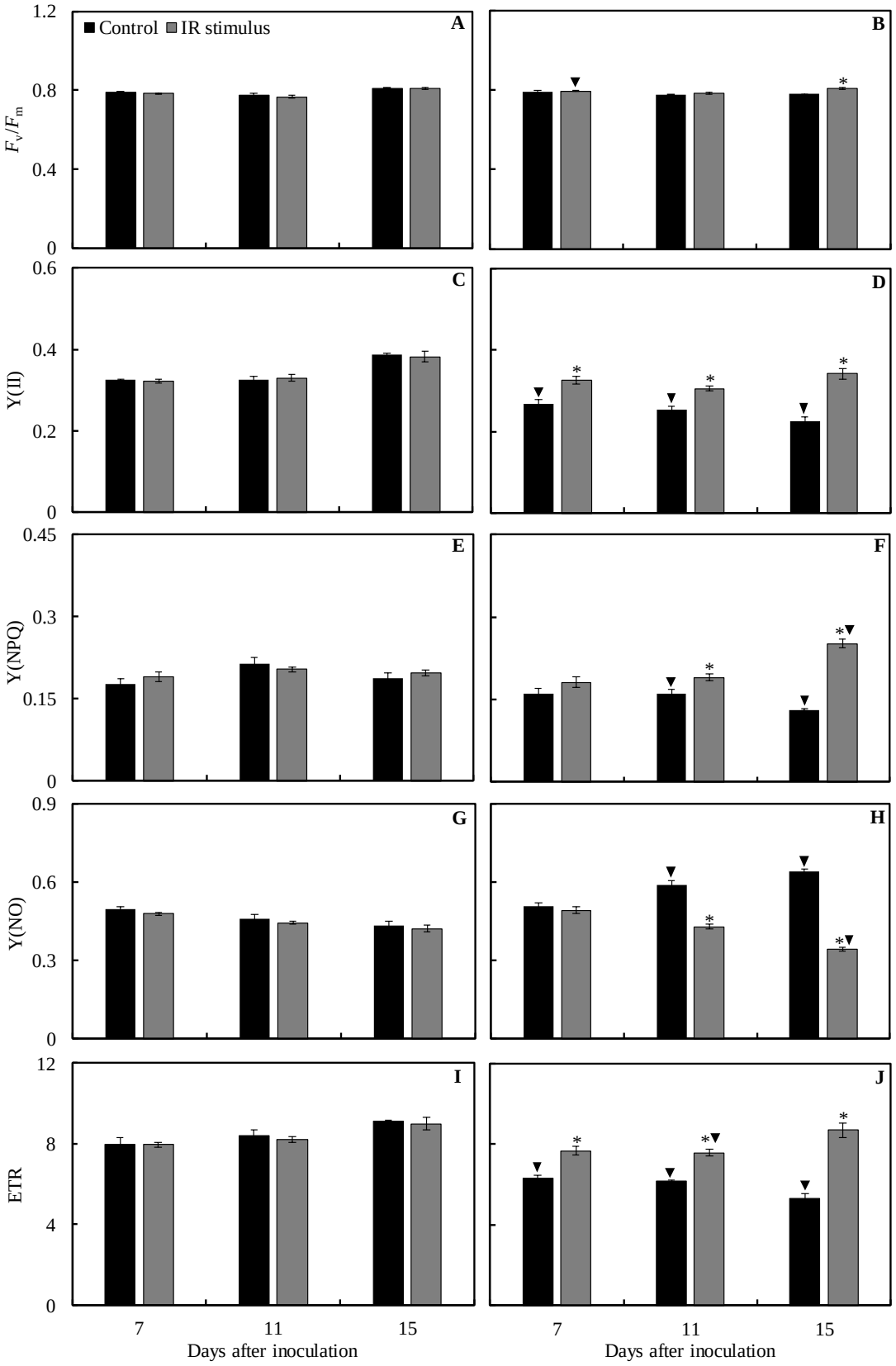
Control
IR stimulus
A
B
C
D
E
F
G
H
I
J
F_v/F_m
Y(II)
Y(NPQ)
Y(NO)
ETR
1.2
0.8
0.4
0
0.6
0.4
0.2
0
0.45
0.3
0.15
0
0.9
0.6
0.3
0
12
8
4
0
7
11
15
Days after inoculation
Days after inoculation

Figure 8. Images of chlorophyll *a* fluorescence parameters: maximum photosystem II quantum yield (F_v/F_m), effective photosystem II quantum yield (Y(II)), quantum yield of regulated energy dissipation [Y(NPQ)] and quantum yield of non-regulated energy dissipation [Y(NO)] determined in leaflets of soybean plants sprayed with water (control) and induced resistance (IR) stimulus and non-inoculated (NI) or at 7, 11 and 15 days after inoculation with *Phakopsora pachyrhizi*.

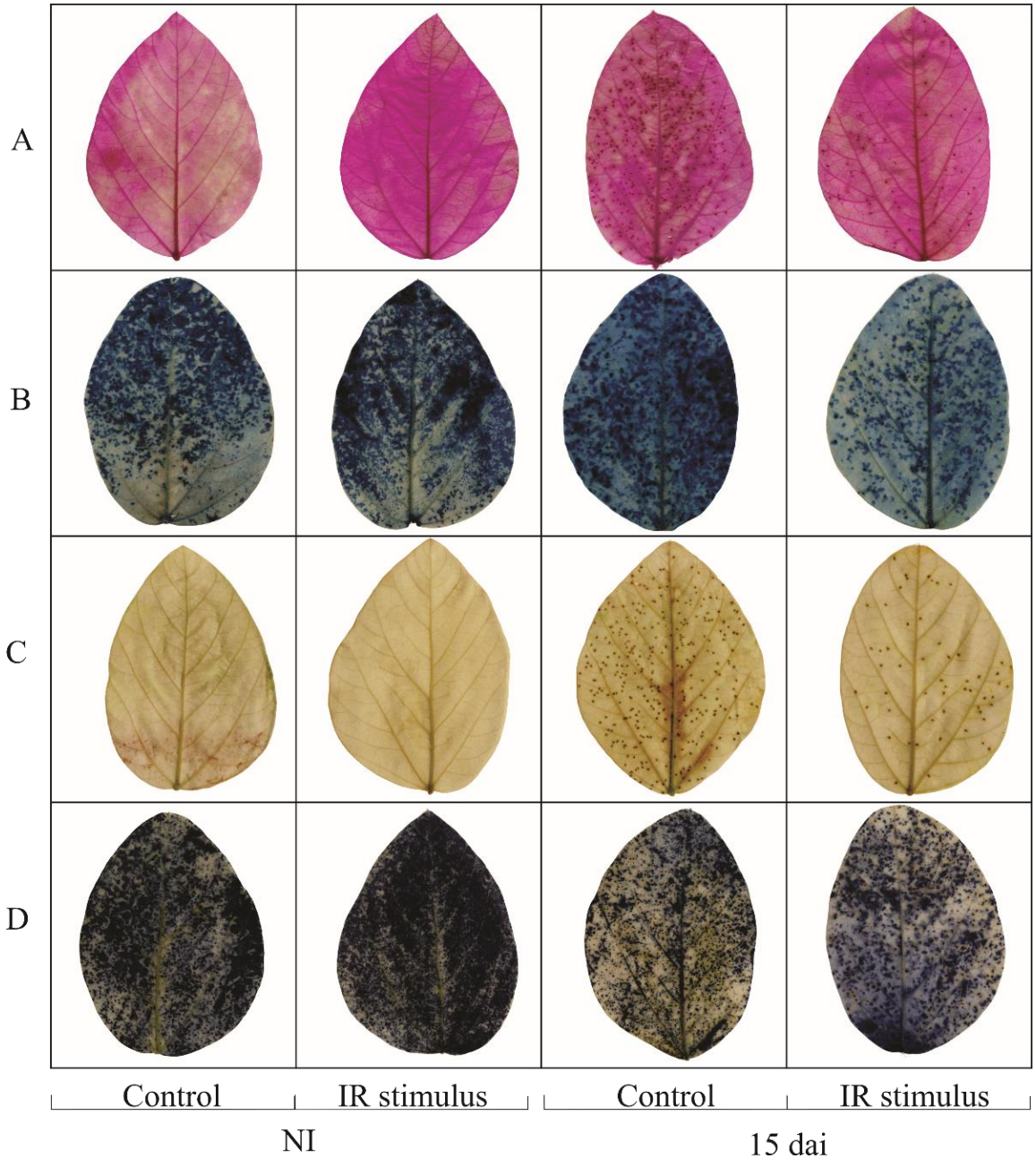

Figure 9. Histochemical detection of lipid peroxidation (A), membrane damage (B), hydrogen peroxide (C), and superoxide anion radical (D) on leaves of soybean plants non-inoculated (NI) or at 15 days after inoculation (dai) with *Phakopsora pachyrhizi* previously sprayed with water (control) or with the induced resistance (IR) stimulus.

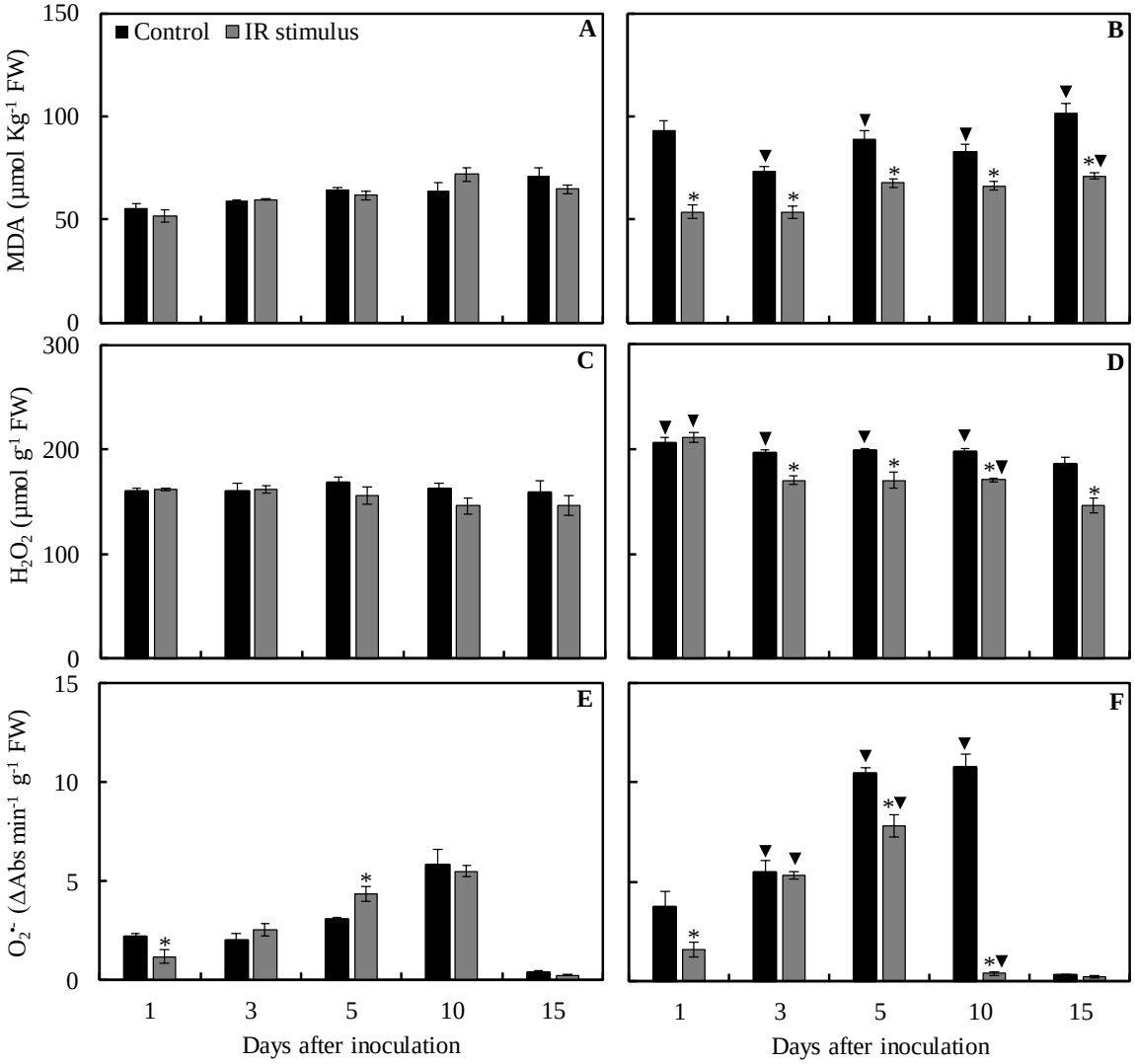

Figure 10. Concentration of malondialdehyde (MDA) (A and B), hydrogen peroxide (H_2O_2) (C and D), and superoxide anion radical ($O_2^{\bullet-}$) (E and F) determined in leaflets of soybean plants sprayed with water (control) and induced resistance (IR) stimulus and non-inoculated (A, C, and E) or inoculated (B, D, and F) with *Phakopsora pachyrhizi*. Means for control and IR stimulus treatments followed by an asterisk (*) and means for NI and I plants followed by an inverted triangle (▼), at each evaluation time, are significantly different ($P \leq 0.05$) according to the *F* test. Bars represent the standard error of the means. FW = fresh weight.

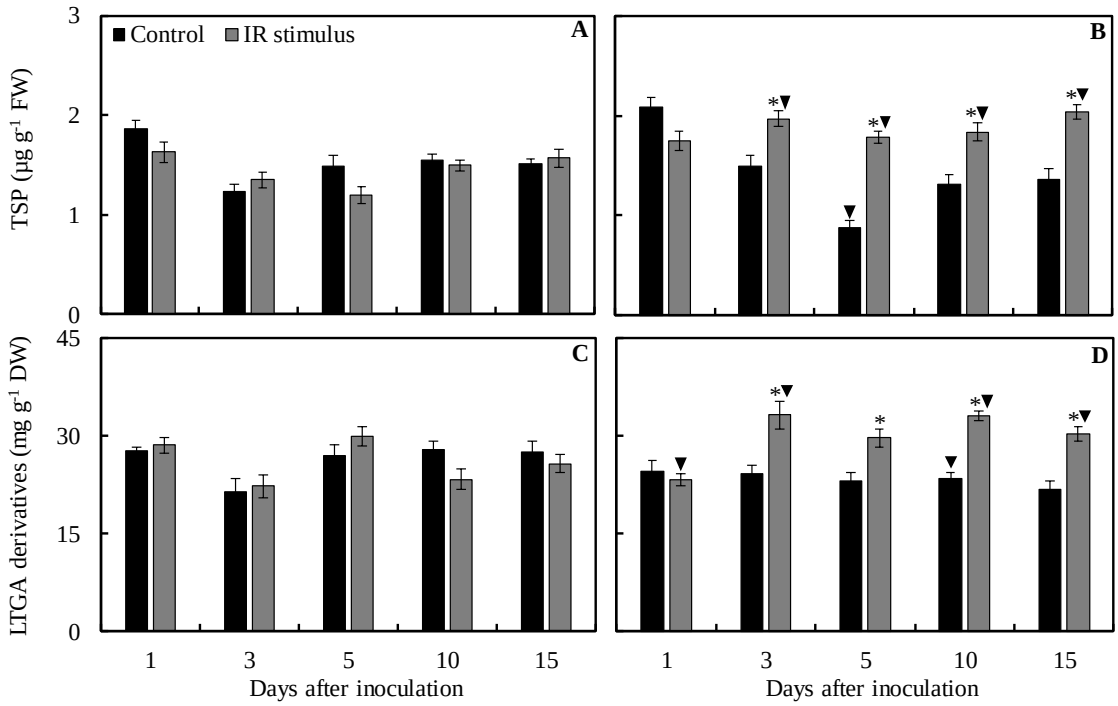

Figure 11. Concentration of total soluble phenolics (TSP) and lignin-thioglycolic acid (LTGA) derivatives determined in leaflets of soybean plants sprayed with water (control) and induced resistance (IR) stimulus and non-inoculated (A and C) or inoculated (B and D) with *Phakopsora pachyrhizi*. Means for control and IR stimulus treatments followed by an asterisk (*) and means for NI and I plants followed by an inverted triangle (▼), at each evaluation time, are significantly different ($P \leq 0.05$) according to the *F* test. Bars represent the standard error of the means. FW and DW = fresh weight and dry weight, respectively.

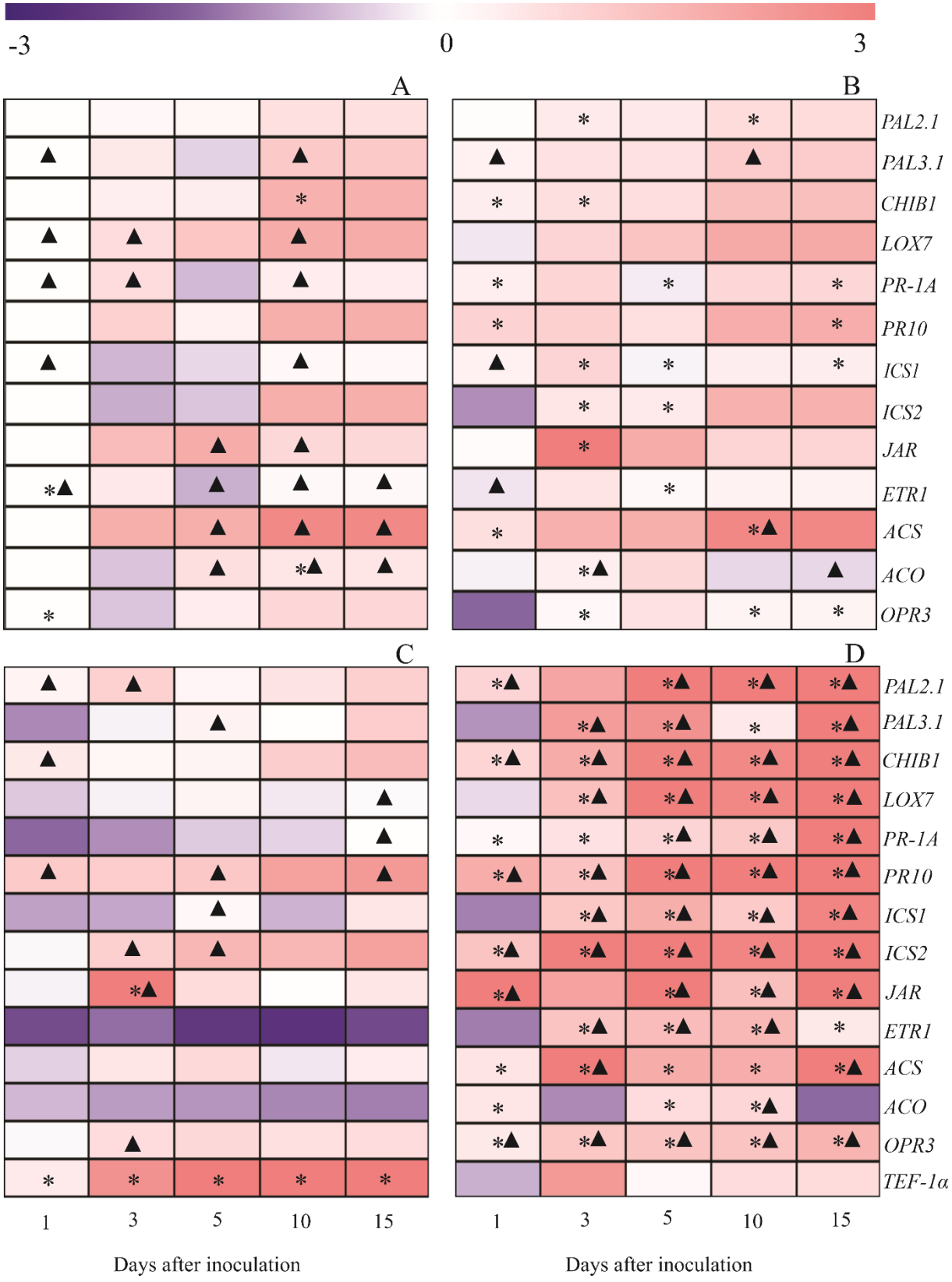
-3
0
3
A
B
C
D
PAL2.1
PAL3.1
CHIB1
LOX7
PR-1A
PR10
ICS1
ICS2
JAR
ETR1
ACS
ACO
OPR3
TEF-1α
1
3
5
10
15
Days after inoculation
Days after inoculation

Figure 12. Expression profile of genes determined in leaflets of soybean plants sprayed with water (control) (A and C) and induced resistance (IR) stimulus (B and D) and non-inoculated (NI) (A and B) or inoculated (I) (C and D) with *Phakopsora pachyrhizi*. Color cells ranging from blue (-3.0) to red (+3.0) represent the relative transcript levels for the genes studied. Amplification of Ubiquitin-3 (*UBIQ*) and glyceraldehyde 3-phosphate dehydrogenase (*GAPDH*) genes from soybean was used as an internal control for data normalization. Fold changes were calculated based on transcript level for NI plants from control treatment at 1 day after inoculation (dai), except for the *TEF-1α* gene. In this case, transcript levels of *TEF-1α* for I plants from control treatment at 1 dai were used in the calculation. Four biological replications were used for each leaf sample with their respective two technical replicates. Means for control and IR stimulus treatments, at each evaluation time, followed by an asterisk (*) are significantly different ($P \leq 0.05$) according to Tukey's test. Means for NI and I plants, for each treatment at each evaluation time, with a triangle (▼) are significantly different ($P \leq 0.05$) according to the *F* test.

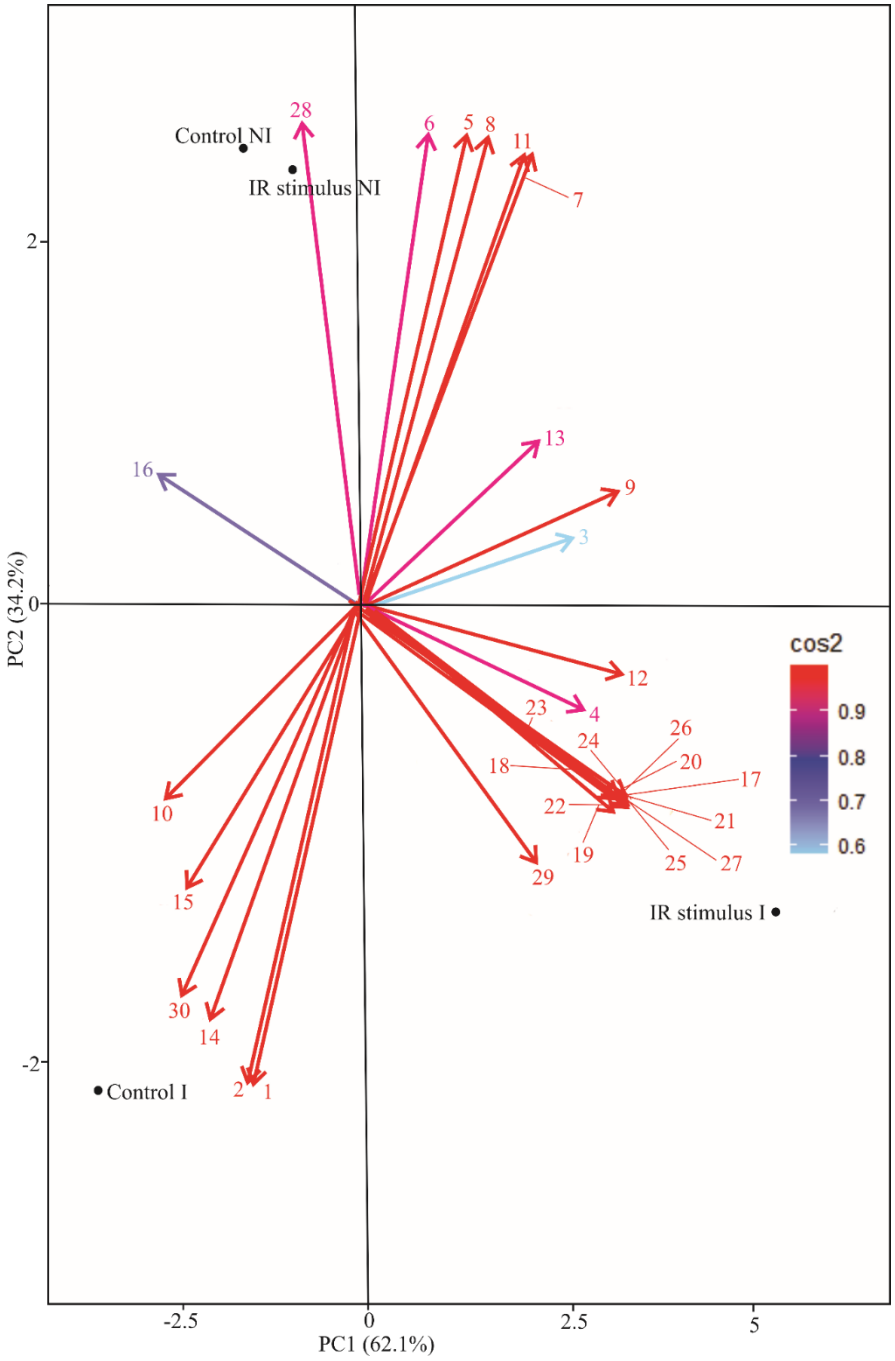
Control NI
IR stimulus NI
Control I
IR stimulus I
28
6
5
8
11
7
13
16
9
3
12
4
23
26
24
20
18
17
22
21
10
19
25
27
29
15
30
14
2
1
cos2
0.9
0.8
0.7
0.6
2
0
-2
-2.5
0
2.5
5
PC2 (34.2%)
PC1 (62.1%)

Figure 13. Score plots and loading values in the principal component analysis (PCA) for variables and parameters evaluated in soybean plants sprayed with water (control) and induced resistance (IR) stimulus and non-inoculated (NI) or inoculated (I) with *Phakopsora pachyrhizi*. Numbers in the PCA are as follow: severity (1), the area under disease progress curve (2), foliar Ni and K concentrations (3 and 4, respectively), concentrations of photosynthetic pigments (5 and 6, respectively, to Chl *a* + *b* and carotenoids), parameters of chlorophyll *a* fluorescence (7, 8, 9, 10 and 11, respectively, to F_v/F_m, Y(II), Y(NPQ), Y(NO) and ETR), metabolites (12, 13, 14, 15 and 16, respectively, to TSP, LTGA derivatives, MDA, H_20_2, and $O_2^{\bullet-}$), and gene expression (17, 18, 19, 20, 21, 22, 23, 24, 25, 26, 27, 28, 29, and 30, respectively, to *PAL2.1*, *PAL3.1*, *CHIB1*, *LOX7*, *PR-1A*, *PR10*, *ICS1*, *ICS2*, *JAR*, *ETR1*, *ACS*, *ACO*, *OPR3*, and *TEF-1α*). Groups were generated from cluster analysis with complete linkage and Pearson distance. Data from variables and parameters used in the PCA were obtained 15 days after inoculation for plants NI or I with *P. pachyrhizi*.